



Fermi National Accelerator Laboratory

FN-549

Gravity for the Masses *

Dan Green
Fermi National Accelerator Laboratory
P.O. Box 500
Batavia, Illinois 60510

October 1990

* Academic lectures presented at Fermi National Accelerator, Batavia, Illinois, January 22 - February 2, 1990.



Operated by Universities Research Association Inc. under contract with the United States Department of Energy

Gravity for the Masses

Dan Green

Fermilab

TABLE OF CONTENTS

| | |
|----------------------------------|-----|
| LIST OF FIGURES..... | i |
| LIST OF TABLES..... | iii |
| ABSTRACT..... | 1 |
| 1 INTRODUCTION..... | 2 |
| 2 THE EQUIVALENCE PRINCIPLE..... | 16 |
| 3 LINEARIZED GRAVITATION..... | 26 |
| 4 SCHWARZCHILD SOLUTION..... | 36 |
| 5 OTHER SOLUTIONS..... | 51 |
| 6 KERR SOLUTION..... | 60 |
| 7 RADIATION..... | 70 |
| 8 NEUTRON STARS..... | 84 |
| 9 HAWKING "EVAPORATION"..... | 102 |
| 10 ACKNOWLEDGMENTS..... | 105 |
| 11 REFERENCES..... | 106 |
| APPENDIX A..... | 107 |
| APPENDIX B..... | 108 |
| APPENDIX C..... | 110 |
| APPENDIX D..... | 111 |

LIST OF FIGURES

| | |
|----------|--|
| Fig. 1.1 | Field line representation of the tidal field of a point mass.....5 |
| Fig. 1.2 | a) Electroweak diagrams for four fermion coupling and W exchange. b) Coupling constants for photon and graviton exchange..... 7 |
| Fig. 1.3 | Kinematic definitions for energy transfer in a collision..... 14 |
| Fig. 2.1 | Equivalence Principle figures. a) Equivalent situations b) Local inertial frames c) Red shift d) Light deflection..... 17 |
| Fig. 3.1 | Light Deflection. a) Kinematic definitions b) Refraction due to inhomogenous index of refraction..... 30 |
| Fig. 3.2 | a) Light deflection as a function of b b) Interferometer at Owens Valley..... 33 |
| Fig. 3.3 | Gravitational Lensing by intervening galaxy splits images of a QSO. Bottom, one image removed showing intervening galaxy. 35 |
| Fig. 4.1 | Turntable. Inertial observer in S with accelerated frame S' of a turntable. 36 |
| Fig. 4.2 | Radar ranging tests. a) Kinematic definition of quantities b) Earth/Venus superior conjunction c) Mariner VI spacecraft as reflector..... 43 |
| Fig. 4.3 | a) Dropping into a black hole. b) Coordinate time (solid line) and proper time (dot-dashed line) near $r=r_S$ 47 |
| Fig. 4.4 | a) Light cones near $r=r_S$ b) World lines near $r=r_S$ 48 |
| Fig. 4.5 | Binary system of black hole and normal star..... 50 |
| Fig. 5.1 | a) Definitions for interior solution b) Newtonian interior solution matching to exterior solution at $r=R$ 55 |

LIST OF FIGURES

| | |
|----------|--|
| Fig. 6.1 | Geometry of the turntable appropriate to the EP metric discussion.61 |
| Fig. 6.2 | Layout of the dynamical vectors in the gyroscopic tests. The spin-orbit and spin-spin vectors are shown for clarity in the two orientations.....66 |
| Fig. 6.3 | Kerr metric singularity surfaces. The horizon, infinite red shift, and ergosphere are indicated.....68 |
| Fig. 7.1 | a) Orbital data for the binary pulsar. b) Measured slowing down of the pulsar. The curve ascribes the deceleration to the emission of gravitational radiation.....78 |
| Fig. 7.2 | a) Layout of interferometer for detection of gravity waves. b) Specifications for existing and proposed interferometers.....82 |
| Fig. 7.3 | Sensitivity of bar and interferometric gravity wave detectors as a function of time.....83 |
| Fig. 8.1 | a) Schematic for density of normal matter. b) Schematic for density of nuclear matter.....85 |
| Fig. 8.2 | Masses of known pulsars in units of solar masses. Note that no rotating neutron star appears to be much above M_{CH}89 |
| Fig. 8.3 | Density and structure for a neutron star.91 |
| Fig. 8.4 | Lowest order neutral current Feynman diagram for neutrino elastic scattering.94 |
| Fig. 8.5 | Data from IMB and Kamioka on the Supernova 1987 neutrino burst. a) Arrival time distribution. b) Energy distribution of neutrinos.....96 |
| Fig. 8.6 | Inferred surface magnetic fields of rotating neutron stars as a function of rotational period.....99 |

LIST OF TABLES

| | | |
|------------|--|----|
| Table 1.1 | Tests of $m_I = m_G$ | 4 |
| Table 2.1a | Redshift Tests..... | 20 |
| Table 2.1b | Details of Direct Clock Tests..... | 20 |
| Table 3.1 | Light deflection measurements..... | 32 |
| Table 4.1 | Perihelion advance measurements..... | 41 |
| Table 4.2 | Radar Ranging Measurements..... | 45 |
| Table 7.1 | Astrophysical sources of gravitational radiation. Energies are quoted at a distance of 100 ly..... | 74 |
| Table 7.2 | Binary system sources of gravitational radiation..... | 80 |
| Table 8.1 | Properties of Supernovae..... | 97 |

*"Now I a fourfold vision see,
and a fourfold vision is given to me
'tis fourfold in my supreme delight
and threefold in soft Beulah's night
and twofold aways, may God us keep
from single vision and Newton's sleep".*

William Blake, 1802

Gravity for the Masses

Dan Green

Fermilab

Abstract

The purpose of this set of lectures is to provide an introduction to general relativity which relies only upon simple physical arguments. The study of the metric is begun with free particle special relativity. A red shift metric is then derived by Equivalence Principle arguments. Linearized gravity is presented as a relativistic generalization of Newton's laws. Finally, the Schwartzchild solution is made plausible using physical arguments.

All the solar system tests are derived by using the formalism of the Lagrangian. Since this method is familiar from classical mechanics, no new mathematics is required. This technique evades geodesic equations and Christoffel symbols.

The Kerr metric is motivated using a turntable example. Gyroscopic tests of this metric are then derived. Correspondences with the familiar quantum mechanical spin-orbit and spin-spin forces are made.

Radiation formulae are made plausible in electromagnetism by making dimensionless replacements to static solutions. Given that success, the corresponding gravitational formulae follow simply. Detection of gravity waves is discussed.

The neutron star mass limit is derived. Further discussion of densities, \bar{B} fields, and neutrino diffusion in supernova events is made.

All the derivations are slanted towards an audience of High Energy physicists.

1 INTRODUCTION

It has often been said that the two major triumphs in 20th century Physics were the development of quantum mechanics in the 1920's and the revelations of relativity theory, beginning in 1905, with the Special Theory and culminating in 1915 with the General Theory. Throughout the 20th century, quantum mechanics has made enormous strides. Presently we have arrived at the Standard Model with quantum electrodynamics, quantum chromodynamics, and the unification of quantum electrodynamics with the weak interactions. By contrast, in relativity, the lack of familiarity with differential geometry, Christoffel symbols, and the Riemann tensor has often left this field impenetrable to students in particle physics. It is also to be noted that, despite spectacular successes in experimental tests of the classical theory of general relativity, until recently, theoretical development floundered on the inability to write a renormalizable quantum field theory of gravity. Recently, of course, with the advent of string theory, there is new hope raised that this theoretical impasse will be overcome.

The goal of these lecture notes is to provide an introduction to the point solutions of general relativity which is accessible to the typical graduate student. There will be essentially no attempt to discuss the cosmological implications of general relativity, given the fact that there are so many excellent texts available. In particular, the discussion will be slanted towards experimentally verified tests and astrophysical tests which are of interest to Fermilab physicists; both theorists, and experimentalists. A collection of references has been given at the end of this note. They are completely idiosyncratic and merely reflect the author's limited reading in this field. These references are extremely useful and are meant to be referred to for a deeper, more mathematical understanding of the topics covered in this paper.

In general, the mathematical details, where they have not been totally evaded, will be provided in a series of Appendices. Basically, there will be no tensor analysis. We will limit ourselves to the usage of well known mathematical techniques, appealing to a presumed shared

knowledge of special relativity, classical dynamics, and electromagnetic theory. Constant analogies will be made between electromagnetic theory and the gravitational theory which we will be "boot-strapping." As mentioned, we will be concentrating on point solutions and local solar system tests of the classical theory of general relativity. Provided in Appendix A is a set of useful astronomical constants having some utility in calculating the quantities which go into these solar system tests.

In order to begin, it seems natural to start with a brief review of Newtonian gravity. Although this is not relativistically correct, because it implies action at a distance, it is a starting point for attempting to derive, or at least motivate, the general relativistic theory. If we use the Lagrangian formalism, we write the Lagrangian as the total kinetic energy minus the potential energy. The potential energy for a gravitational system is always proportional to the gravitational mass. We will factor this out and define a reduced potential Φ . The kinetic energy depends on the inertial mass, because it defines the response of the system to forces as represented by the potential energy. In this case, the Euler-Lagrange equations lead to the equations of motion. The relationship of the reduced potential to the mass density, σ , is that the Laplacian of the reduced potential is driven by the mass density. It is the mass density which defines the potential. There is a proportionality constant G , which is the Newtonian coupling constant. The acceleration is proportional to the gradient of the reduced potential.

$$\begin{aligned}
 L &= T - V, \quad V = m_G \Phi, \quad T = m_I v^2 / 2 \\
 \vec{a} &= -\vec{\nabla} \Phi \quad (m_I = m_G) \\
 \nabla^2 \Phi &= 4\pi G \sigma(x).
 \end{aligned}
 \tag{1.1}$$

This is true only if the inertial and gravitational masses are strictly equal. In this case, motion is independent of the mass (inertia) of the particle. All particles in a gravity field therefore respond with the same motion, independent of mass.

In Newtonian physics, this equality of inertial and gravitational mass seems to be entirely accidental. As seen in Table 1.1, however, the equality holds good to a part in 10^{12} . This fact must give rise to the suspicion that Nature is telling us something. It cannot be an accident that the inertial and gravitational masses are the same to this finely tuned level of accuracy. As an amusing aside, Table 1.1 shows that Newton measured the equality of inertial and gravitational mass to a part in 10^3 .

| <i>EQUALITY OF m_I AND m_G</i> | | | |
|--|-------------|----------------------|-------------------------------------|
| Experimenter | Year | Method | $m_I - m_G /m_I$ |
| Galileo | ~1610 | pendulum | $< 2 \times 10^{-3}$ |
| Newton | ~1680 | pendulum | $< 10^{-3}$ |
| Bessel | 1827 | pendulum | $< 2 \times 10^{-5}$ |
| Eötvös | 1890 | torsion-balance | $< 5 \times 10^{-8}$ |
| Eötvös et al. | 1905 | torsion-balance | $< 3 \times 10^{-9}$ |
| Southerns | 1910 | pendulum | $< 5 \times 10^{-6}$ |
| Zeeman | 1917 | torsion-balance | $< 3 \times 10^{-8}$ |
| Potter | 1923 | pendulum | $< 3 \times 10^{-6}$ |
| Renner | 1935 | torsion-balance | $< 2 \times 10^{-10}$ |
| Dicke et al. | 1964 | torsion-balance; sun | $< 3 \times 10^{-11}$ |
| Braginsky et al. | 1971 | torsion-balance; sun | $< 59 \times 10^{-13}$ |

Table 1.1: Tests of $m_I = m_G$.

This equality implies that all particles, independent of mass, have the same acceleration under the action of gravity. Thus, if one goes into a free fall coordinate system, particles will act as if they were weightless. One can “wipe out” gravity by going into a free fall coordinate system. This is very familiar to those who watch space shuttle astronauts cavort in Earth orbit. If one looks at the relative trajectory of two free fall particles, defining η to be the difference between their coordinates, using Eq. 1.1 the relative acceleration between them is proportional to the second derivative of the potential and to the separation.

$$\begin{aligned}
\eta^i &\equiv x^i - (x^i)' \\
\frac{d^2\eta^i}{dt^2} &= \frac{-\partial\Phi}{\partial x^i} + \frac{\partial\Phi}{\partial(x^i)'} \\
&= -\left(\frac{\partial^2\Phi}{\partial x^i\partial x^j}\right)\eta^j.
\end{aligned}
\tag{1.2}$$

Thus, the free fall deviation depends on the second derivative of the potential; one is left with tidal forces. This is obvious because the first derivative (gradient) of the potential is a common acceleration which can be locally wiped out by going into free fall coordinates. This fact leads us to believe that it is only the second derivative of the potential which is a physically meaningful quantity because the first derivative (acceleration) can be removed by going to an appropriate coordinate system. We will expect, therefore, that the tidal field is intrinsic to gravity. A pictorial representation of the tidal fields is shown in Fig. 1.1.

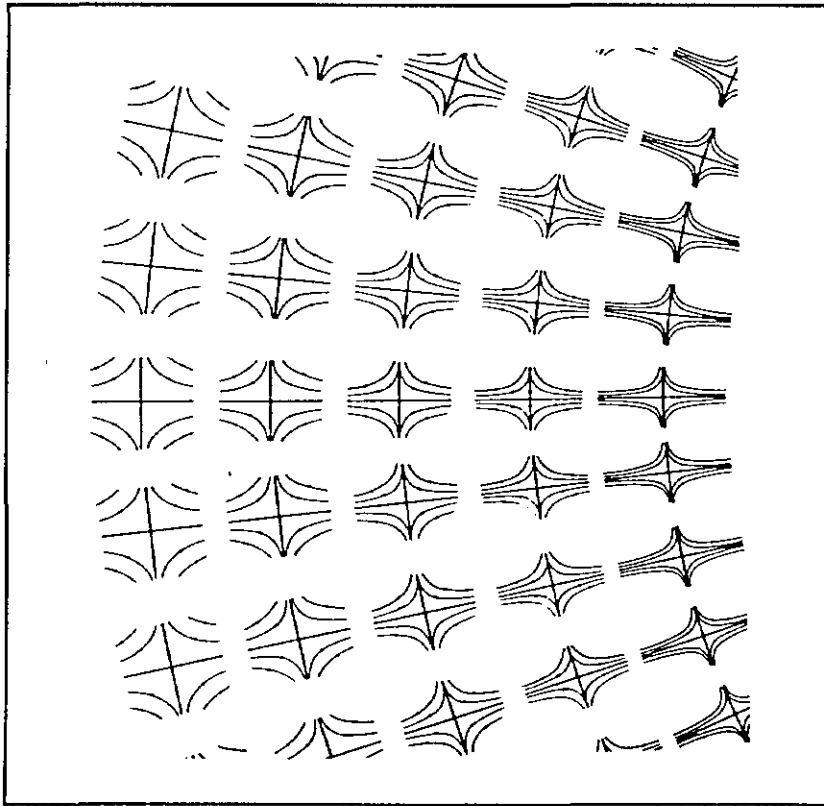


Fig. 1.1: Field line representation of the tidal field of a point mass.

Tidal fields are a local measure of gravity in a free fall coordinate system. Figure 1.1 depicts tidal fields (represented by lines of force) near a point particle source of gravity.

As mentioned, there is a universal coupling between the reduced potential and the source of that potential - the mass density. As wallet card carrying particle physicists, one of the first questions to ask is: "What is the nature of the coupling constant in the problem of gravity?" Reviewing electromagnetism, there is an inverse square force law, which is proportional to the product of the charges. This force leads to the famous dimensionless coupling constant α .

$$f_{EM} = q_1 q_2 / r^2, \quad \alpha = e^2 / \hbar c. \quad (1.3)$$

Consider the case of weak interactions. There is an effective four fermion coupling constant, G_F , which at first looks rather different due to its dimensions of inverse square mass. As learned in particle physics, this is only an apparent difference due to the large masses of the gauge bosons responsible for the weak interactions. If we recall that the Fourier transform of the Yukawa potential is just the propagator in momentum space for a massive particle, and if we are at low momentum transfers, then the propagator is just a constant. The effective four point interaction is thus due to the exchange of a rather heavy gauge boson, as shown in Fig. 1.2.

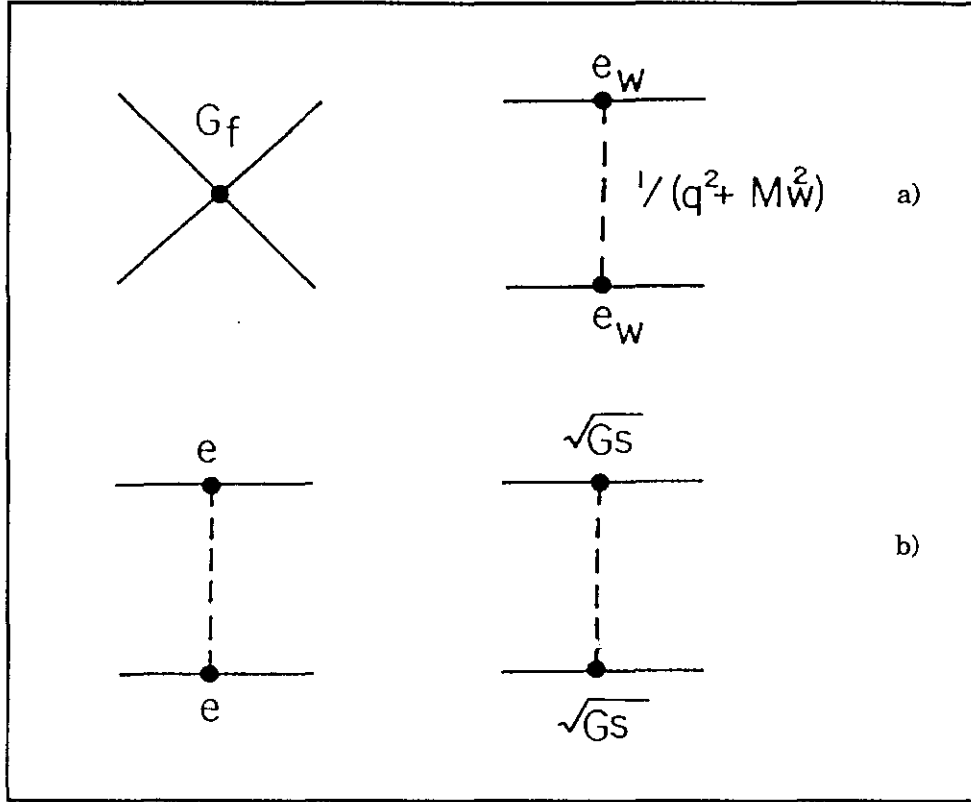


Fig. 1.2: a) Electroweak diagrams for four fermion coupling and W exchange.
 b) Coupling constants for photon and graviton exchange.

The Yukawa length is proportional to the inverse of the gauge boson mass. Heavy objects are thus confined to very small spatial regions allowing one to define an effective four point interaction. The triumph of electroweak physics is that the real coupling constant, once one can probe inside these small distances, is just the electromagnetic coupling constant. This means although we thought we had a weak coupling constant with dimensions, we really had a dimensionless coupling constant and a heavy propagator.

$$\begin{aligned}
 G_F &\sim \alpha_w / M_W^2, \quad \alpha_w = \alpha / \sin^2 \theta_w \\
 &= 1.16 \times 10^{-5} / \text{GeV}^2 \\
 1/(q^2 + M_W^2) &\leftrightarrow e^{-r/\lambda_w} / r \\
 \lambda &\equiv (\hbar / Mc).
 \end{aligned}
 \tag{1.4}$$

What is the situation for gravity? In this case there is a force which is proportional to the product of the masses and has inverse square spatial behavior. The coupling constant has dimensions of inverse mass squared, somewhat comparable to the situation for the weak interactions.

$$\begin{aligned}
 f_G &= Gm_1m_2 / r^2 \\
 G &= 6.6 \times 10^{-11} \text{ m}^3 / (\text{kg sec}^2).
 \end{aligned}
 \tag{1.5}$$

However, in contrast to the weak interaction case, there is a $1/r^2$ force. This means that the quantum in the problem - the gravitino - has zero mass, because any long range force implies a zero mass quantum. The problem of a coupling constant which has dimensions is now unavoidable. We can still, however, define a gravitational coupling constant which will become large, meaning α_G is of order one, at an energy scale, which is the Planck mass. This mass sets an enormously high energy scale of order 10^{19} GeV, and the scale is achieved at distances comparable to the Planck distance, which is 10^{-35} meters.

$$\begin{aligned}
 M_{PL} &= \sqrt{\hbar c / G} = 1.2 \times 10^{19} \text{ GeV} \\
 \alpha_G &= GM^2 / \hbar c \\
 R_{PL} &= \sqrt{\frac{G\hbar}{c^3}} = \frac{\hbar c}{M_{PL}c^2} \sim 10^{-35} \text{ m}.
 \end{aligned}
 \tag{1.6}$$

The situation which contrasts electromagnetism and gravity is sketched in Fig. 1.2b. In both cases, one has a zero mass quantum. However, the coupling constant of electromagnetism is dimensionless, whereas the effective gravitational coupling grows with mass. At first blush the theory should diverge when gravity becomes strong, i.e., at center of mass energies on the scale of the Planck mass. This divergence of gravity is certainly a serious issue and one which is by no means resolved. These divergences cannot be avoided in constructing a quantum field theory of

gravity. In fact, the non renormalizable features of such a point particles theory is a well known and long standing problem. We will only be considering classical, weak fields.

Another possibility is that we can imagine gravity as being merely a fictitious force caused by our being in an accelerated reference system. These forces are well known. Examples include the coriolis and centrifugal force - both being fictitious in the sense that they are caused by our being in an accelerated reference frame and not in an inertial frame.

The name given to this hypothesis is Mach's principle which says that the inertial properties of matter must be determined by its acceleration with respect to all matter in the Universe. For example, let us consider a particle accelerated with respect to a local inertial frame and transform to an accelerated frame, S' , where that force is "wiped out". The extra force must come from acceleration with respect to the Universe as a whole. If we consider the contribution due to a mass M , then the static contribution will go $1/r^2$. This is obviously much too weak; what is needed is a transformation from static fields to radiation fields. We will appeal to a substitution proportional to (due to) acceleration in which the fields fall off as $1/r$ (the flux through unit area will be constant) which is a characteristic of a radiation field. The radiation fields are found by substitution of a dimensionless quantity which is proportional to acceleration and radius.

$$df' = GMm_G / r^2 \left[\frac{ar}{c^2} \right] \quad (1.7)$$

We will use this same substitution later in appealing to an analogy with electromagnetism by which we derive the power radiated by a gravitational system in comparison to that of electromagnetic radiation. If we now smear out the galaxies into a uniform mass distribution, σ , we can integrate over all the galaxies out to a maximum radius.

$$\begin{aligned}
df' &= GMm_G(a/rc^2) \\
df' &= \frac{Gm_G a}{c^2} \left[\frac{\sigma dr}{r} \right] \\
f' &= \frac{Gm_G a \sigma}{c^2} [2\pi r_{MAX}^2].
\end{aligned} \tag{1.8}$$

There is a maximum radius; the cut off comes from the horizon, when the apparent recession velocity of the galaxies is equal to that of light. One can remember what that effective horizon is by referring to the Hubble constant. Remembering that the Universe is about 20 billion years old, means that the Hubble constant is 50km per megaparsec.sec. Then r_{MAX} is c divided by the Hubble constant, which is 20 billion light years, or 2×10^{26} meters. For a mass density, one can take the visible mass density (obtained from counting stars), of 3×10^{-28} kg/m³, or roughly 0.2 protons per cubic meter. This fact is easy to remember because there is basically one baryon per cubic meter, and 10^{10} photons per cubic meter in the observed Universe. The inertial force can be wiped out by inducing an equal but opposite force while going to the accelerated reference frame. If there is a relationship between the Newtonian coupling constant, the Hubble constant, and the mass density, as shown below, then Mach's principle is upheld. This also requires that the inertial mass be equal to the gravitational mass.

$$\begin{aligned}
r_{MAX} &\sim c/H_0 \\
f' &= m_I a \quad \text{Iff} \\
G &= H_0^2 / 2\pi\sigma.
\end{aligned} \tag{1.9}$$

Inserting the numbers, we find experimentally, that the equality is certainly obeyed within an order of magnitude. In fact, if we allowed for a critical closure density 10 times larger (due to the existence of, say, dark matter) then the equality shown in Eq. 1.9 would be much closer to being satisfied (within factors of 2). Mach's principle is thus a tantalizing assertion. It is unproven, but certainly plausible that the numbers appear to be within the right order of magnitude. This means

that the gravitational constant, thought of as a fundamental constant, is perhaps defined by the structure of the Universe as embodied by the Hubble constant and the mass density. In general, it might be a function of time as the Universe evolves. However, for a zero curvature matter dominated cosmology, it is in fact, not a function of time (as can be found in any cosmology text book). It is certainly thought provoking, that the gravitational constant might be related to the structure of the Universe, if Mach's principle were to be obeyed.

For the remainder of this note, we will prosaically consider the gravitational constant to be just that - a fundamental constant of nature in the same way that the fine structure constant α is. Aside from the Newtonian theory of gravity, the other necessary ingredient in constructing a relativistic theory of gravity is, obviously, special relativity. We will assume a familiarity with special relativity, since it is a common tool of the practicing particle physicist. Hence, the relevant formulae will be relegated to Appendix B. Appendix B depicts the Minkowski flat space metric and the invariant length, which is the same in all inertial frames. We also quote the four dimensional position, velocity, acceleration, momentum, and force. For completeness, we quote the four dimensional version of the derivative, divergence, gradient, and Laplacian. In addition, the covariant form of Maxwell's equations is shown. In particular, since the source of Newtonian gravity is known to be mass, we need its relativistic generalization in the form of the mass tensor, stress energy, and pressure tensor. For example, one can note that pressure has dimensions of an energy density so that it is natural that the mass tensor has a relationship with the pressure stress tensor.

The basic premise of the special theory of relativity is that the laws of physics are the same in all inertial frames. In particular, free particles are straight lines in space-time having no acceleration and travel along geodesic paths. The free particle Lagrangian and the relativistic Euler-Lagrange equations are shown below.

$$\begin{aligned}
\mathfrak{L} &= U_\mu U^\mu \\
&= g_{\mu\nu}^0 \left(\frac{dx^\mu}{ds} \right) \left(\frac{dx^\nu}{ds} \right) \\
\frac{d}{d(s/c)} \left[\frac{\partial \mathfrak{L}}{\partial U^\mu} \right] - \frac{\partial \mathfrak{L}}{\partial x^\mu} &= 0 \\
\frac{d}{d(s/c)} [p_\mu] &= F_\mu.
\end{aligned} \tag{1.10}$$

The physical meaning of the Euler-Lagrange equations is merely that the proper time rate of change of the 4 momentum is the 4 force, which for a free particle is proportional to the 4 dimensional acceleration, which is zero. The invariant element in special relativity is the 4 dimensional coordinate length interval between two events and it is the same in all inertial frames. Mathematically, this means it is a distance because distance is invariant under 4 dimensional pseudo rotations (Lorentz transformations).

$$(ds^2)_{SR} = (cdt)^2 - (d\vec{x})^2. \tag{1.11}$$

This interval between events has a causally relevant sign. If it is positive, it represents transmission between two points by less than the speed of light, therefore, it is a possible interval between events which particles can connect. If the length is zero, Eq. 1.11 shows that it represents light moving along the null interval of the light cone. Negative values of the length represent space-time separations which cannot be causality connected, and which are hence outside the causal light cone.

Appendix B shows that the mass density is proportional to a component of the matter tensor, therefore, there is a tensor source for gravity and it is graceful to assume that there is a tensor field. A rank (spin) two field is always attractive, as distinct from a spin one field such as electromagnetism. This means there can be no shielding of the gravitational fields and there is no such thing as a Faraday cage for gravity. One implication is that you cannot get free particles, so the next alternative is to use free fall particles, which was attempted in Eq. 1.2.

As previously mentioned, the fields display $1/r^2$ behavior to a very good approximation. A glance at Eq. 1.4 indicates that a measurement of the magnetic field power law behavior around Jupiter would allow one to put a limit on photon mass. The present limit is 10^{-15} eV due to precisely such a measurement. Similar measurements of gravitational fields power law behavior lead one to put a limit on the gravitino mass of less than 10^{-26} eV. In what follows, we will rigorously assume that the gravitino mass is zero, the gravitational coupling constant is a fundamental constant, and that the source of gravity is proportional to the energy-momentum mass tensor. This implies that gravity is described by a second rank tensor field.

Before explaining the Equivalence Principle, this first introductory Section will end with a comment on a proposed possible Fermilab experiment to study the tensorial rank of gravity. The kinematic definitions for studying the energy transfer in a collision are shown in Fig. 1.3. In the non-relativistic case, the short range power law nature of the force leads you to a transverse momentum impulse which is the force times the time over which the force acts. The force is the potential at the point of closest approach, divided by the impact parameter b . The time of interaction is just b divided by the velocity of the incoming particle. In the case of the electromagnetic interaction, this means that the momentum impulse just goes as $1/b$.

$$\begin{aligned} \Delta p_{\perp} &\sim f(b)\Delta t \sim \frac{V(b)}{v}, \quad \Delta t \sim b/v \\ (\Delta p_{\perp})_{EM} &\sim q^2/(bv) \rightarrow q^2/bc. \end{aligned} \tag{1.12}$$

In the ultra-relativistic case for electromagnetism, special relativity reveals that the fields become stronger by a factor γ , but the time dilation effect means that the time over which those fields act decreases as $1/\gamma$. Vector fields (fields caused by the spin one photon) have a transverse momentum impulse which is independent of γ . This is a very well known phenomenon in experimental particle physics because it leads (in a Coulomb collision) to a constant dE/dx for relativistic particles, or to the concept of a minimum ionizing particle, which is familiar to us all.

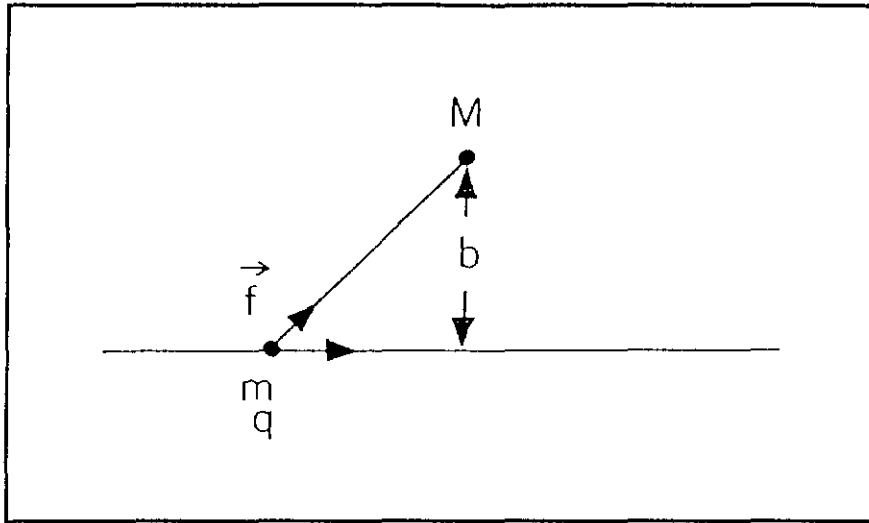


Fig. 1.3: Kinematic definitions for energy transfer in a collision.

In the case of a gravity field, the force is proportional to the square of the masses. Since mass is proportional to energy, and energy transforms with one power of γ , it is easy to see that the second rank field has a force which rises as γ^2 in the ultra-relativistic case. The time, due to time dilation, falls as $1/\gamma$ as in the electromagnetic case, meaning that there is a transverse momentum impulse, which increases as γ . This is another evidence of divergent processes. For mnemonic purposes, instead of the transverse momentum impulse, we quote a change in velocity which increases as γ and is proportional to the dimensionless quantity Φ/c^2 . Note that for an inverse square law $ar=\Phi$, which relates our 2 dimensionless quantities ar/c^2 and Φ/c^2 . The gravitational impulse increases as γ , due to the spin two nature of the graviton field, in contrast to the constant value of transverse momentum impulse with which we are familiar from electromagnetism, a vector field. Unfortunately, even utilizing the γ factor inherent in the Tevatron accelerated beam, and all current technologically feasible noise reduction techniques, this experiment appears, at present, to be impossible.

$$\begin{aligned}
(\Delta p_{\perp})_G &\equiv Mc\Delta\beta \\
\Delta\beta &\sim \frac{Gm\gamma}{bc^2} = \frac{\gamma\Phi(b)}{c^2}.
\end{aligned}
\tag{1.13}$$

This first introductory Section has been a catch-all of topics preparing the stage by reviewing Newtonian physics and special relativity with sidelines into the unexplained equivalence of gravitational and inertial mass, the dimensional nature of the gravitational coupling constant, and its associated high energy divergences. In later Sections, we will gather this material together and start to derive the metrical interval between events appropriate to other gravitational situations.

2 THE EQUIVALENCE PRINCIPLE; RED SHIFT

We now assume the equivalence of inertial and gravitational mass in light of the experimental data shown in Table 1.1. A consequence of this fact is that a uniform gravity field is equivalent to an inertial frame under constant acceleration for mechanical measurements. The Equivalence Principle states that it is equivalent for all possible physical measurements. An inertial frame, where one can apply special relativity, is equivalent to a free fall system in a uniform gravity field. This means we can "wipe out" gravity by going to a free fall coordinate system. The situation is schematically shown in Fig. 2.1a. It is important to realize that any free fall frame is by definition only local in space and time. In special relativity, an inertial frame has infinite spatial and temporal extent. A free fall laboratory, however, needs to be local because any real gravity field is not uniform.

A nonuniform field causes tidal forces as seen in Section 1. This means particles initially at rest will either draw together or apart in time, as shown in Fig. 2.1b. Figure 2.1b is a very good representation of the effect of tidal forces. Tidal forces imply that gravity is equivalent to acceleration only at a single space-time point. We can only use a local inertial frame due to the nonuniform nature of the field which is embodied in the tidal fields.

The Equivalence Principle seems like an extremely innocuous assertion, but it will imply that gravity affects time. In a completely analogous manner, velocity affects time in special relativity. In order to derive the relationship between the gravity field and clock time, consider the situation shown in Fig. 2.1c. On the left hand side, there is a rocket in free space. An observer in that rocket does not see a Doppler shift because he is in free space. By comparison, an observer on the right, observer A, in an equivalent free fall lab, also does not see a Doppler shift. Observer B is instantaneously at rest with respect to A when the light is emitted. Observer B, therefore, has a relative velocity β , when the light is received, and being at rest in the gravity field, moves into the light, relative to observer A. Observer B, therefore, sees a blue shift as shown below.

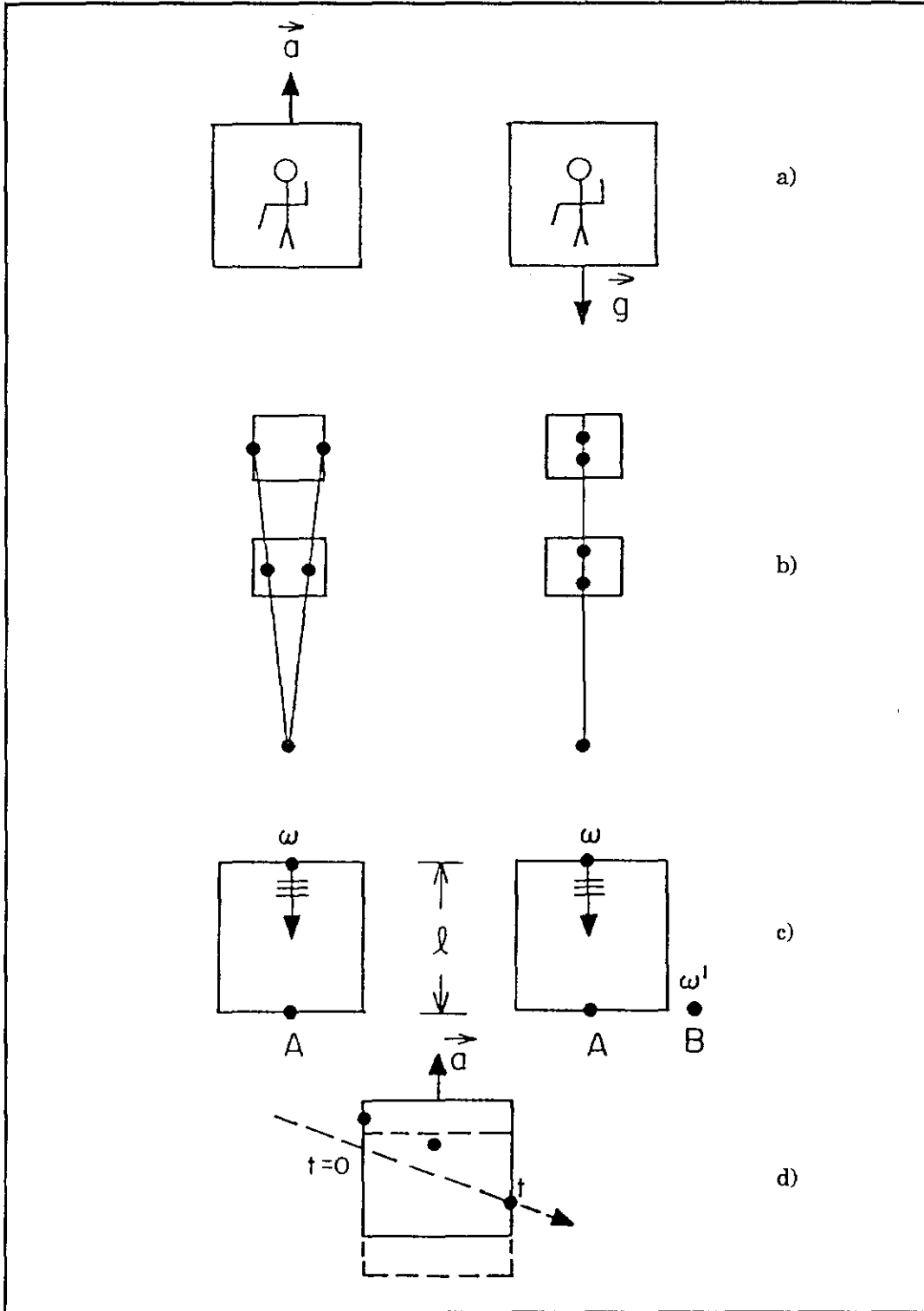


Fig. 2.1: Equivalence Principle figures. a) Equivalent situations b) Local inertial frames c) Red shift d) Light deflection.

$$\begin{aligned}
\omega' &= \omega(1 + \beta) \\
&\sim \omega(1 + gl/c^2) \\
\Delta\omega / \omega &\sim -\Phi/c^2.
\end{aligned}
\tag{2.1}$$

The classical Doppler shift and the Newtonian expression for the relative velocity under constant acceleration is used here. This can be generalized to the case of nonuniform fields. Keeping in mind that this generalization has not been properly motivated. The fractional frequency shift is proportional to the dimensionless ratio Φ/c^2 as seen in Eq. 2.1.. This is a ratio that will be continuously seen. It is the ratio of the gravitational potential energy to the rest energy which, in Newtonian physics, is obviously a small quantity.

Now, what of the frequency? Atomic clocks can be thought of as a standard used to define clock ticks. Frequency is the inverse spacing of clock ticks which means time (or clocks) runs slowly in a gravity well. Extending the situation to nonuniform fields, this can be written as a modified interval between two space-time events.

$$(ds^2)_{RED} \equiv (cdt)^2 \left(1 + \frac{2\Phi}{c^2} \right) - (d\vec{x})^2.
\tag{2.2}$$

Obviously, if the potential goes to zero, then the red shift interval in Eq. 2.2 reduces to the free particle relativistic interval given in Eq. 1.11. In the expression for the red shift interval, t refers to proper time on a clock at rest in a field free region, i.e., far away from all masses. The term ds refers to the proper time on a clock at rest in a field Φ (for small values of the dimensionless quantity Φ/c^2), therefore, using Eq. 2.2, the result given in Eq. 2.1 is recovered. This prediction is so astounding that caution must be taken to experimentally verify it. In Table 2.1, a collection of some of the data is given. The early data comes from observing the red shift due to photons fighting their way out of the gravity well of white dwarfs. The expected frequency shift is given below.

$$\frac{\Delta\Phi}{c^2} \cong GM / Rc^2. \quad (2.3)$$

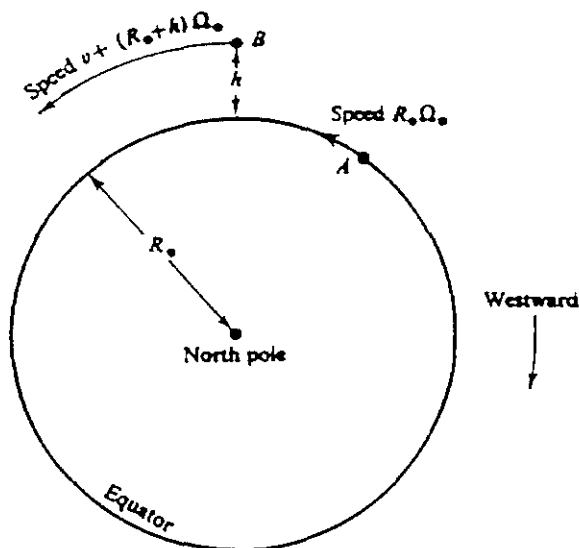
The fractional frequency shift for white dwarfs such as Sirius is roughly 3×10^{-4} . By comparison, less compact sources, such as the sun, have frequency shifts of 10^{-6} . In addition, there are complications, such as convection currents and Doppler shifts caused by proper motion in the sun's atmosphere which set a limit on observational accuracy of a few percent of the shift. Finally, there are measurements made on the Earth which were done in the 1960's. In this case, one is looking at the frequency shift of the 14.4 KeV γ from Fe^{57} falling (at Princeton) 23 meters. Calculations show that the fractional frequency shift is 2×10^{-15} . This is a very precise experiment using Mössbauer technology. These are all very small effects, because they are characterized by the dimensionless ratio of the gravitational potential energy to the rest energy. Nevertheless, these frequency shifts experimentally test the fact that time depends on where you are to a few percent in a gravity field.

Finally, there has been a direct test - one simply picks up a Cesium beam clock, goes to some altitude, waits, and then returns to compare to a Cesium clock at rest on the Earth's surface. This is an absolute direct measurement of the gravitational time dilation or, if you wish, the gravitational twin paradox. Details of this measurement are shown in Table 2.1b. Since the Earth is rotating and because the clocks were on an airplane moving with some velocity, there are also special relativistic time dilation effects. One thing to note now (the reason will be explained later), is that all the special relativistic corrections are of the same order of magnitude as the gravitational effects. Therefore, they must be taken care of carefully. To get an idea of the order of magnitude of the numbers, the acceleration due to gravity on the Earth's surface is 10 m/sec^2 . If one flies at 30,000 feet, or roughly 10,000 meters, $\Delta\Phi/c^2$ is roughly 10^{-12} , and the fractional time lost is just that. If one flies at 500 mph around the Earth for 25,000 miles, (a 50 hour flight), the time shift is predicted to be roughly 200 nsec. Table 2.1b shows that this is indeed the correct order of magnitude.

TIME DILATION EXPERIMENTS

| Experimenter(s) | Year | Method | $\Delta v_{ex} / \Delta v_{th}$ |
|--------------------|-----------|-------------------------------------|---------------------------------|
| Adams, Moore | 1925,1928 | redshift of H lines on Sirius B | 0.2 to 0.5 |
| Popper | 1954 | redshift of H lines on 40 Eridani B | 1.2 \pm 0.3 |
| Pound and Rebka | 1960 | redshift of γ -rays on Earth | 1.05 \pm 0.10 |
| Brault | 1962 | redshift of Na lines on sun | 1.0 \pm 0.05 |
| Pound and Snider | 1964 | redshift of γ -rays on Earth | 1.00 \pm 0.01 |
| Greenstein et al. | 1971 | redshift of H lines on Sirius B | 1.07 \pm 0.2 |
| Snider | 1971 | redshift of K lines on sun | 1.01 \pm 0.06 |
| Hafele and Keating | 1972 | time gain of cesium-beam clocks | 0.9 \pm 0.2 |

Table 2.1a: Redshift Tests.



| Direction of circumnavigation | $\tau_B - \tau_A$ (nanoseconds) | |
|-------------------------------|---------------------------------|--------------|
| | Experiment | Theory |
| Westward | 273 \pm 7 | 275 \pm 21 |
| Eastward | -59 \pm 10 | -40 \pm 23 |

Table 2.1b: Details of Direct Clock Tests.

In addition to the time dilation effect, the Equivalence Principle, properly interpreted, leads to Newton's laws. They come for free, given the interval shown in Eq. 2.2. To investigate, first look at the free particle Lagrangian and the interval for special relativity which are given in Eqs. 1.10 and 1.11. As recalled from Appendix A, this Lagrangian implies that the 4 dimensional momentum is constant, the 4 dimensional acceleration is zero, and a free particle moves in a straight line in space-time (the path of maximal proper time).

$$\begin{aligned}
\mathfrak{L}_{SR} &= \left((ct)^2 - (\vec{x})^2 \right)^{\cdot} \equiv \frac{d}{ds} \\
\frac{\partial \mathfrak{L}_{SR}}{\partial (ct)} &= 2(ct) = \text{const} = \sqrt{E} \\
\frac{\partial \mathfrak{L}_{SR}}{\partial (\dot{x})} &= -2\dot{x} = \text{const}.
\end{aligned} \tag{2.4}$$

Throughout this note, except where stated otherwise, the dot over a quantity means a derivative with respect to proper time. We find that, given the interval appropriate to special relativity, the acceleration (the 2nd proper time derivative of the position) is zero for a free particle.

In the case of a gravity field, the same Euler-Lagrange formulation is used. The effect of gravity on clock rates for clocks immersed in such a field must be monitored. The resulting Euler-Lagrange equations are given below in Eq. 2.5. The time coordinate equation implies a constant energy for static fields, while the position coordinate equations give an acceleration related to the gradient of the reduced potential.

$$\begin{aligned}
\mathfrak{L}_{RED} &\equiv (ct)^2 \left(1 + \frac{2\Phi}{c^2} \right) - (\vec{x})^2 \\
\frac{\partial \mathfrak{L}_{RED}}{\partial (ct)} &= 2(ct) \left(1 + \frac{2\Phi}{c^2} \right) = \text{const} = \sqrt{E} \\
\frac{d}{ds} \left(\frac{\partial \mathfrak{L}_{RED}}{\partial (\dot{x})} \right) &= -2\ddot{x} = (ct)^2 \left(2 \overrightarrow{\nabla \Phi} / c^2 \right).
\end{aligned} \tag{2.5}$$

By direct substitution, the interval has a kinematic piece which is the special relativistic time dilation factor, $\gamma = 1/\sqrt{1-\beta^2}$, and a dynamic piece which is the clock rate shift in a gravity field. As we discussed, the dimensionless dynamic quantity should be very small (weak fields). β is also very small, which means that ds is roughly cdt , or $ci = 1$. Therefore, we get back Newton's laws as the weak field approximation to the Equivalence Principle Lagrangian.

$$\begin{aligned}
 \vec{x} &= (i)^2 \left(-\vec{\nabla}\Phi \right) \\
 ds_{RED}^2 &\sim (cdt)^2 \left(1 + \frac{2\Phi}{c^2} - \vec{\beta}^2 \right) \\
 &\sim (cdt)^2 \\
 \vec{a} &\equiv \frac{d^2\vec{x}}{dt^2} \equiv -\vec{\nabla}\Phi.
 \end{aligned} \tag{2.6}$$

This means that we have the right weak field limit. Newtonian mechanics is the weak field limit of the Lagrangian. Our task is, henceforth merely to find the appropriate form of the metric. The dynamics will then follow from the standard machinery (Euler-Lagrange equations) of classical mechanics. No geodesic equations are needed. The geodesic equations are simply the Euler-Lagrange equations in the case when the Hamiltonian is the interval. The extremal action of special relativity is then the geodesic.

As an aside, there are some interesting implications of the Equivalence Principle derivation. As recalled in classical mechanics, energy conservation was found to arise from the fact that one had time translation invariance in the Hamiltonian. In special relativity, there is an inertial frame of infinite extent, which implies that energy and momentum conservation are due to space-time translational invariance. It has already been argued that in general relativity only local inertial frames can be used, which means there are no flat space frames. Thus, there is no translational invariance in general and, therefore, globally, there is no energy conservation. This is a generally true statement. Point solutions whose field falls off yielding a space-time which is asymptotically flat will be specifically dealt with. In this case, a globally conserved energy can be

defined. It is, however, important to remember that this is not true in general, and cannot be true by the very nature of general relativity. It is equally important to remember that, locally, there will be energy conservation. The experiments done at Fermilab measuring the kinematics of particle production and invoking momentum and energy conservation are still valid because they are done over cosmologically local distances.

It is also reasonably clear that light will be deflected in a gravity field. This will not be discussed in detail now because the prediction is not correct at this level of our exploration into the theory. It is easy to recognize that it must happen because of the postulated equivalence between inertia and gravity. Because light has energy, it has inertial mass (gravitational mass) meaning that it must be attracted or bent in a gravity field. A simple Equivalence Principle geometric construction showing this effect is given in Fig. 2.1d. To an observer in an inertial frame the light must be straight, however, in an accelerated laboratory, the lab moves in the time, t , that it takes the light beam to transit the laboratory. Thus, an observer in that lab will see light go in a curved path as indicated by the small circles in the figure. By the Equivalence Principle, an observer at rest in a gravity well will see light deflect and as discussed in Section 1, the null interval light cone surfaces define the causal boundaries of space-time. Because gravity influences the trajectory of light, it must also, therefore, define the causal structure of space-time. In a gravity well, it will be expected that the simple notion of a light cone of infinite extent will suffer some modification.

As a final topic, it is amusing to look at the Equivalence Principle in non-relativistic quantum mechanics. One can start with the Schrödinger equation for a free particle, which is the analogue of working in an inertial frame. The Schrödinger equation is a statement that the kinetic energy (with no potential) is equal to the total energy. One then makes the quantum mechanical replacements of energy-momentum with differential operators - spatial and temporal. This replacement leads to the Schrödinger equation.

$$\begin{aligned}
(p^2 / 2m)\psi &= \epsilon\psi \\
p_\mu &= -i\hbar\partial_\mu \\
\frac{\hbar^2}{2m}\nabla^2\psi &= i\hbar\partial\psi / \partial t.
\end{aligned}
\tag{2.7}$$

This equation is valid in a local inertial frame. Let us transform to an accelerated frame and determine if the result is equivalent to the Schrödinger equation in a gravity well. The Galilean transformation to an accelerated frame, which is appropriate in the non-relativistic case, leads to the following equation.

$$\begin{aligned}
Z' &= Z + at^2 / 2, \quad t' = t \\
\frac{\hbar^2}{2m}(\nabla')^2\psi &= i\hbar\left[\partial\psi / \partial t' + at' \frac{\partial\psi}{\partial Z'}\right].
\end{aligned}
\tag{2.8}$$

This is fairly ugly and not very transparent. We use the freedom to redefine the overall wave function phase in quantum mechanics. It is known that it is permissible at a single space-time point, because we are dealing with a local inertial frame. We also know that the overall phase is not an observable in quantum mechanics. We then make the transformation;

$$\begin{aligned}
\psi &= \psi' e^{i\phi}, \quad \phi = mat'Z' / \hbar - ma^2(t')^3 / 6\hbar \\
\frac{\hbar^2}{2m}(\nabla')^2\psi' + (maZ')\psi' &= i\hbar\partial\psi' / \partial t'.
\end{aligned}
\tag{2.9}$$

Having done that, we find that the Equivalence Principle indeed works in non-relativistic quantum mechanics. What remains is the Schrödinger equation for a particle in a gravity field defined by the acceleration a .

It is true that the Equivalence Principle works in quantum mechanics, but, quantum effects of gravity have been measured by looking at neutron interferometry using very cold neutrons. The neutron beam is split and subsequently, the beams suffer a phase change by passing through

different potentials, one part of the beam going up, one part going down. This phase change, upon recombination, leads to interference effects. The scale of those interference effects is shown below.

$$\begin{aligned} \psi &\sim e^{ikz}, \quad k = 2\pi/\lambda \\ \frac{\hbar^2}{2m}(k + \delta k)^2 + m(\Phi + \delta\Phi) &= \hbar\omega \\ \delta k &\sim 1/k \left(\frac{1}{\lambda}\right)^2 \delta(\Phi/c^2), \quad \lambda \equiv \hbar/mc. \end{aligned} \tag{2.10}$$

The effect depends on our old friend, $\Delta\Phi/c^2$. In Eq. 2.10, the Schrödinger equation given in Eq. 2.9 has been solved. In the static case ω is constant, and the change in gravitational potential merely leads to a change in the wave number k , and not the frequency.

The Equivalence Principle has thus given the first test of general relativity which is the gravitational red shift. Time depends on where you are in a gravity field. The Equivalence Principle implies quantum mechanical tests. The weak field limit of the implied dynamics is Newton's laws.

3 LINEARIZED GRAVITATION; LIGHT DEFLECTION

In this Section, a discussion follows of what would happen if special relativity is applied to Newtonian gravity and if one simply wrote a wave equation in complete analogy to the electromagnetic case. This is precisely what anyone except Einstein would have done and, thus, leads to a linearized approximation. The equivalence of inertial and gravitational mass means that, since the field itself contains energy, it also has mass, therefore, gravity gravitates. Gravity is thus another non-Abelian field. Gluons are colored, gauge bosons have weak charge, and gravity gravitates. This leads to non-linear field equations which means we cannot superimpose solutions as we can for electromagnetism. The fact that photons have no charge means that the electromagnetic theory is linear leading to the superposition principle.

In this Section, nonlinearity will be ignored and we will begin by trying to write a linear generalization of the Laplace equation relating the gravitational potential to the mass density. As recalled from Appendix A, mass density is related to the 4-4 component of the energy momentum tensor. Therefore, the source is related to a second rank tensor and the Laplacian is the space component of the d'Alembertian. If we are dealing with low velocities, ct is much greater than x , and the d'Alembertian approaches the Laplacian in the non-relativistic limit. Thus, the left hand side of the equation can be written as a wave equation.

$$\begin{aligned}\nabla^2\Phi &= 4\pi G\sigma \\ \partial_\lambda\partial^\lambda\Phi &\equiv \frac{-4\pi G}{c^2}T^{44}.\end{aligned}\tag{3.1}$$

Given the non-relativistic limit, we will now simply assume a tensor field with a coupling constant κ and a gauge condition as shown below.

$$\begin{aligned}(\partial_\lambda\partial^\lambda)\phi^{\mu\nu} &= -\kappa T^{\mu\nu} \\ \partial_\mu\phi^{\mu\nu} &= 0.\end{aligned}\tag{3.2}$$

The nature of the wave equation form assures that there are zero mass gravitons... An assumption that the 4-4 piece of the field tensor is proportional to the Newtonian reduced potential Φ is made. In constructing the Lagrangian, which determines the interaction of this field with matter, the free particle Lagrangian is used and we construct an interaction piece. Fundamentally, the only tensors available for the interaction term are the field tensor itself and the tensor made up as the direct product of the 4 velocity. The symbol ϕ is the trace of $\phi^{\mu\nu}$.

$$\begin{aligned}\mathfrak{L} &= \left[g_{\mu\nu}^0 + \kappa \left(\phi_{\mu\nu} - \frac{g_{\mu\nu}^0}{2} \phi \right) \right] U^\mu U^\nu \\ &= \mathfrak{L}_{FREE} + \mathfrak{L}_{INT}.\end{aligned}\tag{3.3}$$

This construction is made in direct analogy to the electromagnetic case, which is given in Appendix C. The coupling constant by appeal to the non-relativistic weak field limit of this Lagrangian can be evaluated. First, we assume that only the 4-4 component of the field tensor is important. The Euler-Lagrange equations then become Newton's laws as we know, giving a relationship between the 4-4 component of the field tensor and the reduced Newtonian potential.

$$\begin{aligned}\mathfrak{L} &\sim \left[(ci)^2 \left(1 + \frac{\kappa\phi_{44}}{2} \right) - (\vec{x})^2 \left(1 - \frac{\kappa\phi_{44}}{2} \right) \right] \\ \frac{\partial \mathfrak{L}}{\partial \dot{x}} &\sim 2\dot{x}, \quad \frac{\partial \mathfrak{L}}{\partial x} \sim (ci)^2 \frac{\kappa}{2} \left(\vec{\nabla} \phi_{44} \right) \\ \therefore \ddot{x} &\sim \frac{-\kappa}{4} \left(\vec{\nabla} \phi_{44} \right) \\ \ddot{a} &\equiv d^2 \vec{x} / dt^2 \equiv \frac{-\kappa c^2}{4} \vec{\nabla} \phi_{44} \sim -\vec{\nabla} \Phi.\end{aligned}\tag{3.4}$$

The field equations given in Eq. 3.2 give us the other piece of the non-relativistic relationship (see Eq. 1.1).

$$\begin{aligned}\nabla^2 \phi^{44} &\equiv -\kappa c^2 \sigma \\ \nabla^2 \Phi &\equiv 4\pi G \sigma.\end{aligned}\tag{3.5}$$

These two relations give enough information to determine the coupling constant κ in terms of Newtonian constant G and the relationship between the Newtonian potential Φ and the 4-4 component of the field tensor ϕ_{44} .

$$\begin{aligned}\Phi &\equiv (\kappa c^2 / 4) \phi_{44} \\ \kappa^2 &\equiv 16\pi G / c^4.\end{aligned}\tag{3.6}$$

Plugging these results back into the Lagrangian given in Eq. 3.3, $(\kappa\phi)/2$ is found to be proportional to the dimensionless ratio $2\Phi/c^2$, and the interval in linearized general relativity is as given below.

$$\begin{aligned}g_{\mu\nu} &= g_{\mu\nu}^0 + \kappa \left(\phi_{\mu\nu} - \frac{g_{\mu\nu}^0}{2} \phi \right) \\ \kappa\phi / 2 &= 2\Phi / c^2 \\ (ds^2)_{LGR} &\equiv (cdt)^2 \left(1 + \frac{2\Phi}{c^2} \right) - (d\vec{x})^2 \left(1 - \frac{2\Phi}{c^2} \right).\end{aligned}\tag{3.7}$$

We find that we have both spatial and temporal curvature. In particular, the temporal curvature is exactly what has been derived via the Equivalence Principle by looking at a red shift metric. In the low velocity weak field limit, the interval given in Eq. 3.7 has a spatial part being proportional to the velocity squared. As such, this interval may be thought of as providing a higher order correction to the red shift interval, which has been derived in Eq. 2.5. It is clear why the discussion of light deflection has been deferred until this point because, by definition, the local velocity of light is always c . Thus, the low velocity limit was not expected to be appropriate.

One can see from Eq. 3.7, why Einstein thought in terms of spatial curvature. Starting with a flat space Minkowski metric, as seen in Eq. 3.7, the presence of a gravity field makes that metric basically unobservable. When the interactions are turned on, the effective metric is not a

Minkowski metric. Therefore, there are two ways of looking at the situation. First, either imagine there is an interacting field on a flat space-time which comes most easily to particle physicists, or, second, imagine that the mass distribution defines the space-time structure and that particles are free to move on local straight lines in this space-time, which is more pleasing to geometrically oriented physicists.

As seen in Appendix C, the formal equations for gravity and electromagnetism are very similar. However, the coupling for electromagnetism is proportional to the charge, whereas the Galilean principle (that all particles fall with the same acceleration) requires a coupling which is proportional to the mass. This means, in the presence of interactions, that one has a Hamiltonian which can be construed to mean a curved space-time having started with a flat space-time. The Galilean coupling is what allows one to make a geometric interpretation of gravity.

Using the expression just constructed, we may now look at light deflection. From the Equivalence Principle in Section 2, we realize we must have light deflection. Now having a valid expression at high velocities, consistent with relativity, we can begin our discussion, first looking at the null-trajectories of light.

$$\begin{aligned}
 (ds^2)_\gamma &= 0 \\
 \frac{d\vec{x}}{dt} &\equiv c(1 + 2\Phi/c^2) \equiv c/n \\
 \beta_\gamma &\equiv (1 + 2\Phi/c^2).
 \end{aligned}
 \tag{3.8}$$

In special relativity, the vanishing of the interval given in Eq. 1.11 insures that light has the velocity c in all inertial frames. Using the expression in Eq. 3.7, a null light trajectory, in linearized general relativity (LGR) has a coordinate velocity which is less than c . One can think of this situation as defining a medium with an index of refraction n which is not homogeneous and which follows the Newtonian potential Φ . Recall that the coordinate time t is the time on a clock at rest outside the gravity field. We can easily see that the velocity, given in Eq. 3.8, is not a local

velocity using local clocks and rulers. We know that in special relativity and in our local inertial free fall frame, by construction, we will always find that light goes at velocity c for a local measurement. What we want to stress here is that this is a non-local measurement using clocks and rulers far from the gravitational field.

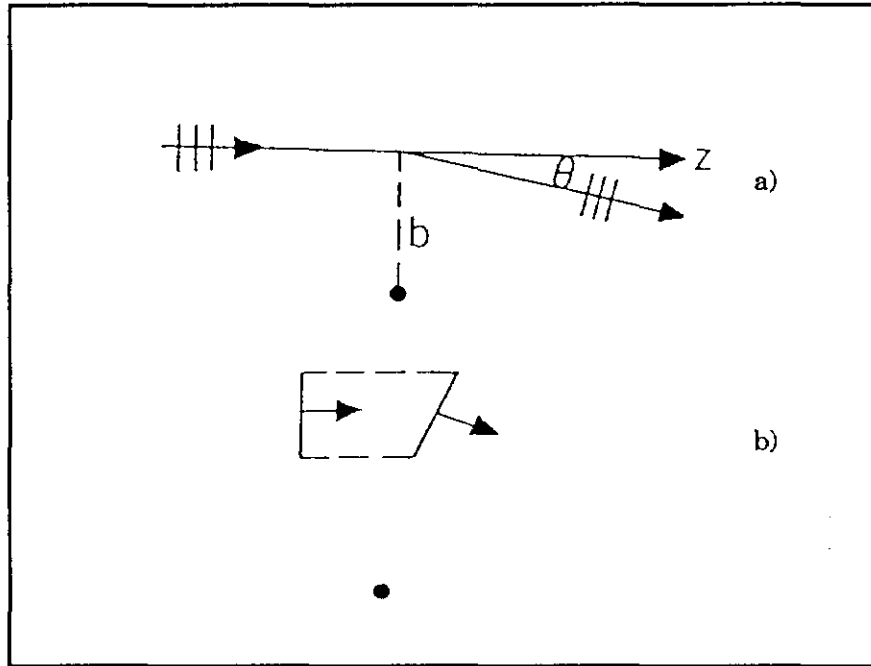


Fig. 3.1: Light Deflection. a) Kinematic definitions
 b) Refraction due to inhomogeneous index of refraction.

The construction for light deflection is shown in Fig. 3.1. Light goes by the sun with impact parameter b and suffers a deflection θ . Given the index of refraction in Eq. 3.8, it is easy to see that the medium defined by that index is inhomogeneous. Thus, a wave near the sun will slow down. The solution is static, so the frequency is constant. Huygen's principle explains that the wave front refracts. The construction for this refraction is shown in Fig. 3.1b. The angle of refraction has to do with the change in index as a function of radius integrated over the travel trajectory.

$$\begin{aligned}
n &\sim 1 + 2GM / c^2 / \sqrt{Z^2 + b^2} \\
d\theta &\sim \frac{\partial n}{\partial b} dZ = \frac{-2GM}{c^2} b dZ / (Z^2 + b^2)^{3/2} \\
\theta &= \int d\theta = \frac{4GM}{bc^2} = 4\Phi(b) / c^2.
\end{aligned}
\tag{3.9}$$

The result of the integration is that the deflection angle is just 4 times our familiar dimensionless ratio Φ/c^2 . Evaluating this expression for the sun, a deflection angle of 8.2 microradians is observed.

$$\begin{aligned}
\theta &= 8.2 \mu\text{rad} = 1.75'' \\
&= 2r_s / b, \quad r_s = 2GM / c^2 \\
(r_s)_\odot &\sim 3.5 \text{ km} \\
(r_s / R)_\odot &\sim 5 \times 10^{-6}.
\end{aligned}
\tag{3.10}$$

It will be extremely useful to define a characteristic length for the gravitational potential in what follows. This length is such that at that length the gravitational potential is comparable to the rest energy. The length for the sun has the value of 3.5 km, therefore, the ratio of that characteristic length to the radius of the sun is 5 parts per million.

Data for light deflection is tabulated in Table 3.1 and the results agree with the prediction to about 1%. Table 3.1 also shows that with time the baseline has increased, resulting in an improved resolution with time. A picture of the radio telescopes that were used is shown in Fig. 3.2. Figure 3.2a depicts the light deflection as a function of impact parameter relative to the sun's radius, while Fig. 3.2b shows the Owen's Valley interferometer. Thinking back to undergraduate physics, you will recall that the resolving power in the diffraction limit is given by the wavelength divided by the baseline. For a 3 cm radio wave with a 3 km baseline, such as in Owen's Valley, a diffraction limit of about 0.2 sec results. Table 3.1 shows that the error is indeed this order of magnitude.

$$\begin{aligned}
d\theta &\sim \lambda / d \\
\lambda = 3 \text{ cm}, d = 3.1 \text{ km}, d\theta &\sim 0.2''.
\end{aligned}
\tag{3.11}$$

| EXPERIMENTAL RESULTS ON THE DEFLECTION OF RADIO WAVES | | | |
|---|-----------------|---------------|---|
| Radio Telescope | Wavelength (cm) | Baseline (km) | θ (sec) |
| Owen's Valley | 3.1 | 1.07 | 1.77 ± 0.20 |
| Goldstone | 12.5 | 21.56 | $1.82 \begin{cases} +0.26 \\ -0.17 \end{cases}$ |
| National RAO | 11.1 and 3.7 | ~ 2 | 1.64 ± 0.10 |
| Mullard RAO | 11.6 and 6.0 | ~ 1 | 1.87 ± 0.30 |
| Cambridge | 6.0 | 4.57 | 1.82 ± 0.14 |
| Westerbork | 6.0 | 1.44 | 1.68 ± 0.09 |
| Haystack and National RAO | 3.7 | 845 | 1.73 ± 0.05 |
| National RAO | 11.1 and 3.7 | 35.6 | 1.78 ± 0.02 |
| Westerbork | 21.2 and 6.0 | ~ 1 | 1.82 ± 0.06 |

Table 3.1: Light deflection measurements.

A few other experimental comments are in order. If one tried to do this experiment on the Earth's surface, for a 1 km path, the light would fall, (deflect) only about 1 Angstrom - which is certainly unobservable. This small hand calculation explains the importance of using observations of the solar deflection of light. This is not as simple as it appears because the sun does not have a hard edge, it is surrounded by plasma and solar corona. Reading basic books on electromagnetism, one remembers that the index of refraction for a plasma is frequency dependent, and is characterized by a plasma frequency, ω_p . Because we are measuring an effective index of refraction, this is something that can get in the way. The plasma frequency depends on the number density of the plasma, the characteristic size of the electrons, and the coupling constant, as one might expect.

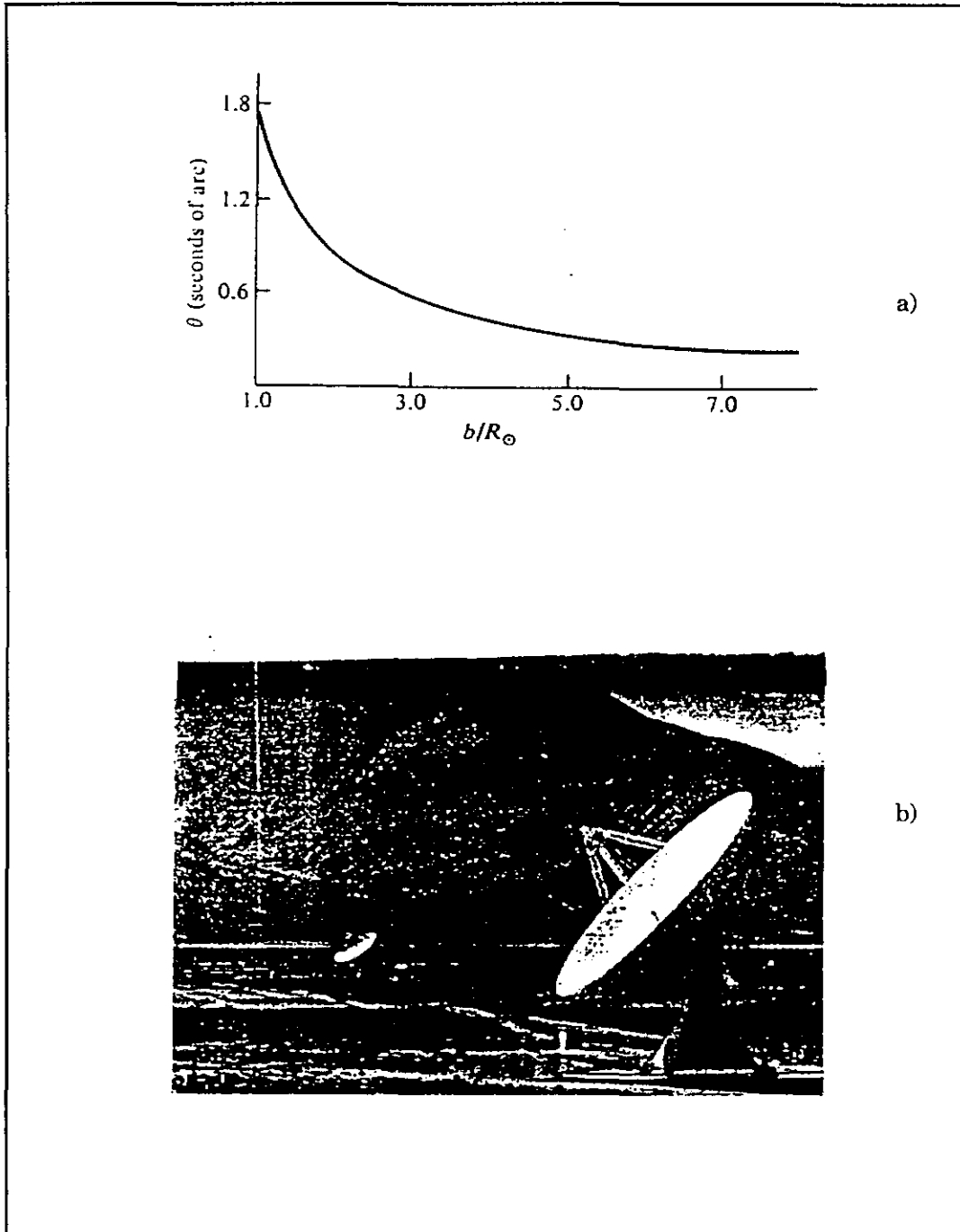


Fig. 3.2: a) Light deflection as a function of b b) Interferometer at Owens Valley.

$$n = \sqrt{1 - \left(\frac{\omega_p}{\omega}\right)^2} \quad (3.12)$$

$$\frac{\omega_p}{c} \sim \sqrt{\rho_e \lambda_e \alpha}.$$

If one takes a number density of 10^{14} electrons per cubic meter, one finds a plasma frequency shift per frequency of 3 times 10^{-7} for 6000 Angstrom light. This is a very small effect, and it is ω dependent, therefore, one is able to make a correction. For 10 cm radio waves, however, the ratio of the plasma frequency to the radio frequency is 10%. This is a major effect since we are looking for a gravitational effect which is parts per million, as stated earlier. The corona density which we took should be compared to 1 atom per cubic Angstrom which, as will be discussed later, is a reasonable density for a solid. This solid density leads to a number density of 10^{30} electrons (atoms) per cubic meter - or Avogadro's number. Therefore, we have assumed a corona which is in fact a very good vacuum - i.e., a density 10^{-16} that of normal matter. This small digression should serve merely to point out that there are systematic effects and systematic uncertainties in these astronomical observations which one must realize.

Finally, instead of dealing with small effects, like parts per million, one can go to astronomical observations and look for the gravitational lense effects of matter in bulk. The resulting split image of a quasi stellar object is shown in Fig. 3.3. The splitting of the images is due to an intervening galaxy which is somewhat fainter. It is easy to show from a generalization of our previous work that the deflection angle in traversing an extended body is a sort of Gauss' law, proportional to the expression given in Eq. 3.9 - where the mass is interpreted as the mass inside of the trajectory.

$$\theta \cong 4GM(b) / bc^2$$

$$M(b) = M \left[1 - \left(\frac{R^2 - b^2}{R^3} \right)^{3/2} \right]. \quad (3.13)$$

The observation of these gravitational lensing effects, giving rise to an even larger number of images - multiple images - is irrefutable macroscopic evidence of the gravitational deflection of light.

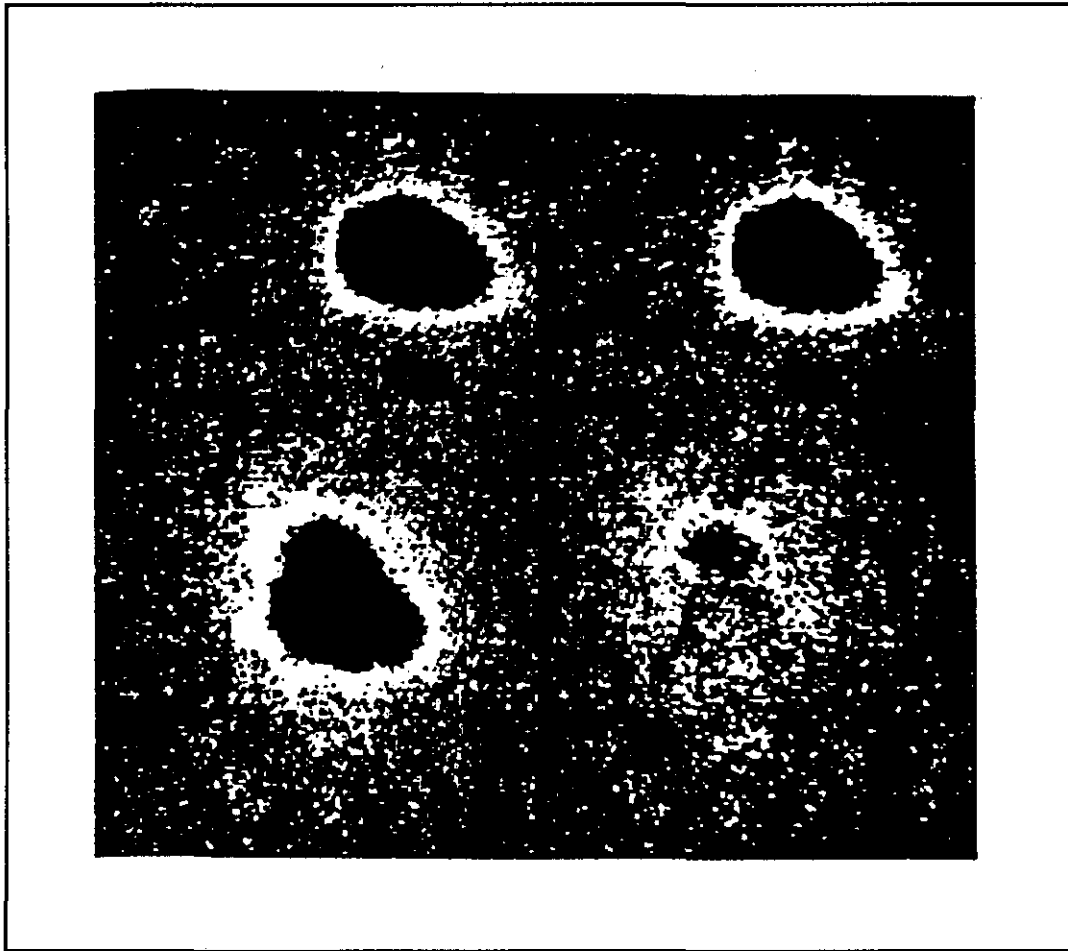


Fig. 3.3: Gravitational Lensing by intervening galaxy splits images of a QSO.
Bottom, one image removed showing intervening galaxy.

4 SCHWARZCHILD SOLUTION; PERIHELION ADVANCE, RADAR RANGING, SINGULARITIES

In order to proceed beyond the point of Green's function solution for linearized general relativity, we need to motivate the derivation of the Schwartzchild metric. To do this, we consider the situation shown in Fig. 4.1. There is an inertial observer with clock t in frame S , and there is a rotating turntable frame S' . The Equivalence Principle tells us that a particle at rest in a gravity field is equivalent to a particle in an accelerated frame. The inertial observer in frame S is able to use special relativity.

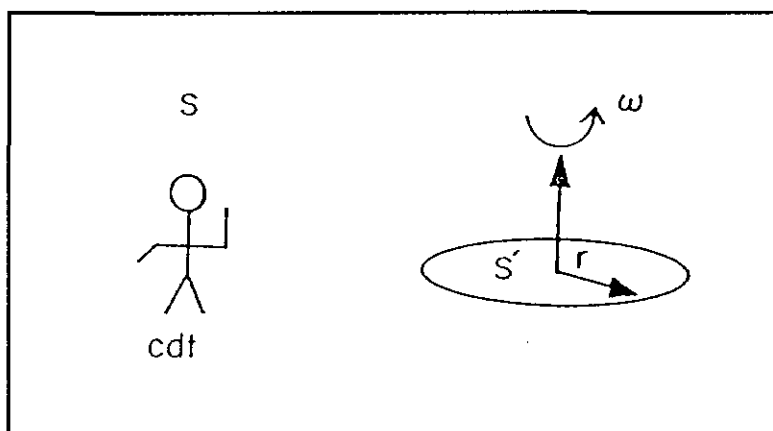


Fig. 4.1: Turntable. Inertial observer in S with accelerated frame S' of a turntable.

There is an effective velocity of a clock at rest in a gravity field with respect to an observer at rest in a flat space - or far from the sources of a gravity field. If we choose to equate the kinetic energy in an inertial frame to the potential energy in a gravity field as a statement of the Equivalence Principle, then we find that the effective velocity squared in the gravity field is $2\Phi/c^2$. This is a familiar factor already seen several times. It underscores the statement that special relativistic effects are the same order of magnitude as general relativistic effects.

$$\begin{aligned}
T_{EP} &\equiv |V| \\
\frac{\beta_{EP}^2}{2} &= -\Phi / c^2.
\end{aligned}
\tag{4.1}$$

By time dilation we have the following relationship between clocks t and s , $ds = (cdt) / \gamma_{EP}$.

So far, all we have succeeded in doing is re-deriving the red shift metric. The reason for using a turntable, is because the acceleration field is inhomogeneous. Since the inertial observer can use special relativity, he can say that there is a length contraction. The observer in frame S will see rulers contracted along the direction of velocity. An observer in frame S' can lay down rulers of length r . He will find a circumference less than $2\pi r$ since the rulers are azimuthally contracted by the kinematic γ factor. So, an observer in S' has two inequivalent definitions of the radius. To pick one, define r to be such that a circle of radius r has circumference $2\pi r$. Radial distance is equal to $(\sqrt{g_{rr}})dr$. By the length contraction hypothesis, g_{rr} is equal to γ_{EP}^2 .

$$\begin{aligned}
(ds)^2 &= (cdt)^2(1 - \beta_{EP}^2) = (cdt)^2 / \gamma_{EP}^2 |d\vec{r} = 0 \\
(dl)^2 &= g_{rr}dr^2 + r^2d\Omega^2 \\
g_{rr} &= \gamma_{EP}^2.
\end{aligned}
\tag{4.2}$$

These arguments allow us to motivate the Schwartzchild metric as being a modified flat space metric whose modifications have to do with time dilation and length contraction. We use an Equivalence Principle argument to state that an object at rest in a gravity field is equivalent to an object in an accelerated frame.

$$\begin{aligned}
(ds)_S^2 &\sim (cdt)^2(1 - \beta_{EP}^2) - \frac{dr^2}{(1 - \beta_{EP}^2)} - r^2d\Omega^2 \\
\beta_{EP}^2 &= -2\Phi / c^2 = 2GM / rc^2 \equiv r_S / r \\
r_S &\equiv 2GM / c^2.
\end{aligned}
\tag{4.3}$$

In Eq. 4.3, we have again defined the Schwartzchild radius. For example, on the Earth, the Schwartzchild radius is 0.9 cm, so the Schwartzchild radius divided by the Earth's radius is about 10^{-9} .

There are various limiting forms for the Schwartzchild metric. If the potential goes to zero, we recover the flat space, special relativistic metric. The meaning of the coordinates are that clocks t refer to clocks at rest as r goes to infinity, while clocks at rest in the gravity field are labeled by the proper time ds . We know that ds is slow, because Φ is less than zero, which means ds is less than dt . The percentage difference is Φ/c^2 , as seen in the red shift Section. The new ingredient is that there is spatial curvature, as there was in the linearized theory, and that it is anisotropic due to the fact that the acceleration field is anisotropic.

We have "derived" the Schwartzchild metric by appealing to special relativity (in the guise of time dilation and length contraction) and the Equivalence Principle. We will now assume that this is the correct solution for space-time around a spherically symmetric mass. Looking at the dynamics, the interval is just proportional to the Lagrangian. The same situation obtains as in classical mechanics, the proper time rate of change of θ is zero. Thus, we have a motion in a plane which, for simplicity, we choose to be the plane defined by the angle $\theta=\pi/2$.

$$\begin{aligned} \mathfrak{L}_S &= \left(1 - \frac{r_S}{r}\right) (ct)^2 - \frac{(\dot{r})^2}{\left(1 - \frac{r_S}{r}\right)} - r^2 d\Omega^2 \\ \dot{\theta} &= 0, \quad \theta = \pi/2 \\ \mathfrak{L}_S &= \left(1 - \frac{r_S}{r}\right) (ct)^2 - \frac{(\dot{r})^2}{\left(1 - \frac{r_S}{r}\right)} - r^2 (\dot{\phi})^2. \end{aligned} \tag{4.4}$$

The Lagrangian in Eq. 4.4 is not a function of time nor of the angle ϕ . Classical mechanics explains that there are then two constants of the motion. One of those constants we define to be J which we will see is proportional to angular momentum. The other constant is the total system energy.

$$\frac{\partial \mathfrak{L}}{\partial \dot{\phi}} = -2r^2 \dot{\phi} = \text{CONST}, \quad J' \equiv r^2 \dot{\phi} \quad (4.5)$$

$$\frac{\partial \mathfrak{L}}{\partial \dot{t}} = 2 \left(1 - \frac{r_s}{r}\right) c^2 \dot{t} = \text{CONST}, \quad \sqrt{\varepsilon} \equiv \left(1 - \frac{r_s}{r}\right) (c\dot{t}).$$

Plugging these two constants of motion back into the Lagrangian, a simple expression for the total energy is found.

$$\begin{aligned} d\mathfrak{H} &= 0 \\ \mathfrak{L} = \mathfrak{H} = I &= \frac{\varepsilon}{\left(1 - \frac{r_s}{r}\right)} - \frac{(\dot{r})^2}{\left(1 - \frac{r_s}{r}\right)} - \frac{(J')^2}{r^2} \\ (\dot{r})^2 + \left[1 + \frac{(J')^2}{r^2}\right] \left(1 - \frac{r_s}{r}\right) &= \varepsilon. \end{aligned} \quad (4.6)$$

This result is a reminder that in an asymptotically flat space, a globally conserved energy can be defined - this is a specific realization. Looking at Eq. 4.6 on the right hand side, we have the total energy, and on the left, we have a term which is obviously the kinetic energy. The remaining terms will be assigned to be the potential in a Schwartzchild space. This effective potential has a term which is the known Newtonian potential, a term which is the centrifugal potential (due to the fact that we have a finite angular momentum) and finally, a third term. These potentials go as $1/r$, $1/r^2$, and $1/r^3$ respectively.

$$\begin{aligned} \frac{2\Phi'_{EFF}}{c^2} &= \frac{-r_s}{r} + \frac{(J')^2}{r^2} - \frac{r_s(J')^2}{r^3} \\ \Phi_{EFF} &= \frac{-GM}{r} - \frac{GMJ^2}{m^2 c^2 r^3} \end{aligned} \quad (4.7)$$

$$J = mr^2 d\phi / dt \sim mr^2 d\phi / d(s/c).$$

We define J to be the Newtonian angular momentum, or $mr^2 d\phi / dt$. We know that at least in the low velocity weak field limit, we can make that $mr^2 c \dot{\phi}$. Therefore, we have the relationship between J' and the Newtonian angular momentum J used in Eq. 4.7.

This problem can now be solved using the machinery of Euler-Lagrange equations, finding the constants of the motion and solving for the orbital parameters just as one does in Newtonian mechanics. A shorter way to arrive at the solution is to realize that, looking at Eq. 4.7, it is a Newtonian problem, but with an extra force which goes like $1/r^4$. Therefore, since the acceleration is the derivative of the potential, the effective force in the Schwartzchild space can be immediately written down.

$$\begin{aligned}
 a &\sim -\partial\Phi_{EFF} / \partial r, \quad J \sim mc\beta r \\
 &\sim \frac{GM}{r^2} \left[1 + \frac{3J^2}{m^2 c^2 r^2} \right] = \frac{GM}{r^2} [1 + 3\beta^2].
 \end{aligned}
 \tag{4.8}$$

In nearly circular orbits, there is a simple relationship between the angular momentum and the velocity. This allows us to express the extra acceleration term as a function of β . It is well known from classical mechanics, that for an inverse square force law the orbits are re-entrant ellipses. Therefore, this extra perturbation causes an orbit that is modified, and the perihelion of the ellipse is not re-entrant. There is a perihelion advance which is proportional to this perturbing term. It is not surprising that the fractional perihelion advance per orbit is just the perturbation term $3\beta^2$.

$$\begin{aligned}
 \frac{\Delta\phi}{2\pi} &\equiv 3\beta^2 = 3r_s / 2r \\
 &= 3\Phi / c^2 = 3GM / bc^2 \\
 &= 43'' / \text{CENTURY FOR MERCURY} \\
 (\beta^2)_{\text{MERCURY}} &\sim (3 \times 10^{-8}).
 \end{aligned}
 \tag{4.9}$$

The prediction for the perihelion advance is given in Eq. 4.9. It is a triumph of this theory that indeed the perihelion advance was an observation made before the theory. General relativity

therefore provides an explanation for the troublesome advance of the perihelion, which had been observed for some time. It is easy to see that the perihelion advance builds up per orbit. Using the numerical data given in Appendix A, the perihelion advance for Mercury can be calculated to be 43" of arc per century. Obviously, since the velocity of the planets decreases with radial distance, the most accurate measurement does indeed come from Mercury. A tabulated set of results for the inner three planets is given in Table 4.1 The data is good to about 1%, although one should realize that the observed perihelion advance is at least 10 times larger due to the perturbing effects of the other planets on Mercury. Classical mechanics results must be under control to very high accuracy before one quotes a 1% agreement between the prediction and the observed perihelion advance.

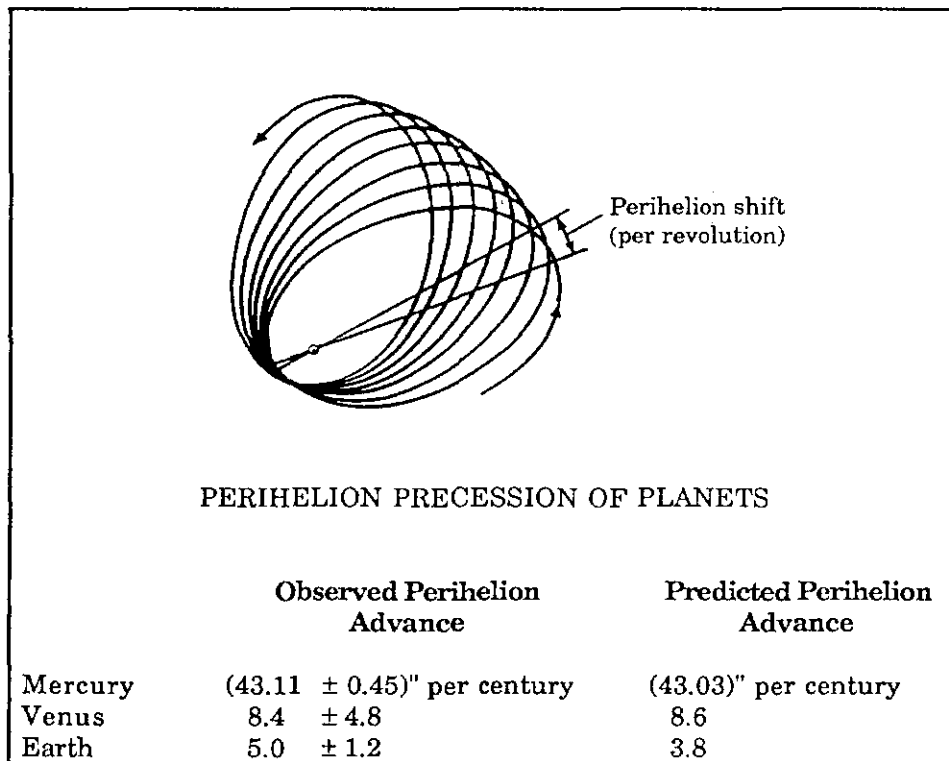


Table 4.1: Perihelion advance measurements.

Just a final word about other possible systematic errors. We have assumed that we have a spherically symmetric source, so we can treat it as a point particle located at the origin. This is not

necessarily the case when the source is the sun. In general, one relates the potential to the sources, as in Eq. 1.1. The integral form of Eq. 1.1 is given in Eq. 4.10.

$$\begin{aligned}\Phi(\vec{x}) &= -G \int \frac{\sigma(\vec{x}') d\vec{x}'}{|\vec{x} - \vec{x}'|} \\ \Phi(r) &\sim -\frac{G}{r} \left[M + Q(3\cos^2\theta - 1)/r^2 \right] \\ Q^{kl} &= \int \left[3(x')^k (x')^l - (r')^2 \delta_i^k \right] \sigma(\vec{x}') d\vec{x}' \\ &\sim MR^2.\end{aligned}\tag{4.10}$$

Expanding the integral solution, we first have the monopole term which is just the mass. The dipole term is zero if we pick the origin of coordinates to be the center of mass, therefore, it cannot have a physical meaning. Finally, the quadrupole moment term leads to a potential which goes as $1/r^3$. Clearly, if the sun possessed a quadrupole moment, the potential would be functionally exactly the same as the effective potential given in Eq. 4.7. The observational limits on the smallness of the sun's quadrupole moment lead to a possible 4" per century² correction to the observation. At present, this is the systematic error which one needs to attach to the measurements of the observed perihelion advance.

An independent test of the Schwartzchild metric comes from radar ranging of either planets or artificial satellites and space probes. The purpose is to send a radar pulse on a round trip. As the pulse nears the sun, one monitors the slowing down effect that has already been seen in the discussions of the linearized theory. The kinematic definitions that we will be using are shown in Fig. 4.2a. Since one is traveling on nearly a radial geodesic and since the Schwartzchild and linearized intervals are radially the same, we will use the effective velocity of light which has been derived in Eq. 3.8. It is then easy to integrate over a travel time ignoring any small deflections. A straight line trip is assumed.

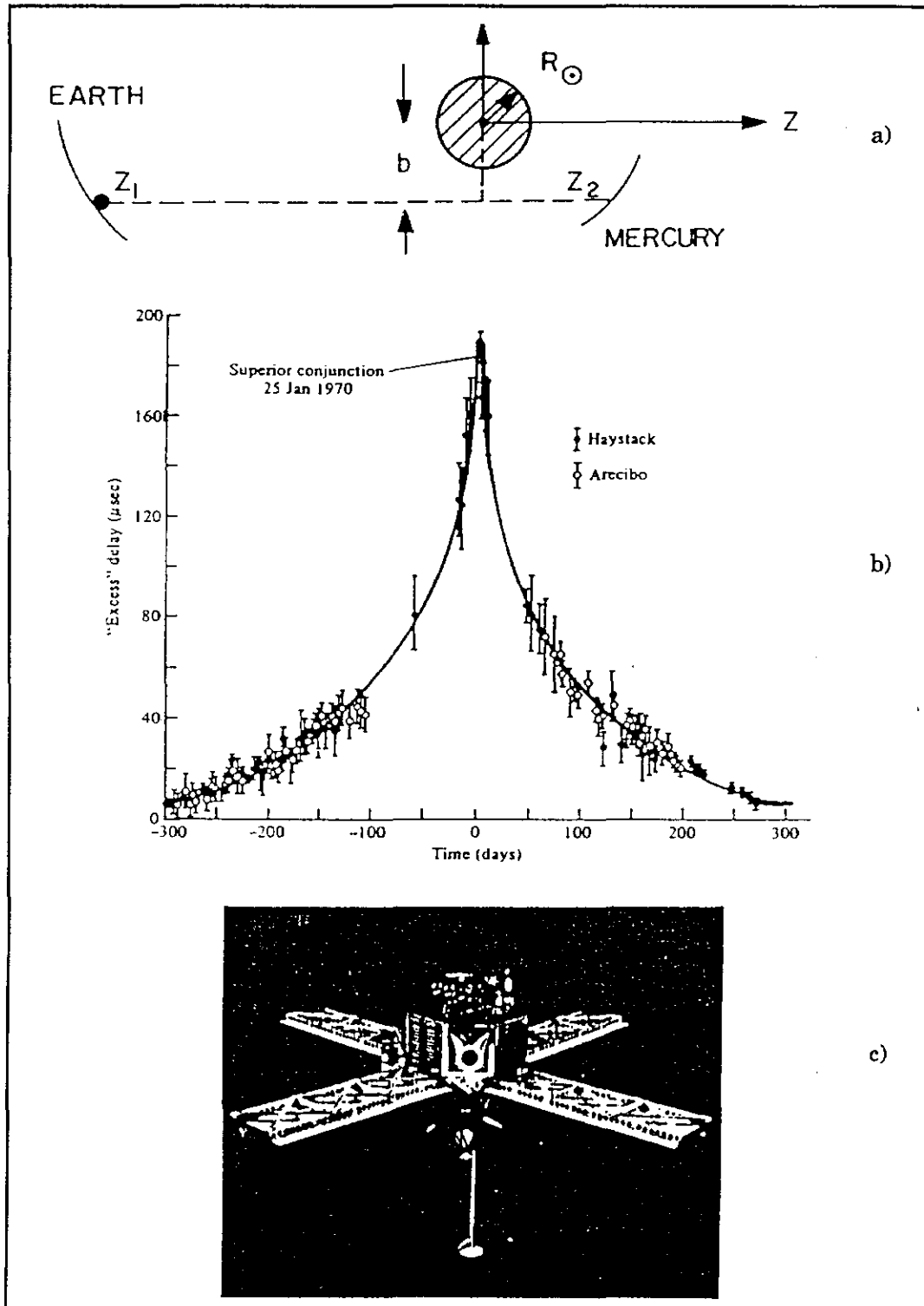


Fig. 4.2: Radar ranging tests. a) Kinematic definition of quantities b) Earth/Venus superior conjunction c) Mariner VI spacecraft as reflector.

$$\begin{aligned}
c\Delta t &\sim \int_{Z_1}^{Z_2} dZ / \beta_\gamma \sim \int_{Z_1}^{Z_2} \left[1 + \frac{r_s}{\sqrt{Z^2 + b^2}} \right] dZ \\
&\sim (Z_2 - Z_1) + r_s \ln \left[\frac{Z_2 + \sqrt{Z_2^2 + b^2}}{Z_1 + \sqrt{Z_1^2 + b^2}} \right].
\end{aligned} \tag{4.11}$$

The excess time or the time beyond what one expects from a flat space is shown below. In particular, the approximation is that the location Z of the transmitting and reflecting objects are much larger than the impact parameter b . One sees that the effect, which is typically of size equal to the Schwartzchild radius, is enhanced by a logarithmic factor. If one calculates the impact parameter equal to the radius of the sun, the time delay corresponding to the Schwartzchild radius is 12 microseconds. The logarithmic factor, however, is of order 10 so the round trip excess delay time is about 200 microseconds, which is equivalent to 70 km.

$$\begin{aligned}
c\delta t &\sim 2r_s \ln \left(\frac{4|Z_1||Z_2|}{b^2} \right) \\
(r_s)_\odot &\sim 3.5 \text{ km} \sim 12 \mu \text{ sec} \\
c\delta t &\sim 220 \mu \text{ sec} \sim 70 \text{ km}.
\end{aligned} \tag{4.12}$$

Figure 4.2b shows data for an Earth-Venus superior conjunction; the maximum excess time delay is indeed 200 microseconds. Table 4.2 shows data that has been taken with both planets and artificial satellites. The level of accuracy is good to about 4 or 5%. As mentioned earlier, some of the limitations arise in using radio waves, in that the plasma frequency relative to the source frequency is not particularly small. Therefore, there is another index of refraction which needs to be under systematic control.

| Dates of observation | Radar telescopes | Reflector | Experimenters and reference | Wave length | (Observed Delay) (Einstein prediction) | Formal standard error | One-sigma error |
|------------------------------|--------------------------------------|-------------------------------|------------------------------------|-------------------|--|-----------------------|-----------------|
| November 1966 to August 1967 | Haystack (MIT) | Venus and Mercury | Shapiro (1968) | 3.8 cm | 0.9 | | ± 0.2 |
| 1967 through 1970 | Haystack (MIT) and Arecibo (Cornell) | Venus and Mercury | Shapiro, Ash, <i>et al.</i> (1971) | 3.8 cm, and 70 cm | 1.015 | ± 0.02 | ± 0.05 |
| October 1969 to January 1971 | Deep Space Network (NASA) | Mariner VI and VII spacecraft | Anderson, <i>et al.</i> (1971) | 14 cm | 1.00 | ± 0.014 | ± 0.04 |

Table 4.2: Radar Ranging Measurements.

As a final topic in this Section, we can observe the apparent singularities seen in Eq. 4.4, when the radius is equal to the Schwartzchild radius. At that radius, the time-dilation becomes infinite and the length contracted rulers go to zero length. The question is, Is this a real physical singularity or does it just appear to be so, because we are in a non-simple frame of reference? To begin looking at the situation, one can try drop testing particles into the “singularity.” The simplest way to do this is to solve the radial Euler-Lagrange equations. Using the energy conservation of Eq. 4.6, we can look at the special case of purely radial motion in which case, $\dot{\phi} = 0, J' = 0$.

$$\begin{aligned}
\dot{\phi} &= 0, \quad J' = 0 \\
(\dot{r})^2 &= \varepsilon - (1 - r_S/r) \\
\varepsilon &= (1 - r_S/r_0) \\
(\dot{r})^2 &= r_S(1/r - 1/r_0).
\end{aligned}
\tag{4.13}$$

There is a simple relationship for the velocity as a function of radius if one drops a test particle starting at rest. One can then integrate that equation from the starting radius to the origin. One finds that the proper time is finite and well behaved. As you recall, the proper time is time on a clock in a freely falling laboratory. Thus, observers falling into this region will see nothing out of

the ordinary. We can, however, use the relationship between clocks and energy as given in Eq.4.5 to look at the situation as seen by observers at infinity using clocks at rest. As seen in Eq. 4.14, clearly, the relative clock rate between observers in free fall labs and observers at infinity suffers a divergence at the Schwartzchild radius.

$$\begin{aligned}
 s &= \int_0^S ds \\
 (s)_{r=0} &= r_0 \left[1 + \frac{\pi}{2} \sqrt{\frac{r_0}{r_S}} \right] \\
 \frac{cdt}{ds} &= \sqrt{1 - \frac{r_S}{r_0}} / (1 - r_S / r) \\
 r_\infty &= r_S, \quad r_\gamma = r_S.
 \end{aligned}
 \tag{4.14}$$

This situation is also shown in Fig. 4.3b. Therefore, as far as observers at infinity are concerned, it takes an infinite amount of time on their clocks in order to approach the Schwartzchild radius. As we have seen for observers themselves, the time is finite and perhaps all too short on a radial geodesic. There is an infinite red shift surface at the Schwartzchild radius which is labeled as r_∞ . This surface occurs where g_{44} vanishes, such that the red shift for observers at infinity becomes infinite.

Using Eq. 3.8, we can also examine the region where the velocity of light goes to zero. This happens at a radius r_γ , which is also equal to the Schwartzchild radius. The region $r < r_\gamma$ is the event horizon. One cannot send signals to the region $r > r_\gamma$, because light signals cannot escape to infinity since their coordinate velocity is zero at r_γ . The causal structure near the Schwartzchild radius is shown in Fig. 4.4. As mentioned earlier, since gravity effects light, we expect modifications to the causal properties of space-time near strong gravitational fields. The light cone at the Schwartzchild radius is tipped over so that the velocity using t clocks is effectively zero. Any object that has a radius less than the Schwartzchild radius must be in a forward light cone and then must intercept $r=0$. As an amusing note, if one works out the Newtonian problem of escape velocity, one finds that it is equal

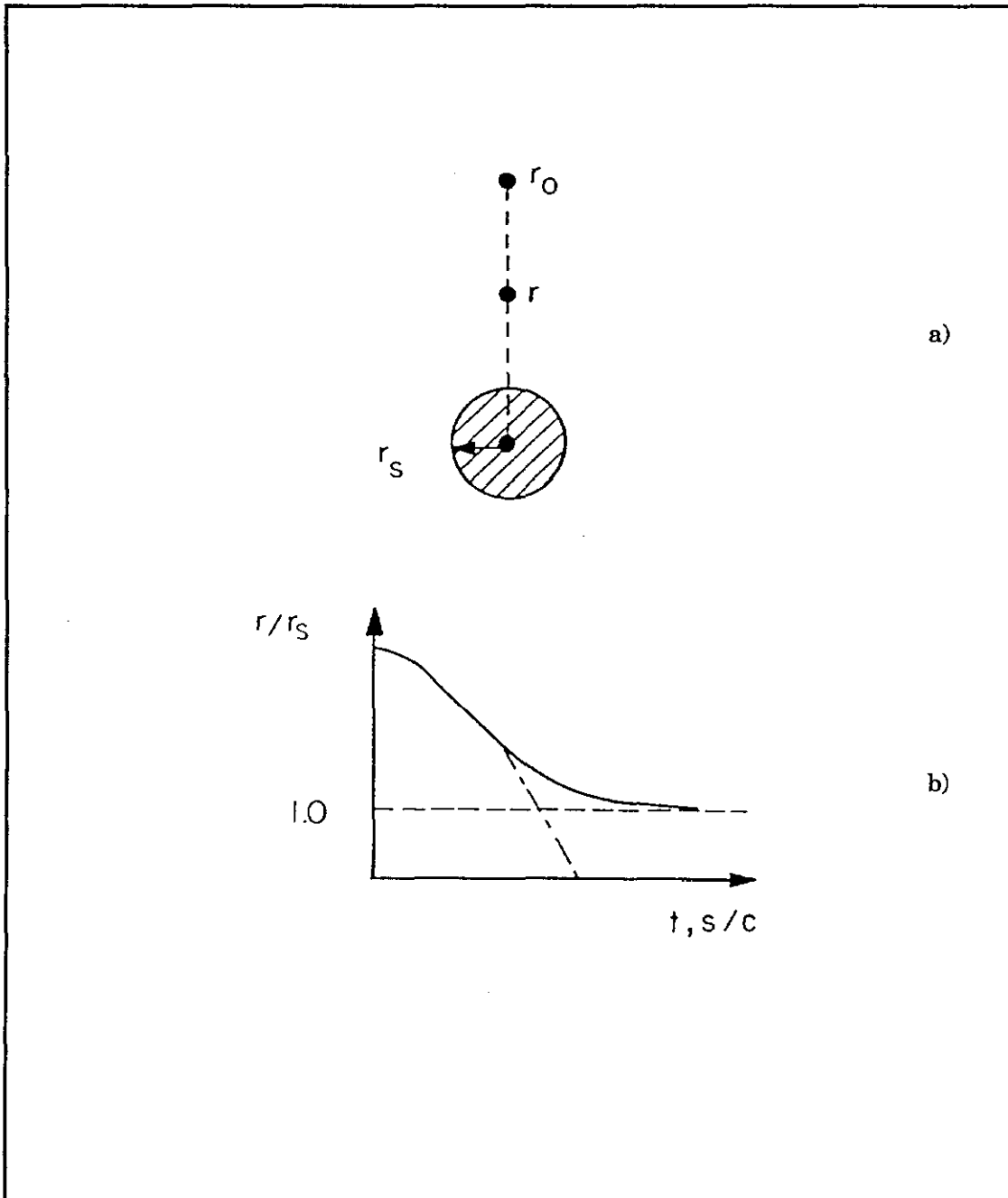


Fig. 4.3: a) Dropping into a black hole. b) Coordinate time (solid line) and proper time (dot-dashed line) near $r=r_s$.

to the velocity of light at the Schwartzchild radius. It is also interesting to note that, in special relativity (flat space) an observer will eventually see all of space-time in the sense that the forward light cone encloses all of space. In the presence of a gravitational field, however, there are horizons or regions of space-time which will never become accessible to an observer.

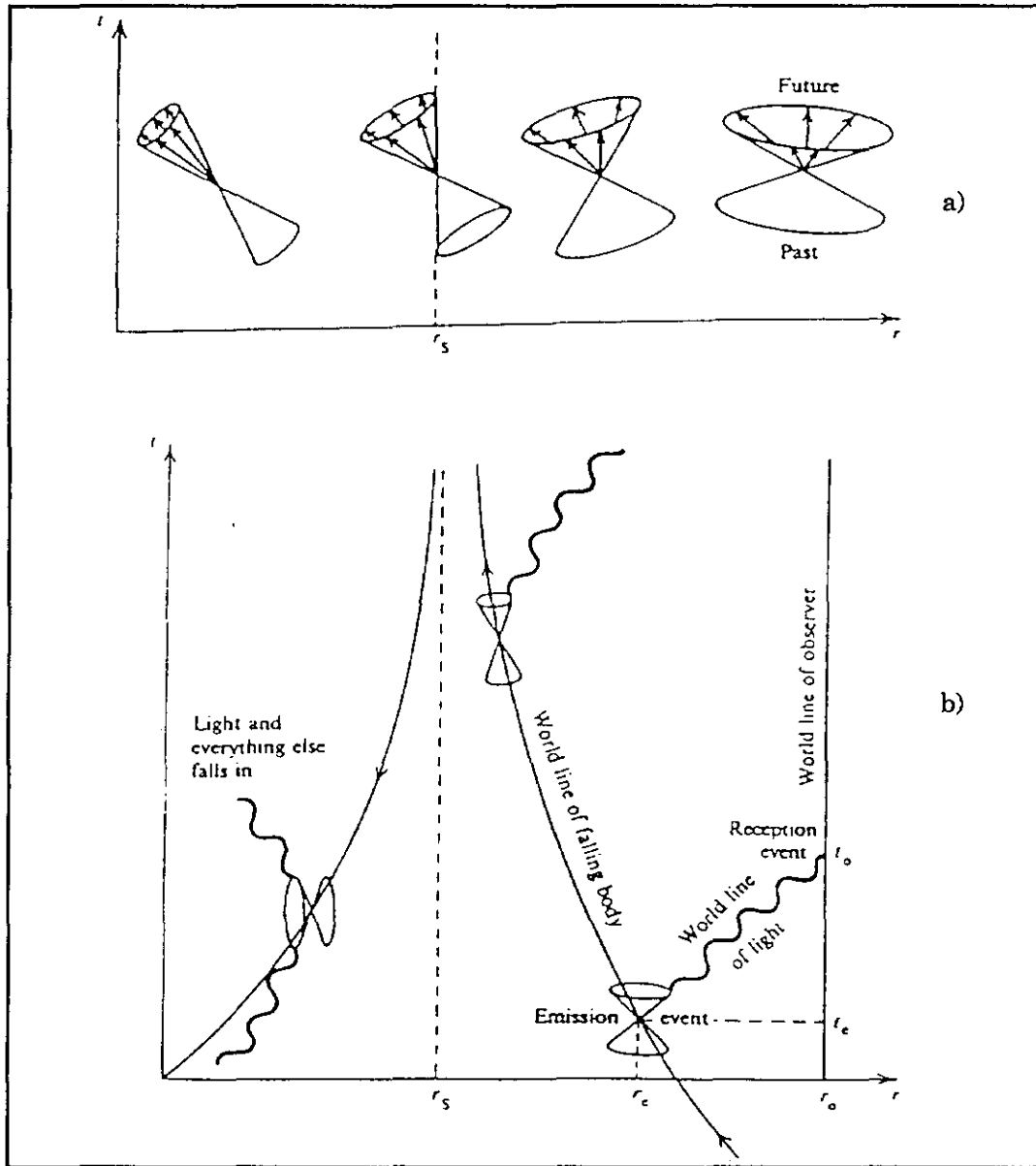


Fig. 4.4: a) Light cones near $r=r_S$ b) World lines near $r=r_S$.

One can use the formula derived for the deviation between geodesics, Eq. 1.2, and the effective potential that was written down in a Schwartzchild space, Eq.4.7, to get an idea of the order of magnitude of the forces that might act on observers falling into such a region. This potential is finite and well behaved at the Schwartzchild radius. In fact, the Newtonian piece - which goes as $1/r$, will be used. As discussed in thinking about the Equivalence Principle, an observer falling into this space-time region will suffer a longitudinal elongation and a lateral compression. If a characteristic longitudinal size l is taken, given the acceleration of a mass element, one can easily derive the stress or pressure which is the force per unit area integrated over the entire area of the object. For r near r_S ;

$$\begin{aligned} \frac{\partial^2 \Phi'_{EFF}}{\partial x \partial x} &\sim (r_S / r^3) c^2 \\ P &\sim \frac{r_S}{r^3} \sigma (lc)^2. \end{aligned} \quad (4.15)$$

As an example, a person might have a mass of 75 kg, a length of 1.8 meters, a density of 1 gm/cm^3 , i.e., water. For the Schwartzchild radius we pick a value of order the sun's Schwartzchild radius, 3.5 km. There would then be a pressure at the Schwartzchild radius of 10 million atmospheres. This is the tidal pressure which is trying to rip the person apart. To set the scale, 1 atmosphere is 10 meters of water. The deepest type of deep sea dive takes place under pressures of 1000 atmospheres. Thus, the tidal pressure is about 10,000 times the pressure that one normally might encounter on Earth.

$$\begin{aligned} l &= 1.8m, \quad \sigma = 1gm/cm^3 \\ P &\sim 10^{12} \text{ Nt/m}^2, \text{ for } (r_S)_\odot = r \\ &\sim 10,000,000 \text{ ATM.} \end{aligned} \quad (4.16)$$

What this means of course, is that if black holes existed, when objects accrete to them, they would suffer enormous forces far beyond the situations existing in a normal environment. This is

illustrated in Fig. 4.5 which shows a sketch of a normal star and a black hole in a binary system. As material falls into that hole, you can imagine that accelerations are such that one might have x-ray point sources. In particular, at Fermilab, there is a small experiment looking for muons from point sources which exists as a side line of a test of the muon system for D0.

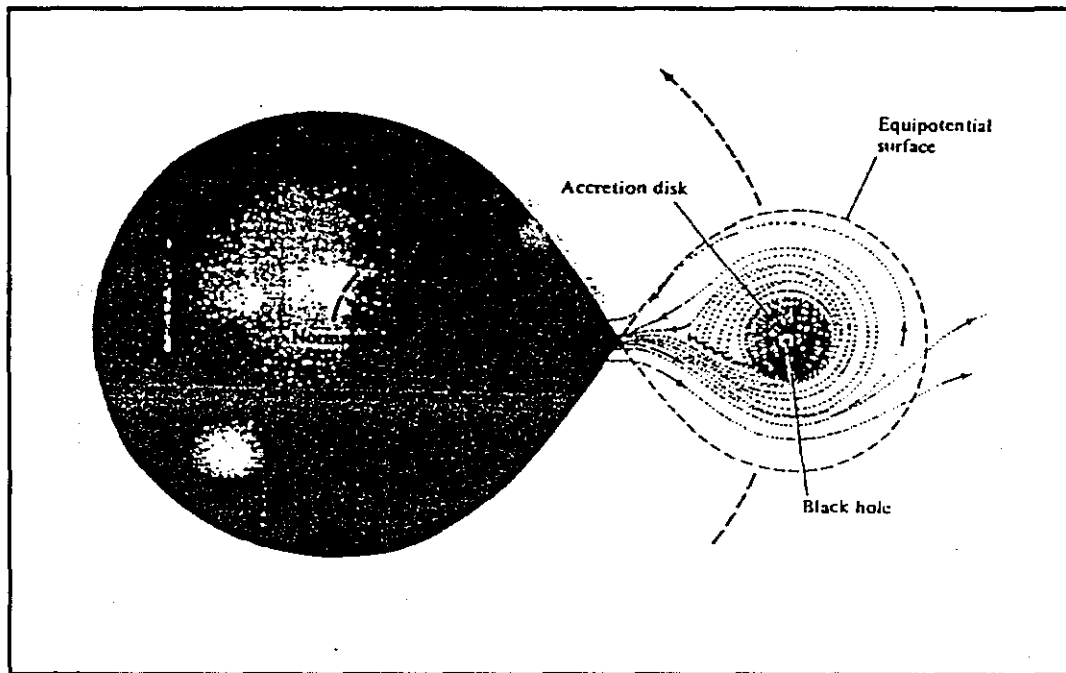


Fig. 4.5: Binary system of black hole and normal star.

5 OTHER SOLUTIONS; CHARGED MASS, COSMOLOGICAL TERM, INTERIOR SOLUTION

There are several distinct solutions which are generalizations of the Schwartzchild solution which will be discussed in this Section. Fundamentally, a black hole's singularity is characterized by charge, mass and spin. So far we have only discussed mass. In this Section we will discuss charge, and in the next Section, we will discuss solutions for singularities with spin angular momentum. First, consider the Schwartzchild solution for a charged mass. The existence of charge means, classically, that we have electric fields and thus, electric self energy. We know by the Equivalence Principle that all energy gravitates. Because the mass is the total energy of the system, we need a effective mass which takes into account the electromagnetic self energy. The solution is called the Nördstrom Reissner metric. However, it is intimately related to the Schwartzchild solution, being identical with the substitution of M_{EFF} for M .

$$\begin{aligned}
 M_{EFF} &\equiv M - q^2 / 2rc^2 \\
 r_c &\equiv q^2 / Mc^2 \\
 q &= Ne, \quad M = Nm \\
 r_c &= N\alpha\lambda.
 \end{aligned}
 \tag{5.1}$$

The second term in M_{EFF} is the electromagnetic self energy within a sphere of radius r containing charge q . Since the electromagnetic self energy is repulsive, it comes in with a negative sign such that the effective mass is reduced from the Schwartzchild mass.

As with the Schwartzchild radius, one can define another characteristic radius, r_c , which is the size where the electromagnetic self energy is equal to the rest energy. This definition is obviously related to the classical electron radius. It is in complete analogy to the Schwartzchild radius which is the radius where the potential energy is equal to the rest energy. The Coulomb radius for a totally charged object is equal to the Yukawa wavelength of the individual objects

making up that system, times the coupling constant, times the number of particles in the system. Clearly, since the self energy depends on the square of the charge, whereas the gravitational mass depends only on the first power of the number density, the electrical interaction will dominate at some point.

Calculating the expression for the effective mass back into the Schwartzchild metric, one can find g_{44} . We have an additional term to what we had in the Schwartzchild case which goes like $1/r^2$. It is second order in the characteristic radii, $r_S r_C$.

$$\begin{aligned}
 g_{44} &= 1 - r_S / r + r_S r_C / 2r^2 \\
 g_{44} &= 0 \\
 r_\infty &= \frac{r_S}{2} \left(1 \pm \sqrt{1 - 2r_C / r_S} \right) \\
 \alpha &\geq (m / M_{PL})^2.
 \end{aligned}
 \tag{5.2}$$

We can look at the infinite red shift surface where the g_{44} piece of the metric disappears. By doing this, we have to solve a quadratic equation. Clearly, looking at Eq. 5.2, if the charge were to go to zero, then the Coulomb radius would go to zero and we would get back that the infinite red shift surface is just the Schwartzchild radius. It is also true that a solution for the infinite red shift ~~surface does not exist beyond a certain magnitude for r_C .~~ This is merely a statement that the Coulomb repulsion will overcome the gravitational attraction for a charged black hole and will not allow the formation of such a singularity. Obviously by looking at Eq. 5.2, this situation occurs when $r_S = 2r_C$. In the case where all objects comprising this system have the fundamental electron charge, the ratio of the mass of the constituents to the Planck mass squared needs to be $\leq \alpha$.

We should also consider the possibility of non-classical sources for the field equations. In discussing linearized general relativity, for example in Appendix C, we always used the energy tensor and used as sources the classical mass. Suppose, however, the vacuum itself has an energy density. Quantum mechanics is replete with examples of zero point energy. The Standard Model of particle physics has an electroweak vacuum expectation value. This energy will also gravitate and

therefore, should be included in the field equations. The vacuum contribution to the energy tensor then leads to a term in the Laplace equation having a solution which increases as the square of the radius. There is a characteristic vacuum size, the vacuum radius, as defined in Eq. 5.3, which leads to a vacuum contribution to g_{44} and g_{rr} .

$$\begin{aligned}
\langle T^{\mu\nu} \rangle_V &= g^{\mu\nu} \sigma_V c^2 \\
\nabla^2 \Phi &= 4\pi G \sigma - \Lambda c^2 \\
\Phi_V &= -\Lambda c^2 r^2 / 6, r_V = \sqrt{3/\Lambda} \\
-2\Phi_V / c^2 &= (r/r_V)^2.
\end{aligned} \tag{5.3}$$

The parameter Λ corresponds, as seen in Eq. 5.3, to a uniform effective mass density which leads to a characteristic length scale. This vacuum energy density is something like the classical ether and was initially introduced by Einstein in order to have a stable Universe. This was of course before Hubble's discovery that all galaxies appear to recede from us. Einstein then characterized the introduction of this parameter as his biggest mistake.

$$\begin{aligned}
\sigma_V &= -\Lambda c^2 / 4\pi G \\
g_{44} &= 1 + \frac{2}{c^2} (\Phi + \Phi_V) \\
&= 1 + r_s / r - (r/r_V)^2.
\end{aligned} \tag{5.4}$$

As an aside, one should note that the energy tensor in Eq. 5.3 has the metric subsumed in it, defining the vacuum energy density, whereas the sources given in Appendix B, for example, do not. Therefore, as the metric evolves, for example, as the Universe expands, the matter density decreases from a denser, earlier era, while the vacuum energy density remains a constant. The vacuum energy density has a potentially strong effect on the evolution of the Universe because it does not dilute with expansion. In fact, this perception is the basis for the recent inflationary scenarios where exponential growth is driven by the vacuum expectation value of hypothesized scalar fields.

It is necessary to point out that there is a problem with the observed smallness of the vacuum energy density. Given that energy controls the evolution of the Universe, then the vacuum energy density cannot have extensively modified the evolution, therefore, σ_V must be comparable or less than the visible density, which we know is about 1 proton per cubic meter.

$$\begin{aligned}
 \sigma_V &\leq 1p / m^3 \\
 \Lambda &\leq 10^{-58} m^2 \\
 \sigma_{VEV} &\sim (100 GeV)^4 \\
 &\sim 10^{55} GeV / m^3 \\
 &\sim 10^{55} \sigma_V \\
 &(\hbar c = 2 \times 10^{-16} GeV \cdot m).
 \end{aligned}
 \tag{5.5}$$

In contrast, the situation in quantum field theory is that the zero point energy should always contribute to the vacuum energy. The most familiar example for particle physicists is the Standard Model vacuum expectation value, which we know is about 100 GeV. Converting to energy density, using Planck's constant, we find that the Standard Model vacuum expectation value energy density or mass density is about 10^{55} times larger than the limit given by cosmologists. This appears at first blush to be something of a problem to the simple minded experimentalist.

One should also note that, if there is a vacuum energy density, then "empty" space does not give us a flat metric, but instead gives a deSitter metric which is not asymptotically flat. We also note that, at least conceptually, the parameter Λ could be positive or negative. Thus, the contribution of the vacuum energy density to the metric could be of either sign. Given that there are a variety of questions and problems, even so, they will be finessed in the future, ignoring any possible non zero value for the vacuum energy density, and assuming r_V is rigorously zero.

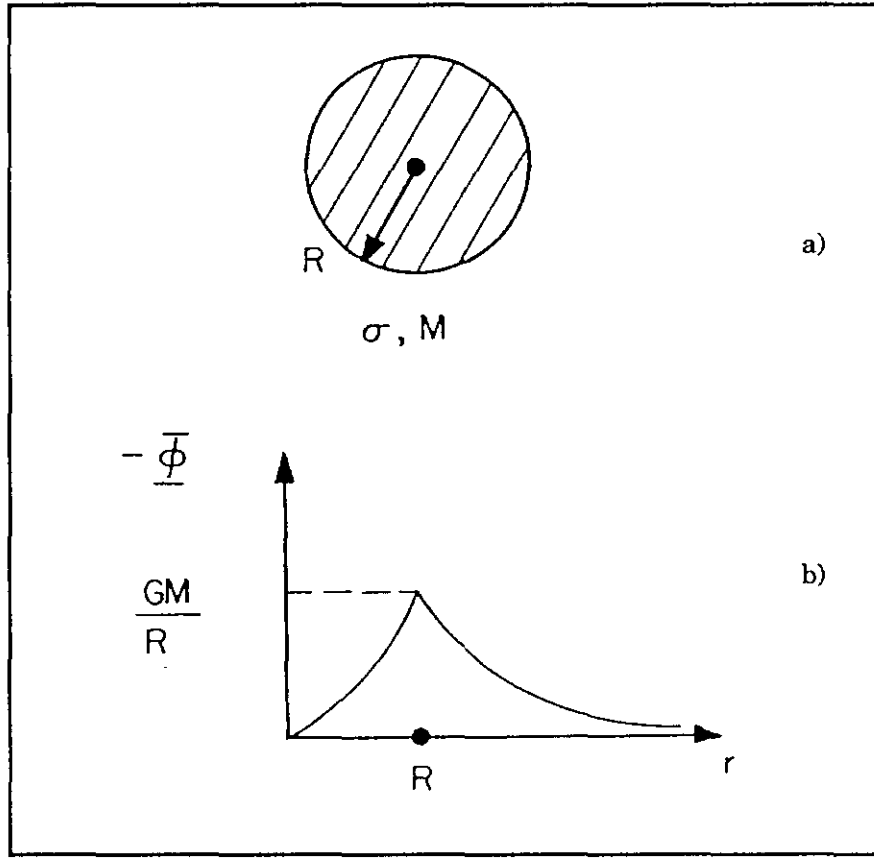


Fig. 5.1: a) Definitions for interior solution b) Newtonian interior solution matching to exterior solution at $r=R$.

As a final topic for this Section, we will consider the interior solution. So far we have discussed the fact that we are either dealing with a point source or that we are outside the mass distribution and therefore, by Gauss's law, consider it to be a point source. The geometric definitions for the interior solution are shown in Fig. 5.1. In Newtonian mechanics, the mass is simply the mass per unit volume times the volume - what could be simpler? If we work out the Newtonian radius at which the object has a radius equal to its Schwartzchild radius, it is simply given in terms of the Newtonian coupling constant and the density.

$$M = \sigma_0 V = \sigma_0 \left(\frac{4}{3} \pi R^3 \right) \tag{5.6}$$

$$\left(\frac{R^3}{r_s} \right)_{R=r_s} \equiv R_0^2 = 3c^2 / 8\pi G \sigma_0.$$

Clearly for densities greater than the density σ_0 , there will not be a solution because the system will exist inside its own Schwartzchild radius which is unstable. The system, as we will see, then collapses into a black hole singularity, thus, the radius of the system has to be larger than the Schwartzchild radius.

The Newtonian expression for the interior solution is quite familiar. One can easily write down the interior solution $-2\Phi_{IN}/c^2$. In the case of Newtonian mechanics, this solution is continuous with the exterior solution as shown in Fig. 5.1b.

$$\begin{aligned} \Phi_{IN} &= -GM_{IN} / r \\ &= \frac{-GM}{R^3} r^2 = \frac{-c^2}{2} \left(\frac{r}{R_0} \right)^2 \\ -\frac{2\Phi_{IN}}{c^2} &= \frac{r_s r^2}{R^3} = \left(\frac{r}{R_0} \right)^2 \end{aligned} \tag{5.7}$$

$$(ds)_{IN}^2 = \left[\frac{3}{2} \sqrt{1 - (r_s / R)} - \frac{1}{2} \sqrt{1 + \frac{2\Phi_{IN}}{c^2}} \right]^2 (cdt)^2 - dr^2 / (1 + 2\Phi_{IN} / c^2) - r^2 d\Omega^2.$$

What results, unfortunately without proof but hopefully with some motivation, is the interior metric appropriate to this problem. The spatial part is very simple; it corresponds to the Schwartzchild solution simply modified by replacing the exterior Newtonian potential by the interior Newtonian potential which is exactly what we might expect. For the temporal part of the interval, the resulting expression is similar to the spatial part - except for the fact that there is a constant term which is needed to match the exterior Schwartzchild solution at radius R . We note that the interior solution, as given in Eq. 5.7, matches smoothly onto the exterior solution. This implies

that the parameter M is the total energy since, exterior to a system of point particles that may be interacting, what is important is the total mass-energy, which is the source term for the energy tensor.

Looking closer at the situation, the physical volume is related to the coordinate volume by the elements of the metric. The total volume, therefore, integrated from zero to R , is shown below.

$$\begin{aligned}
 dV &= (\sqrt{g_{11}} dx^1) (\sqrt{g_{22}} dx^2) (\sqrt{g_{33}} dx^3) \\
 &= r^2 dr d\Omega / \sqrt{1 - (r/R_0)^2} \\
 V &= 2\pi R_0^3 [x_0 - \sin x_0 \cos x_0] \\
 \sin x_0 &= R/R_0 \\
 V &\sim \frac{4\pi R^3}{3} \left[1 + 3/10 (R/R_0)^2 \right], \quad \frac{R}{R_0} \ll 1.
 \end{aligned} \tag{5.8}$$

For small values of $\sin x$, the physical volume is $4/3\pi R^3$ times a correction factor. It is positive, which means that the physical volume is larger than the Newtonian coordinate volume. Therefore, there is a mass defect in that the density times the physical volume is greater than the total mass (energy) M . The fractional change in mass is proportional to the dimensionless quantity r_s/R .

$$\begin{aligned}
 \Delta M &= \sigma_0 V - M \\
 \frac{\Delta M}{M} &= \frac{3}{10} (r_s/R).
 \end{aligned} \tag{5.9}$$

This is similar to the situation in nuclei where there is a mass defect. The mass of a nucleus is less than the sum of the masses of its constituents, because of binding energy effects. It takes energy (or mass) to break a nucleus apart, since it is a bound system. The mass defect is caused by energy lost while packing matter under its own gravitational self energy. Take the interior solution for the potential and bring in a spherical shell of matter from infinity to that potential. The energy is lost proportional to the interior potential. The total energy lost in constructing this dust

ball is the energy lost for all radii from zero to R . The mass lost in doing this is the energy loss divided by c^2 .

$$\begin{aligned}
\Phi_{IN}(r) &= \frac{-4\pi G}{3} \sigma_0 r^2 \\
dM &= 4\pi r^2 dr \sigma_0 \\
d\varepsilon &\sim -dM \Phi_{IN}(r) = \frac{-16\pi^2}{3} G \sigma_0^2 r^4 dr \\
\varepsilon &= \int_0^R d\varepsilon = \frac{-16}{15} \pi^2 G \sigma_0^2 R^5 \\
\Delta M &= -\varepsilon / c^2.
\end{aligned} \tag{5.10}$$

This purely Newtonian calculation, shown in Eq. 5.10, agrees perfectly with the weak binding limit given by the expansion shown in Eq. 5.9. Due to this satisfying situation, one can begin to understand the physical mechanisms that may differentiate between coordinate and physical volume.

As a final comment for this Section, we will look at observers inside the dust ball. This solution does have some cosmological implications. And as mentioned, we will concentrate on non-cosmological tests, therefore, limiting ourselves to very brief comments. Suppose you live in the dust ball. You would then use clocks t' which are at rest with respect to the dust and not coordinate clocks t which, as we know, refer to observers outside the mass distribution - because you cannot get outside. For your clocks and rulers, therefore, you have a solution which, for simplicity, we transform as defined by Eq. 5.11 (see Eq. 5.8).

$$\begin{aligned}
(ds^2)_{IN} &= (cdt')^2 - R_0^2 [dx^2 + \sin^2 x d\Omega^2] \\
r &= R_0 \sin x \\
R_0^2 &= 3c^2 / 8\pi G \sigma_0.
\end{aligned} \tag{5.11}$$

These are exactly the transformations expected from examining Eq. 5.8. Note that the length parameter R_0 in Eq. 5.11 is exactly what one has in the interior solution in Eq. 5.6. Note also that

this interior interval is constant in terms of coordinate clocks t and rulers x , except for an overall scale factor R_0 . This scale factor is inversely proportional to the gravitational coupling constant and to the density, therefore, a low density Universe is large. As the density goes to zero, the characteristic curvature radius becomes infinite. As seen in Eq. 5.8, if $R_0 \rightarrow \infty$ the metric becomes Euclidian.

Note that in everything in this Section, and in most of what will be done in this entire note, pressure has been neglected as a source of energy. The metric shown in Eq. 5.11 is called a Friedmann metric, it has been "derived" from semi-Newtonian considerations of the interior of a pressureless dust ball. This metric is useful in cosmology. It arises in a space of constant curvature due to a uniform matter density.

If the characteristic radius R_0 is equal to the Schwartzchild radius, one has the critical closure density which is roughly 10 times the observed visible matter density. For a Universe which is characterized by a Hubble distance of roughly 10 billion light years, one can look back at Eq. 1.9, to see the relationship between the prior discussion and what is implied in Eq. 5.11. Hawking observed that a collapsing star is mathematically equivalent to an expanding Universe with the sense of time reversed. In that context, we have looked at the interior dust ball solutions in some detail because of the implications for cosmology.

6 KERR SOLUTION; DRAG AND PRECESSION, ERGOSHERE

In this Section the properties of point solutions with both mass and spin will be investigated. In the Newtonian problem from the Schwartzchild solution in Section 4, we know that the potential is the static Newtonian potential plus a centrifugal term which we have already seen in the discussion of the conserved energy. As in the case of mass and charge, we will define a characteristic length, the Kerr radius which is defined to be the radius where the rotational kinetic energy is comparable to the rest energy.

$$\begin{aligned}
 \Phi_{ROT} &\sim \Phi + J^2 / 2m^2 r^2 \\
 r_K &\equiv J / mc \sim r^2 \omega / c \equiv c / \omega \\
 2\Phi_{ROT} / c^2 &= \frac{-r_S}{r} + \left(\frac{r_K}{r} \right)^2.
 \end{aligned} \tag{6.1}$$

The metric associated with a Newtonian turntable will be studied in order to start to build up an intuition about the physical effects. The geometry for this is shown in Fig. 6.1. The idea is similar to the Equivalence Principle arguments were used in motivating the Schwartzchild metric. The time rate of change of the angle is ω . Outside the turntable, one has a local inertial frame and can use special relativity. The transformation to the rotating coordinate system simply comes from adding the angle swept out by the rotating turntable which leads to the metric shown below.

$$\begin{aligned}
 \omega &\equiv d\phi / dt, \beta_{EP}^2 = (\omega r / c)^2 \rightarrow r_S / r \\
 (ds)_{SR}^2 &= (cdt)^2 - (dr^2 + (rd\phi)^2 + dZ^2), \phi \rightarrow \phi + \omega t \\
 (ds)_{TURN}^2 &= (cdt)^2 \left(1 - \left(\frac{\omega r}{c} \right)^2 \right) - (dr^2 + r^2 d\phi^2 + dZ^2) + \frac{2r\omega}{c} (rd\phi)(cdt) \\
 &= (cdt)^2 \left(1 - \frac{r_S}{r} \right) - (dr^2 + r^2 d\phi^2 + dZ^2) + \frac{2r_S r_K}{r^2} (rd\phi)(cdt) \\
 &= (ds)_{RED}^2 + \frac{2r_S r_K}{r^2} (rd\phi)(cdt).
 \end{aligned} \tag{6.2}$$

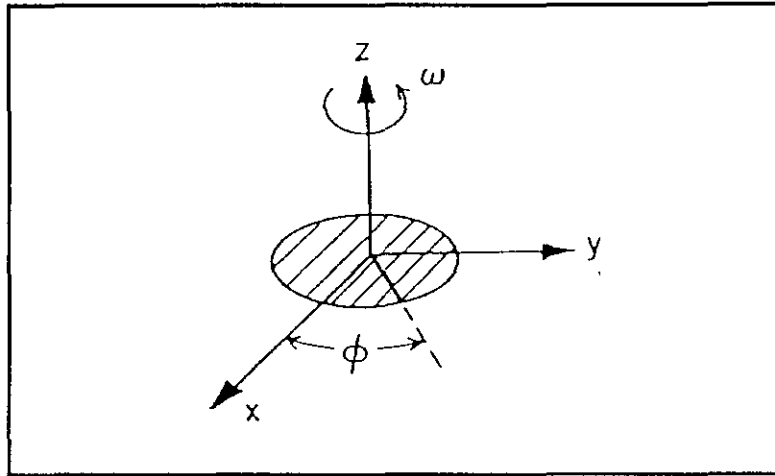


Fig. 6.1: Geometry of the turntable appropriate to the EP metric discussion.

In this expression for the interval the coupling between space and time is of primary importance. This will carry over into general relativity. The coupling implies that there is a dragging of the space-time by the rotations themselves. This is very similar to the situation for magnetic fields in electromagnetism. What we have done so far is effectively an Equivalence Principle argument. Therefore, we expect that when looking at the dynamics, we will recover Newtonian mechanics, as we argued in general. In fact this is true; the Euler-Lagrange equations for the turntable metric given in Eq. 6.2 are shown in Eq. 6.3.

$$\begin{aligned} d^2r / dt^2 + \omega^2 r &= 0 \\ r^2 d^2\phi / dt^2 + 2\omega r dr / dt &= 0. \end{aligned} \tag{6.3}$$

One recovers the centrifugal force, and the Coriolis force. Clearly they are fictitious forces due to the fact that we are writing equations of motion in an accelerated or non-preferred reference system.

The exact Kerr solution in general relativity is something we will not derive, but we will appeal to the Newtonian and Equivalence Principle turntable metrics. This solution was discovered

in 1963, and the derivation is extremely tedious. An approximate solution, valid for slow rotations, $r_K \ll r_S$, is:

$$\begin{aligned} (ds^2)_K &\sim (cdt)^2 \left(1 - \frac{r_S}{r}\right) - dr^2 / \left(1 - \frac{r_S}{r}\right) - r^2 d\Omega^2 + 2(r_S r_K / r^2)(r \sin^2 \theta d\phi)(cdt) \\ &\sim (ds^2)_S + 2(r_S r_K / r^2)(r \sin^2 \theta d\phi)(cdt). \end{aligned} \quad (6.4)$$

Basically, the solution is the Schwartzchild solution for the diagonal parts with a coupling between the ϕ coordinate and the clock coordinate t . This coupling is something expected from the discussion of the turntable metric, see Eq. 6.2. Note here that the parameter r_K has a sign because there is a sense of the rotation, which is the sense of the angular momentum about the z axis, J_z . Looking at Eq. 6.4, it is fairly easy to convince oneself that in most situations, the rotations are a second order effect, because the spin terms in the metric go like $1/r^2$ in contrast to the $1/r$ terms due to the mass sources.

Given the metrical interval for the Kerr solution, one can proceed and calculate the Euler-Lagrange equations. This is a central force problem, so the motion is in a plane - exactly as was the case for the Schwartzchild solution. There are again two constants of the motion since the Lagrangian does not depend on the coordinate ϕ or the coordinate t , however, in this case, the angular momentum is a somewhat more complicated object.

$$\begin{aligned} \dot{\theta} &= 0, \quad \theta = \pi/2 \\ \frac{\partial \mathcal{L}}{\partial \dot{\phi}} &= -2r^2 \dot{\phi} + \frac{2r_S r_K}{r}(ct) \\ J'_K &= r^2 \dot{\phi} - \left(\frac{r_S r_K}{r}\right)(ct) = r^2 \left[\dot{\phi} - \left(\frac{r_S r_K}{r^3}\right)ct \right]. \end{aligned} \quad (6.5)$$

As might be expected from the turntable example, the metric is pulled along and given off-diagonal parts by the angular velocity. There is a shear effect which causes a drag of the inertial

frame, whose value is implicit in Eq. 6.5. The ratio of the inertial drag to the angular velocity of the rotating source is proportional to the ratio of the radius of observation to the Schwartzchild radius.

$$\begin{aligned}\omega_{DRAG} &= \frac{cr_S r_K}{2r^3} \\ (\omega_{DRAG} / \omega) &\sim \frac{1}{2}(r_S / r).\end{aligned}\tag{6.6}$$

The rotational pieces are clearly the gravitational analogue of the magnetic field in electromagnetism. This should be obvious, in a sense, since the electrical part of the potential goes like $1/r$, whereas the magnetic part goes like $1/r^2$. The drag caused by this rotation is called Lense-Thirring or Kerr precession. Numerically, for the Earth, the Schwartzchild radius is about 1cm whereas the Kerr radius is about 3 meters. This means that the first order effect of gravity is roughly one part in 10^9 , whereas the second order rotational part is about 1 part in 10^{15} . This means that the inertial drag is only about $0.1''/\text{year}$.

$$\begin{aligned}(r_S)_\bullet &\sim 0.9\text{cm}, \quad (r_K)_\bullet \sim 3.3\text{m} \\ r_S / R_\bullet &= 1.4 \times 10^{-9}, \quad r_S r_K / R_\bullet^2 \sim 7.0 \times 10^{-16} \\ (\omega_{DRAG})_\bullet &\sim 0.1'' / \text{yr}.\end{aligned}\tag{6.7}$$

The existence of the drag frequency leads us to predict certain precessions. Recalling from special relativity, when looking at the g factor in spin-orbit coupling in quantum mechanics, the Thomas precession of the spin due to being in an accelerated reference system, is proportional to that acceleration.

$$\begin{aligned}
d\vec{S} / dt &= \vec{\omega} \times \vec{S} \\
\vec{\omega}_T &= -\left(\frac{\vec{\beta} \times \vec{a}}{2c} \right) \\
|\vec{\beta}|^2 &= GM / rc^2 = r_s / 2r \\
\vec{a} &= \left(\frac{GM}{r^2} \right) \hat{r} = (r_s c^2 / 2r^2) \hat{r} \\
\omega_T &= \left(\frac{r_s}{2r} \right)^{3/2} \left(\frac{c}{2r} \right) \\
(\omega_T)_{R_\bullet} &\sim 2.3'' / yr.
\end{aligned} \tag{6.8}$$

The time rate of change of the spin is zero in a local inertial frame, whereas the Thomas frequency implies that a gyroscope (which is in this accelerated frame) will change its direction with respect to the fixed stars. Clearly, this particular precession is due to the fact that one is in an accelerated reference system. In a circular orbit, β^2 is just proportional to the dimensionless quantity r_s/r . We can easily work out the acceleration, and therefore find the Thomas precession frequency. Calculating, we find a much larger effect than the Kerr precession which is about 2.3"/year for the Thomas precession. Note that this precession has nothing to do with the Kerr solution and, in fact, is not a general relativistic effect in the sense that one third of it is just the Thomas precession due to special relativity.

Because the direction of velocity is proportional to the momentum, and the acceleration is radial, then the vector time rate change and the spin is proportional to the vector cross product of the angular momentum of the spin just as it is in quantum mechanics. This fact allows one to define a spin-orbit potential just as is done in non-relativistic quantum mechanics. This points out the $\vec{L} \cdot \vec{S}$ nature of the coupling. It is the ratio of the spin-orbit interaction energy to the rest energy times the Schwartzchild radius ratio to the observational radius which is important.

$$\begin{aligned}
\frac{2\Phi_{SO}}{c^2} &= \left(\frac{3r_s}{2r} \right) \left[\frac{(\vec{L} \cdot \vec{S}) / mr^2}{mc^2} \right] \\
\hat{\beta} &\sim \hat{p}, \quad \hat{a} \sim \hat{r}.
\end{aligned} \tag{6.9}$$

We will state without proof that the full machinery of the Euler-Lagrange equations using the Kerr metric gives you the Thomas precession times a factor of 3, or 6.9"/year in Earth orbit. We note in passing that there is presently no experimental proof of the existence of any spin effect in general relativity (either spin-orbit or spin-spin coupling), nor of any charge effect.

Similarly, one can write down a spin-spin interaction potential for the Lense-Thirring precession frequency.

$$\begin{aligned} \omega_{DRAG} &\equiv \left(\frac{r_S}{r}\right) [J / 2mr^2] \\ \frac{2\Phi_{SS}}{c^2} &\sim \left(\frac{r_S}{r}\right) \left[\frac{(\vec{J} \cdot \vec{S}) / mr^2}{mc^2} \right]. \end{aligned} \tag{6.10}$$

This is quite similar in functional form to the spin-orbit coupling as one might expect. The geometric layout for a possible gyroscopic Earth orbit test of general relativity is shown in Fig. 6.2. If the spin is oriented along the acceleration, then we expect a precession of 6.9"/year due to the spin-orbit coupling. By comparison, if the gyroscopic spin is aligned parallel to the Thomas angular frequency, then the spin-orbit precession is wiped out and the much smaller spin-spin precession frequency is tuned in. In the first case, $\vec{\omega} \times \vec{S}$ has a maximum value, whereas in the second case it is zero. Neither of these experiments has been performed, however, it is conceptually possible to make these measurements, and they are planned for future shuttle launches.

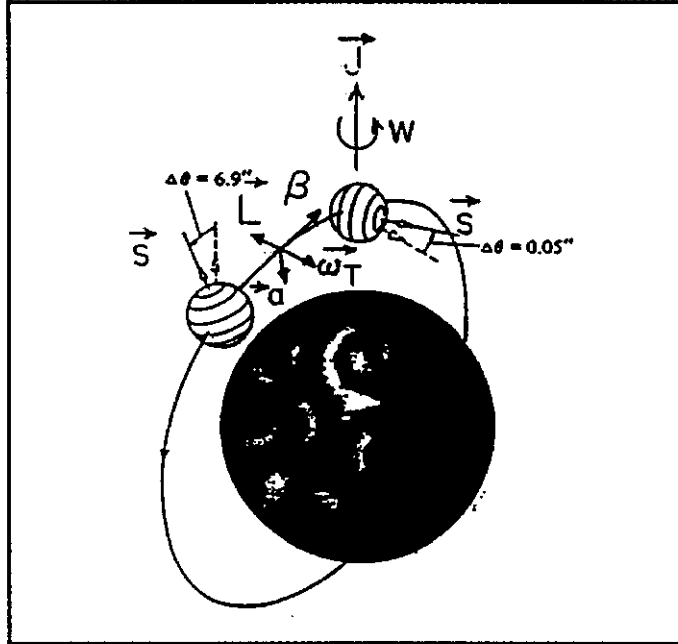


Fig. 6.2: Layout of the dynamical vectors in the gyroscopic tests. The spin-orbit and spin-spin vectors are shown for clarity in the two orientations.

Finally, it is of interest to examine the singularity structure, if any, of the Kerr solution. The exact Kerr metric approaches the limit of the metric given in Eq. 6.4, which is the weak rotation limit. The value of the parameters defining the radial and temporal parts of the exact metric are given below (without proof).

$$\begin{aligned}
 (ds)_K^2 &\sim (cdt)^2 \left(1 - \frac{r_S r}{\rho^2} \right) - \frac{\rho^2}{\Delta} dr^2 \dots \\
 \rho &\sim r + (r_K \cos \theta)^2 / 2r \\
 \Delta &\equiv r^2 (1 + 2\Phi_{ROT} / c^2).
 \end{aligned}
 \tag{6.11}$$

It is interesting to note that the parameter Δ is indeed just the parameter one expects when modifying the Schwartzchild potential using the Newtonian approximation for rotations that were derived in Eq. 6.1. As a limiting case, if r_K is small, one recovers the weak field limit given in Eq. 6.4. If r_K were to vanish, i.e. a non-rotating black hole, one would recover the Schwartzchild

solution. As in our discussion of Schwartzchild singularities, the infinite red shift surface corresponds to the situation where the temporal part, g_{44} , of the metric vanishes. By comparison, the infall sphere, or horizon, occurs when light (which goes on null geodesics) cannot escape. In that case the coordinate velocity of light is zero. These two surfaces are given below.

$$\begin{aligned}
 r_\infty &\sim r_S - (r_K \cos \theta)^2 / 2r_S, \quad g_{44} = 0 \\
 r_\gamma &= \frac{r_S}{2} \left(1 \pm \sqrt{1 - \left(\frac{2r_K}{r_S} \right)^2} \right), \quad \Delta = 0 \\
 &\sim r_S - r_K^2 / r_S.
 \end{aligned}
 \tag{6.12}$$

In a situation exactly analogous to that for a charged black hole, the rotating black hole may not have a solution for the horizon. The physical reason for this is that the centrifugal effects are repulsive and they may overcome the gravitational attraction such that no black hole may form. This is exactly the analogue of the charged self-repulsion.

Unlike the Schwartzchild case, the horizon is not congruent with the infinite red shift surface, therefore, signals can escape for radii less than r_∞ , if they are boosted in the direction of rotation. One can use the vacuum rotation to aid escape. The simplest way to help is to boost yourself equatorially in the direction of the rotation. The horizon and infinite red shift surfaces meet at the poles; the shape of these surfaces is shown in Fig. 6.3. There are some interior singularities which we have not discussed. What is most important is that the infinite red shift surface and the horizon are not congruent. The region between them is called the ergosphere.

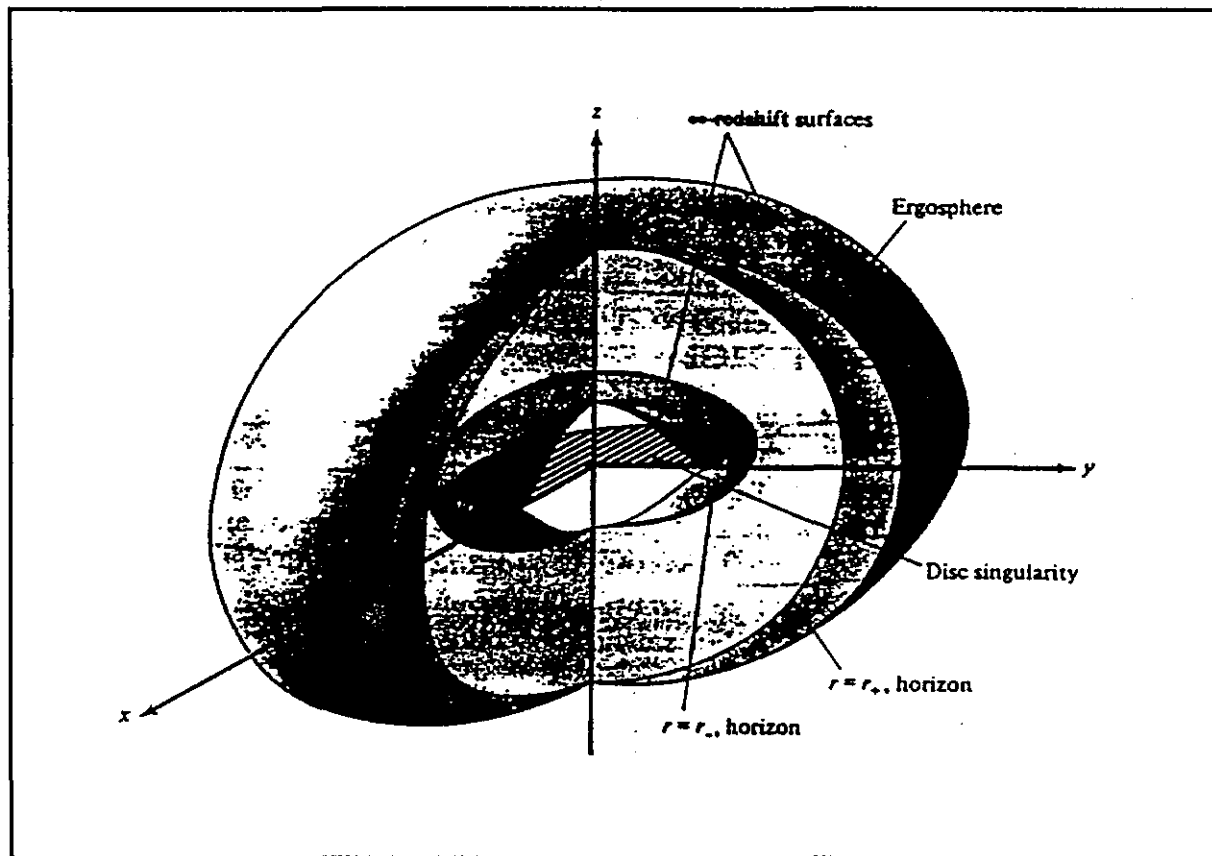


Fig. 6.3: Kerr metric singularity surfaces. The horizon, infinite red shift, and ergosphere are indicated.

Rotational kinetic energy can be extracted from a rotating black hole. Clearly, that reduces the angular momentum until the Kerr radius goes to zero and all the rotational energy is removed. As first noted by Penrose, at the end of this extraction one is left with a non-rotating Schwartzchild solution with reduced mass. Vacuum fluctuations in the ergosphere can be used which decay into a pair of particles: one is in a negative energy orbit, the other escapes with positive energy. Energy can thus leak out near the equator and the rotating hole will spontaneously slow down. A similar concept will be discussed in the last Section of this note.

As seen from Fig. 6.3, an intuitive way to think of this is that there is an equatorial bulge of the infinite red shift surfaces due to the rotation. Rotation can prevent the collapse of a star to a black hole. In particular, if the Kerr radius is greater than half the Schwartzchild radius, no singularity

will form - see Eq. 6.12. We can estimate this situation by observing the angular momentum of a uniform sphere and noting that angular momentum is conserved in collapse. The moment of inertia can be trivially calculated. The resulting expression for r_K depends on the radius and the rotation frequency. We can evaluate the Kerr radius by taking the rotation period of the sun (as observed, for example, by watching the sunspots rotate on the surface of the sun). It turns out to be roughly 2.4 km.

$$\begin{aligned}
 r_K &> r_S / 2 \\
 J &= I\omega = \left(\frac{3MR^2}{5} \right) \omega \\
 r_K &= \frac{3}{5} \omega R^2 / c \\
 T_\odot &\sim 30 \text{ days} \\
 (r_K)_\odot &\sim 2.4 \text{ km.}
 \end{aligned}
 \tag{6.13}$$

Since the Schwartzchild radius is 3.5 km, the rotation of the sun is roughly that which is needed to avoid a collapse. Since the sun is a fairly typical star, it must often be the case that a collapse is evaded by the existence of rotational kinetic energy.

7 RADIATION; GENERATION, DETECTION

So far we have been discussing the static solutions of general relativity. It is clear that, just as in electromagnetism, there are both static and radiative solutions. This is evident from our derivation of the linearized theory with its wave equation. Gravitinos are obviously massless quanta which propagate the gravitational force. Since they are massless spin 2 objects they have 2 helicity states, like photons. We will try to avoid any of these complications with polarization and consider the trace of the gravitational field as a measure of the radiation strength. Like rotations, there has as yet been no direct detection of gravitational radiation, although sightings were reported in the late 1960's. Formally, the fact that linearized general relativity satisfies a wave equation yields the equivalent integral equation between the sources and the field exactly as in electromagnetism. These mathematical formalities are addressed in Appendix D.

The long wavelength approximation allows us to simplify the integral equations and expand the fields in the moments of the source distribution. Given the fields, the time average radiated power can be found which is propagated away by those fields. One thus gets estimates for the radiated power for any particular system. In "deriving" gravitational formulas, because of the strong formal analogy with electromagnetism and because of our familiarity with electromagnetism, we will first look at the electromagnetic case. The approach taken will be to quote the static solution and look at the flux, or Poynting vector, for that solution. Then one makes the familiar dimensionless substitutions such as to get radiation fields. This is very similar to the spirit of the discussion of Mach's principle in Section 1.

In electromagnetism, the static electric dipole field, for 2 charges q separated by a distance b , goes like $1/r^3$. The static flux, which is the energy per unit time, then goes like $1/r^4$. Obviously, in order to have a true radiative solution, we need the flux crossing unit area to be independent of r . The radiation should also be due to acceleration. We therefore make the replacement of the static

distance b by the dynamic harmonic displacement d and replace r by the only other object which has the dimensions of length, the wavelength. The electric dipole moment is D .

$$\begin{aligned}
 E &\sim qb / r^3 \\
 \langle P \rangle_{EM} &\sim cr^2 |E|^2 \sim cq^2 b^2 / r^4 \\
 b &\rightarrow d, \quad r \rightarrow \lambda = c / \omega \\
 \langle P \rangle_{EM} &\rightarrow \frac{q^2 d^2}{c^3} \omega^4 = \omega^4 (\delta D)^2 / c^3 \\
 &= \langle \ddot{D} \rangle^2 / c^3.
 \end{aligned} \tag{7.1}$$

This substitution implies that the radiated power is just proportional to the (acceleration)² of the dipole moment, which is proportional to the fourth power of the frequency. The kinetic definition of these terms is given in a Figure enclosed in Appendix D for reference purposes. What is extremely pleasant in this simple minded dimensional analysis is that, knowing the static solutions, one can “derive” the radiative solutions by simple dimensionless replacements.

For systems with zero dipole moment the next term in the expansion would be a quadrupole. In the case of electromagnetism, the substitutions that give fields which goes like $1/r$ result in (fields)² or an energy flux which goes like ω^6 .

$$\begin{aligned}
 E &\sim \omega^3 / r \\
 \langle P \rangle_{EM} &\sim \frac{\omega^6}{360c^5} (\delta Q_{EM})^2.
 \end{aligned} \tag{7.2}$$

As discussed, gravitational radiation is very similar to electromagnetic radiation. The only difference is that the gravitational dipole moment is zero if the center of coordinates is chosen to be the center of mass of the system. It must therefore be concluded that the dipole moment of the matter distribution has no physical consequences. This is due to the fact that the spin 1 photon results in forces that are attractive or repulsive, but the spin 2 graviton is only attractive. This fact appears in the dipole or quadrupole nature of the electromagnetic and gravitational radiation respectively.

The substitution in the quadrupole moment formula for electromagnetic radiation, Eq. 7.2, in order to convert to gravity, is the replacement of α with α_G as discussed in Section 1. The dynamical quadrupole moment in electromagnetism is approximately the charge times the mean separation times the dynamical separation, as shown in Appendix D. The replacement then is to replace the charged coupling with the gravitational coupling, leading to a gravitational radiation which goes like ω^6/c^5 times the gravitational coupling constant times terms proportional to the dynamical quadrupole moment, δQ , squared.

$$\begin{aligned}
 \alpha &\rightarrow \alpha_G \\
 q^2 &\rightarrow GM^2 \\
 \delta Q_{EM} \sim qbd &\rightarrow \sqrt{GM}bd \\
 \langle P \rangle &\sim \frac{\omega^6}{c^5} GM^2 b^2 d^2 \\
 &\sim \frac{\omega^6}{c^5} G(\delta Q)^2.
 \end{aligned} \tag{7.3}$$

The exact formulae are given without proof in Appendix D and are reproduced below.

$$\begin{aligned}
 \langle P \rangle &= \frac{G}{45c^5} \langle \ddot{Q} \rangle^2 \\
 &= \frac{G\omega^6}{45c^5} (\delta Q)^2.
 \end{aligned} \tag{7.4}$$

There have been no direct observations of gravitational radiation, but there has been an inferred observation based on the slowing down of pulsars. For this reason, we will look at the radiative lifetime of a system that is decaying by the emission of gravitational radiation. For a system of size R , the period is related to the velocity in a circular orbit. The velocity is a quantity we have already derived several times. Therefore, with an expression for the angular frequency ω , the radiated power can be expressed as shown below in Eq. 7.5.

$$\begin{aligned}
\tau &= R/v, \quad \beta = \sqrt{r_s/R} \\
\langle P \rangle &\sim G\omega^6 M^2 R^4 / c^5 \\
&\sim (cr_s/R)^5 / G \\
\langle P_{MAX} \rangle &\sim c^5 / G = 3.7 \times 10^{52} \text{ Joule / sec} \\
&= 10^{26} L_{\odot}.
\end{aligned}
\tag{7.5}$$

This equation gives the average radiated power for a system whose dynamical size d is equal roughly to its static size b , both of which are equal to R . It is easy to see that the maximum radiated power comes from a situation near final collapse when the size of the system is comparable to its Schwartzchild radius. In that case, the maximum radiated power depends only on the gravitational coupling constant G . When calculating the numbers, it is found that this maximum power is roughly 10^{26} times the current luminosity of the sun.

A tabulated series of potential sources of gravitational radiation is given in Table 7.1. The frequency which is quoted for the binary stars is the rotation frequency. The received energy is the energy at a distance of 100 light years. The surface area at a distance of a hundred light years is roughly 10^{41} cm^2 . The pathological system which gives the maximum radiated power, as shown in Eq. 7.5, has a characteristic frequency of order kilocycles if the binaries have typical solar masses. This means that the maximum radiated energy is of order 10^{56} ergs. At a distance of 100 light years, the received energy density would be roughly $10^{15} \text{ ergs/cm}^2$. This is the absolute maximum that would occur if we observe the gravitational collapse of a star of a few stellar masses to form a black hole. In that case, the frequency of one kilocycle is roughly the time it takes light to go one Schwartzchild radius. This leads to an enormous received energy on the Earth's surface. Realistic sources (see Table 7.1) lead to somewhat reduced energies.

ASTROPHYSICAL SOURCES OF GRAVITATIONAL RADIATION

| Source | Spectrum | Energy received |
|--|---|---|
| Binary star system (of the AM CVn type) | discrete, $\nu = 2 \times 10^{-3} / \text{sec}$ | $10^{-9} \text{ erg} / \text{cm}^2 \text{ sec}$ |
| Collapse of neutron binary system | glissando, $\nu \sim 200 / \text{sec}$ increasing to $\nu \sim 2 \times 10^3 / \text{sec}$ | $10^{11} \text{ erg} / \text{cm}^2$ |
| Pulsating neutron star | discrete, $\nu = 10^3 - 10^4 / \text{sec}$ | $10^9 \text{ erg} / \text{cm}^2$ |
| Rotating neutron star star (with rigid deformation) | discrete, $\nu = 3 \times 10^2 / \text{sec}$ | $10^{-1} \text{ erg} / \text{cm}^2 \text{ sec}$ |
| Rapidly rotating neutron star (with rotation-induced deformation) | discrete, $\nu = 1.5 \times 10^3 / \text{sec}$ (slight drift to higher frequency) | $10^9 \text{ erg} / \text{cm}^2$ |
| Neutron star falling into black hole ($10 M_{\odot}$) | continuous, peaked near $\nu \sim 10^4 / \text{sec}$ | $10^{10} \text{ erg} / \text{cm}^2$ |
| Gravitational collapse of a star ($10 M_{\odot}$) to form a black hole | continuous, peaked near $\nu \sim 10^3 / \text{sec}$ | $10^{13} \text{ erg} / \text{cm}^2$ |

Table 7.1: Astrophysical sources of gravitational radiation.
Energies are quoted at a distance of 100 ly.

As previously mentioned, the loss of energy due to gravitational radiation means that the system radius decreases. When the radius decreases, you are more tightly bound and the gravitational radiation rate increases. Similarly, as in the case of classical mechanics with electromagnetic radiation, the system is unstable and spirals inward. This was a problem before quantum mechanics. The hydrogen atom was unstable and, when the decay rate was calculated, it was such that hydrogen atoms must decay at enormous macroscopic rates. This particular problem was solved by quantum mechanics. Since we do not have a quantum mechanical theory of gravity, the possibilities should at least be examined.

The Virial Theorem tells us that the total energy (for power law binding) is of the same order as the kinetic energy. This can be written down in a straightforward way. The gravitational lifetime τ_G is then of order the energy divided by the radiated power. This lifetime is the

characteristic time for light to go a distance equal to the size of the system times the ratio of the system size to the Schwartzchild radius cubed.

$$\begin{aligned}
 \epsilon &\sim T \sim Mc^2 \beta^2 = Mc^2 (r_S / R) \\
 \tau_G &= \epsilon / \langle P \rangle \\
 &= \frac{R}{c} (R / r_S)^3.
 \end{aligned}
 \tag{7.6}$$

The Virial Theorem tells us that the potential and kinetic energies for power law force laws are comparable. Therefore, the energy of the system to its radius can be related. Clearly, smaller radii require larger absolute values of the energy for tighter binding. This fact can be used to convert the lifetime into the change of size of the system as a function of time. If we put this into dimensionless units, we find that it is also in the ratio of the Schwartzchild radius to the system size to the third power.

$$\begin{aligned}
 \epsilon &\sim V \sim GM^2 / R \\
 d\epsilon &\sim \frac{-GM^2}{R^2} dR \\
 dR / d(ct) &\sim (r_S / R)^3, \quad d\epsilon / dt \sim \langle P \rangle.
 \end{aligned}
 \tag{7.7}$$

The system is obviously going at the speed of light if it is collapsing to a size near the Schwartzchild radius, where the system radius approaches the Schwartzchild radius because the dR is roughly cdt . In less pathological situations, such as an object in Earth orbit, we recall that the ratio of the Schwartzchild radius to the Earth's radius is roughly 10^{-9} , which means that the rate of change of, say, a satellite orbit is roughly 10^{-4} fm/sec due to gravitational radiation. This motion is certainly undetectable by means of radar ranging, for example, by making precision measurements of the Moon's orbit with respect to the Earth.

$$(r_S / R)_\oplus^3 c \sim 3 \times 10^{-4} \text{ fm/sec.}
 \tag{7.8}$$

It is clear that gravitational radiation is crucial to collapse and that the collapse is rapid for a binary star system with a system size near the Schwartzchild radius. This can be quantified somewhat by looking at the change of the period as a function of time. That change is just related to the change of radius as a function of the time as given in Eq. 7.7, using the relationship between the period and the radius, Eq. 7.5.

$$\begin{aligned}\tau &\sim R^{3/2} / c\sqrt{r_S} \\ d\tau / dt &\equiv (r_S / R)^{5/2}.\end{aligned}\tag{7.9}$$

We find that the time rate change of the period is a dimensionless quantity given as some power of the ratio of the Schwartzchild radius to the system radius. The amount of energy radiated in the collapse process can be estimated by taking Eq. 7.7 and integrating once. One uses energy conservation to assert that the radiated energy is equal to the change in gravitational potential energy as the system becomes more bound. If one starts from a large distance, the total radiated energy is just equal to the final value of the binding energy. The ratio of the radiated energy to the rest energy is proportional to the ratio of the Schwartzchild radius to the system radius. One can conclude, therefore, that in a process where a tightly bound system emits gravitational radiation at a characteristic size near the Schwartzchild radius, a large fraction of the rest energy will be radiated as gravity waves.

$$\begin{aligned}R^4 - R_0^4 &\sim r_S^3 c(t - t_0) \\ (\Delta\mathcal{E})_{RAD} &\sim GM^2\left(\frac{1}{R_0} - \frac{1}{R}\right) \\ (\Delta\mathcal{E})_{RAD} / Mc^2 &\sim (r_S / R).\end{aligned}\tag{7.10}$$

We now look at the rather sparse experimental data on gravitational radiation. There is a binary pulsar, whose period has been observed since 1974. The system consists of two objects of

roughly 1.4 solar masses, which means that the velocity β is about 0.001, Eq. 7.5. Since the size of this system is about 10^9 meters, the ratio of the Schwartzchild to the system radius is a few parts per million. This is not a particularly spectacular system, however being a binary pulsar, it has an extremely well defined period. This being the case, one can make a very accurate measurement of the time rate change of the period of the system. It has been measured to be increasing at a few parts per 10^{12} .

$$\begin{aligned}
 \tau &= 2790.6 \text{ sec} \\
 d\tau / dt &\sim -2.3 \times 10^{-11} \\
 M_1 \sim M_2 &\sim 1.4 M_\odot \\
 \beta &\sim 10^{-3}, \quad R \sim 10^9 \text{ m.}
 \end{aligned}
 \tag{7.11}$$

The observed slow down rate is consistent with the estimate given in Eq. 7.9 once all the numerical factors, explicitly shown in Appendix D, are put in. The curve given in Fig. 7.1 fits well to the data for the binary. Since it is a binary system, one can evaluate all the kinematic quantities which are needed. The curve shown in Fig. 7.1b is the exact curve expected if the system were radiating gravitational radiation at the expected rate. This is one of the few pieces of evidence, although indirect, for the emission of gravity waves and is perhaps not as compelling evidence as one might hope for.

Looking in Appendix D at dipole radiation for an electromagnetic system, relative to the quadrupole gravitational radiation that we have been discussing, the ratio is just a ratio of the relative coupling constants times some ω factors to make up for the dipole to quadrupole difference. Certainly, one would expect the ratio of the coupling constants if one writes the simplest first order Feynman diagram. Assuming that the binary system is moving at a substantial fraction of the velocity of light, the quantity of $b\omega/c$ is a number of order one.

As an example, if the system consists entirely of protons, then the ratio of the couplings is of order 10^{-36} . Therefore, if the system is charged by even the smallest amount, the electromagnetic

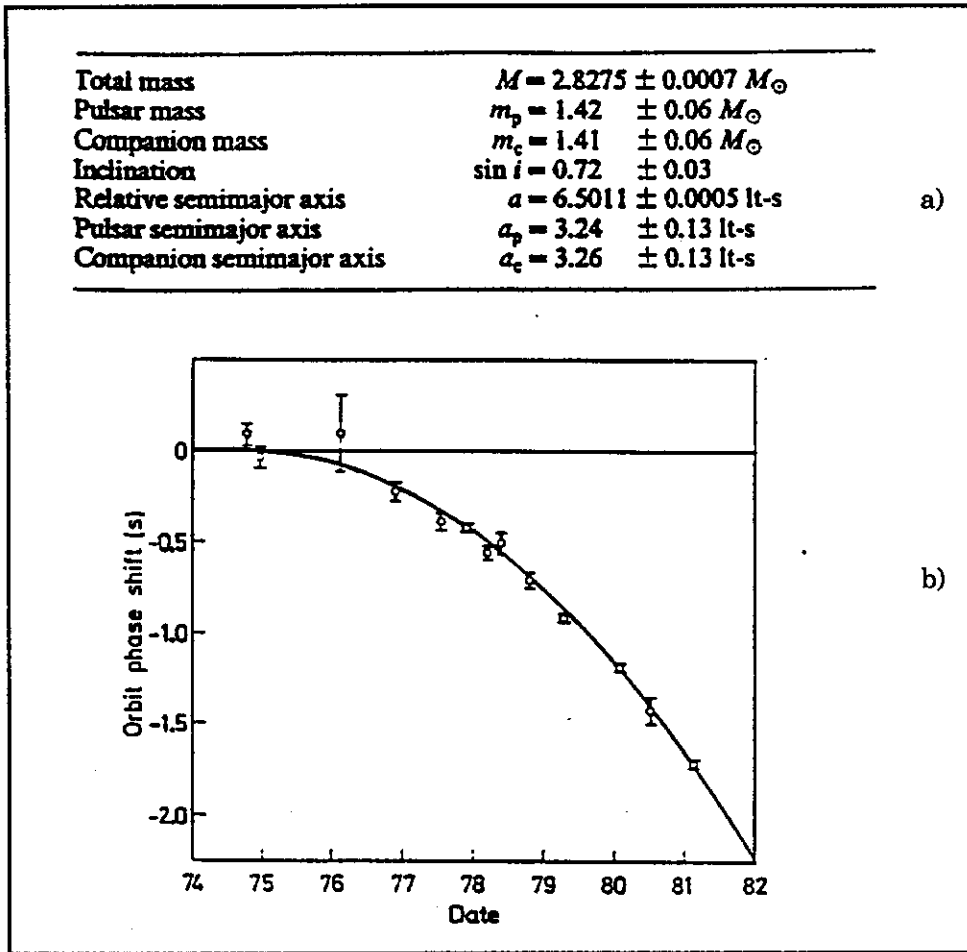


Fig. 7.1: a) Orbital data for the binary pulsar. b) Measured slowing down of the pulsar. The curve ascribes the deceleration to the emission of gravitational radiation.

radiation will dominate. If this is true, the slowing down of the binary system quoted above is fortuitous. For example, there are roughly 10^{57} protons in an object of roughly one stellar mass. Therefore, if gravitational radiation were to dominate, the system must be neutral to roughly 1 part in 10^{18} , because the gravitational coupling constant is relatively so weak.

$$\frac{\langle P \rangle}{\langle P \rangle_{EM}} \sim \frac{\alpha_G (b\omega/c)^2}{\alpha} \tag{7.12}$$

$$\alpha_G / \alpha \sim 10^{-36}.$$

To set the scale for possible detection of radiation, a selected set of binary star systems is given in Table 7.2. Some of the shortest period binaries, which are within a hundred parsecs of the Earth, deliver of order 10^{-16} Joules/(m^2 sec). These are known systems, and therefore give a benchmark, or bottom line, for the detection of gravitational radiation. The nice thing about detection is that you know such systems exist and you know in principle how much they should radiate. The received power sets the scale for the sensitivity of your detector. One is guaranteed a signal without invoking strange and bizarre new astrophysical sources of gravitational radiation. The bad news is, of course, that the power scale is very low.

How can the radiated power be related to the sensitivity of a possible detector? To begin, review the electromagnetic situation. Here the energy density goes as the square of the electric field and so the Poynting vector, the flux or the energy crossing unit area in unit time, is proportional to c times the energy density. This field causes an acceleration which is proportional to the coupling constant and the field itself. Appendix D shows us that the dynamical quadrupole moment is related to the tensor gravitational field. Therefore, it is simple to write down the gravitational Poynting vector.

$$\begin{aligned} |\vec{S}|_{EM} &= \frac{c}{8\pi} |E_0|^2, \quad \ddot{x} = \frac{qE_0}{m} \\ |\vec{S}|_G &= \frac{\omega^2}{2c} |\phi|^2. \end{aligned} \tag{7.13}$$

The difference between the gravitational and electromagnetic Poynting vectors arises from the fact that the lowest order radiation is dipole for electromagnetism and quadrupole for gravity. Recalling from the linearized theory Section, one recalls that a plane wave of the tensor field $\phi_{\mu\nu}$ will lead to a wave of tidal acceleration. Tidal acceleration is expected because we know that it is what is intrinsic to gravity fields. Since the tidal acceleration effects the metric which defines

| Binary | Period | Mass | Distance from Earth (pc) | τ (orbital decay time) | $(-dE/dt)_{\text{grav}}$ (J s ⁻¹) | Gravitational radiation at Earth (J m ⁻² s ⁻¹) |
|---------------------|------------|---------------|--------------------------------|-----------------------------------|--|---|
| η Cas | 480 yr | 0.94 0.58 | 5.9 | 3.8×10^{25} yr | 5.6×10^3 | 1.4×10^{-32} |
| ξ Boo | 149.95 yr | 0.85 0.75 | 6.7 | 1.5×10^{24} yr | 3.6×10^5 | 6.7×10^{-31} |
| Sirius | 49.94 yr | 2.28 0.98 | 2.6 | 2.9×10^{22} yr | 1.1×10^8 | 1.3×10^{-27} |
| Fu 46 | 13.12 yr | 0.31 0.25 | 6.5 | 1.3×10^{22} yr | 3.6×10^7 | 7.1×10^{-29} |
| β Lyr | 12.925 day | 19.48 9.74 | 330 | 2.8×10^{12} yr | 5.7×10^{21} | 3.8×10^{-18} |
| UWCMa | 4.393 day | 40.0 31.0 | 1470 | 3.3×10^{10} yr | 4.9×10^{24} | 1.9×10^{-16} |
| β Per | 2.867 day | 4.70 0.94 | 30 | 1.3×10^{12} yr | 1.4×10^{21} | 1.3×10^{-16} |
| WUMa | 0.33 day | 0.76 0.57 | 110 | 2.5×10^{10} yr | 4.7×10^{22} | 3.2×10^{-16} |
| WZSge | 81 min | 0.6 0.03 | 100 | 4.9×10^6 yr | 3.5×10^{22} | 2.9×10^{-16} |
| 10,000 km binary | 12.2 s | 1.0 1.0 | 1000 | 13.0 yr | 3.25×10^{34} | 2.7×10^{-6} |
| 1000 km binary | 0.39 s | 1.0 1.0 | 1000 | 11.4 h | 3.24×10^{39} | 2.7×10^{-1} |

Mass of each component star is shown in units of one solar mass. The final two entries are hypothetical, very close binaries involving two one-solar-mass objects separated by 10000 km and 1000 km respectively. Data taken from M.J. Rees, R. Ruffini and J.A Wheeler, *Black Holes, Gravitational Waves and Cosmology* (Gordon and Breach, London, 1974).

Table 7.2: Binary system sources of gravitational radiation.

physical distance, a fractional elongation is expected which is proportional to the dimensionless quantity $k\phi$, which is also equal to $2\Phi/c^2$.

$$\begin{aligned}
 g &\sim g_0 + k\phi \\
 (dx/x) &\sim k\phi \sim 2\Phi/c^2 \\
 &\sim k \sqrt{\left(\frac{2c}{\omega^2}\right) \left[\frac{\langle P \rangle}{4\pi r^2}\right]}.
 \end{aligned}
 \tag{7.14}$$

The magnitude of this dimensionless “wobble” in the metric caused by the wave of tidal acceleration can be estimated. We use the maximum collapse case of 10^{15} ergs/cm² quoted previously.

$$\begin{aligned}
 \kappa &= \sqrt{16\pi G} / c^2 = 6.5 \times 10^{-22} \text{ sec} / \sqrt{\text{kg} \cdot \text{m}} \\
 \langle \varepsilon_{MAX} \rangle / 4\pi r^2 \text{ at } 100 \text{ ly} &\sim 10^{12} \text{ Joule} / \text{m}^2 \\
 \omega &\sim 10^3 / \text{sec} \\
 \langle P_{MAX} \rangle / 4\pi r^2 &\sim 10^{15} \text{ Joule} / \text{m}^2 \text{ sec} \\
 \kappa\phi &\sim 5 \times 10^{-13} \\
 x &\sim 10 \text{ km} = 10^{14} \text{ \AA} \\
 dx &\sim x\kappa\phi \sim 50 \text{ \AA}.
 \end{aligned}
 \tag{7.15}$$

The coupling constant κ is related to Newton's constant G , as discussed in Section 3 on linearized general relativity. As previously mentioned, the absolute maximum collapse value of received power at 100 light years distance is 10^{15} Joules/(m² sec). This maximum leads to a dimensionless “wobble” of a few parts in 10^{13} . If one imagines this being studied in a 10 km lever arm interferometer, then one would expect a displacement of 50 Angstroms, which is enormous. In fact, the most useful near binary, which is given in Table 7.2, is not particularly pathological and leads to a dimensionless “wobble” of order 10^{-28} . This is a factor $\sim 10^{15}$ weaker than the maximum.

$$\begin{aligned}
 &\text{Observed Binary:} \\
 &3 \times 10^{-16} \text{ Joule} / \text{m}^2 \text{ sec} \\
 &\kappa\phi \sim 3 \times 10^{-28}
 \end{aligned}
 \tag{7.16}$$

There are a variety of laser interferometer gravity wave detectors which have been, or will soon be, taking data and which are designed to have a sensitivity in this dimensionless quantity of a few parts in 10^{22} . This is certainly getting within hailing distance of detecting known objects. Work on these systems has been going on in the U.S. and elsewhere since the early 1970's. At present, a typical lever arm is physically about 10 meters, and optically, about 80 meters with plans

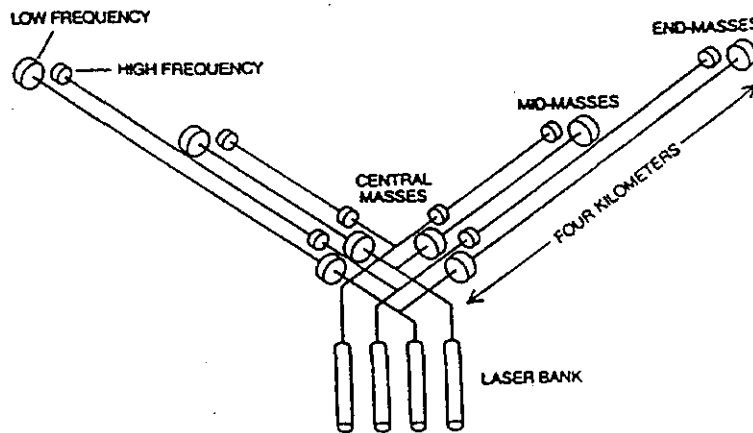
NEW ROUND of DETECTORS
COULD DETECT EXTRAGALACTIC SIGNALS by EARLY 1990's
 prototypes → → → full scale

CalTech (Mohave Desert)

} **Laser Interferometer Gravitation Wave Observatory**

MIT (Columbia, Maine)

LIGO sensitivity $\Delta l/l \approx 10^{-22}$
 several events/year
 Virgo & other nearby clusters
 total cost for 2: \$60,000,000



| | | | | | | | | | |
|--|----------------------|--------------------|--------------------|--------------------|--------|----------------|-------|------|---------|
| Country: | USA | FRG | GBR | USA | FRA | PRC | JPN | ITA | PRC |
| Institute: | MIT | MPQ | Glasgow | Caltech | Orsay | Quanzhou | Tokyo | Pisa | Beijing |
| Prototypes: | | | | | | | | | |
| Start: | 1971 | 1975 | 1976 | 1980 | 1983 | 1985 | 1986 | 1986 | 1985 |
| Technique: | DL | DL | FP | FP | (FP) | - | (DL) | (DL) | - |
| Armlength L : | 1.5 m (5 m) | (3 m) 30 m | (1.5 m) 10 m | 40 m | 5 m | 3 m | 10 m | 2 m | 0.5 m |
| N or $\frac{1}{2} f$: | 50 | 100 | 3000 | 2000 | | (2) | | | - |
| Optical Path L : | (80 m) | 3 km | 30 km | 75 km | | (6 m) | | | |
| Strain sensitivity $\frac{\Delta L}{L} \left[\text{Hz}^{-1/2} \right]$: | $(4 \cdot 10^{-17})$ | $1 \cdot 10^{-19}$ | $1 \cdot 10^{-19}$ | $2 \cdot 10^{-19}$ | | $(> 10^{-15})$ | | | |
| Laser: | Ar | Ar | Ar | Ar | Ar | HeNe | Ar | Ar | HeNe |
| Plans for Large Interferometers: | | | | | | | | | |
| Planning: | 1982 | 1985 | 1985 | 1984 | 1986 | | 1987 | 1987 | |
| Armlength L : | 4 km | 3 km | 1 km | 4 km | (3 km) | (3 km) | | 3 km | |

Fig. 7.2: a) Layout of interferometer for detection of gravity waves.
 b) Specifications for existing and proposed interferometers.

for extending the lever arm to several kilometers. Some data on present and future interferometers are shown in Fig. 7.2.

Finally, one needs to know how to extrapolate the interferometers looking for a few kilocycle radiation sources and the room temperature bars looking for stresses and strains from gravity waves. These latter are now operating in dimensionless elongation ratios of order a few 10^{-17} . Removing thermal noise by going to cryogenic bars seems to allow one to operate at 10^{-18} . It would appear that, momentarily, the interferometers will cross this limit and drive down to their avowed sensitivity of 10^{-22} . This will indeed be an exciting time because we know that gravitational waves should be observed. It is "merely" a question of getting to the proper sensitivity. Once one can see galactic and extragalactic gravitational sources, a whole new spectrum is opened up, which is complementary to the electromagnetic spectrum. Exciting times are clearly ahead in this field.

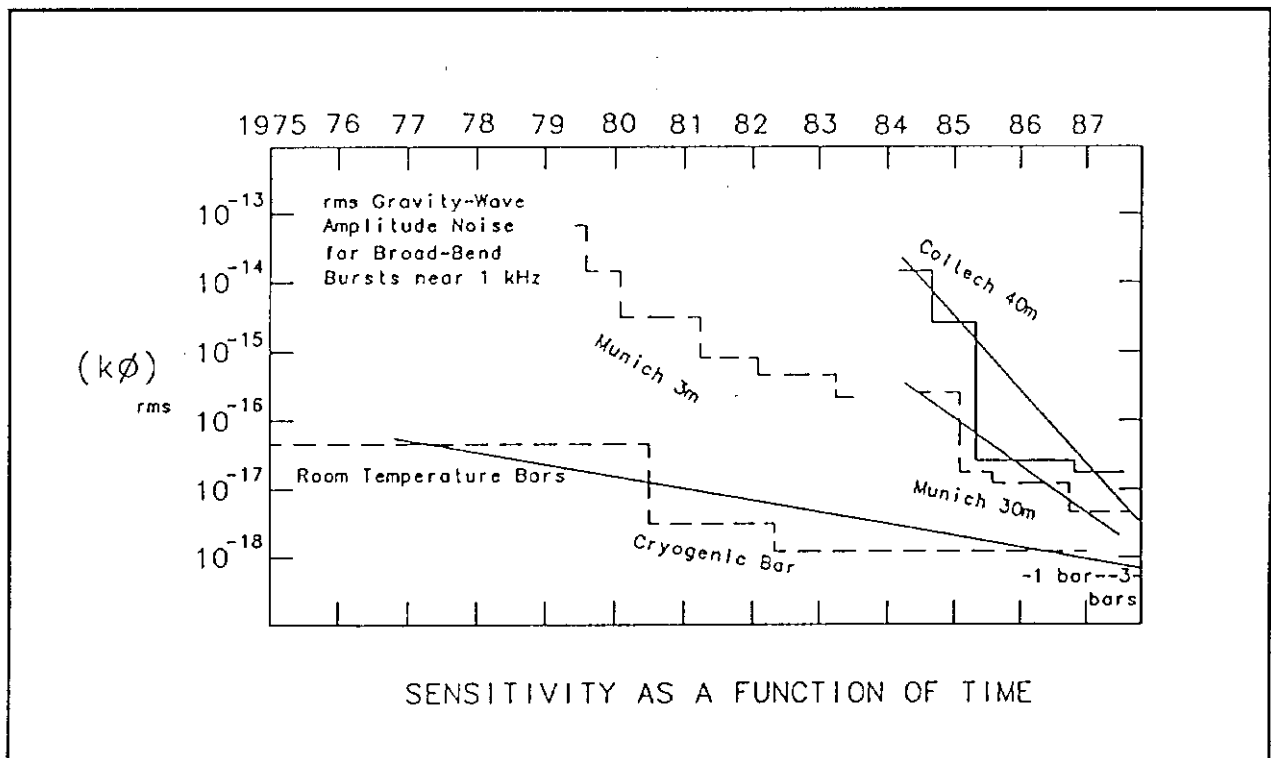


Fig. 7.3 Sensitivity of bar and interferometric gravity wave detectors as a function of time.

8 NEUTRON STARS; COLLAPSE LIMIT, NEUTRINO DIFFUSION, B FIELDS

In this Section, we will consider some of the technical questions about possible collapse of objects into a black hole. The reason for studying this is very simple; we have seen several times that the interesting Physics comes in the pathological situation when the size of the system is near its Schwartzchild radius. We also know that there is no stability for a gravitational system. Because gravity is always attractive, it does not have any stable configuration, a fact which was noted by Newton.

We are going to be looking at densities, so the first question we might ask ourselves is: What is normal density? What we mean by "normal" is what we are used to and what we are used to is the density of atomic systems. Atoms have radii which are set by a competitive balance between Coulomb attraction and the quantum zero point energy associated with localizing a system within a certain region in space. To observe this, write down the Schrödinger equation for a single particle. This is just an operator statement that kinetic energy plus potential energy is total energy as recalled from the Equivalence Principle discussion. Using the uncertainty relation, momentum times position is of order \hbar . The minimum value for ϵ occurs at a_0 .

$$\begin{aligned} \frac{p^2}{2m} - e^2 / r &= \epsilon \\ \frac{\hbar^2}{2mr^2} - e^2 / r &= \epsilon \\ r = a_0 = \hbar^2 / me^2 &= \lambda_e / \alpha \\ &\sim 1\text{\AA}. \end{aligned} \tag{8.1}$$

The expression for the total energy has a minimum which is the ground state. This state occurs at a characteristic radius, which is the Yukawa wavelength for the electron divided by the coupling constant. This makes some sense because, if the coupling were very weak, then the system would get very large as it is loosely bound. The Yukawa wavelength is also the only characteristic

length scale in the problem, so the Bohr radius must be proportional to it. Calculating the Bohr radius, a characteristic size of about one Angstrom results. The characteristic density is then roughly 1 proton per cubic Angstrom, or 1.7 grams/cm³.

$$\sigma_A \sim m_p / (1\text{\AA})^3 \sim 1.7 \text{ gm/cm}^3. \tag{8.2}$$

It is amusing that one can calculate, in a few lines, why most systems have a density about 1 gram/cm³. Figure 8.1a pictorially shows the situation where the size of the atom is the Bohr radius, or about 1 Å. This size is set by the zero point energy of the electrons, whereas the mass of the system is localized in the nucleons, which are about 2000 times heavier.

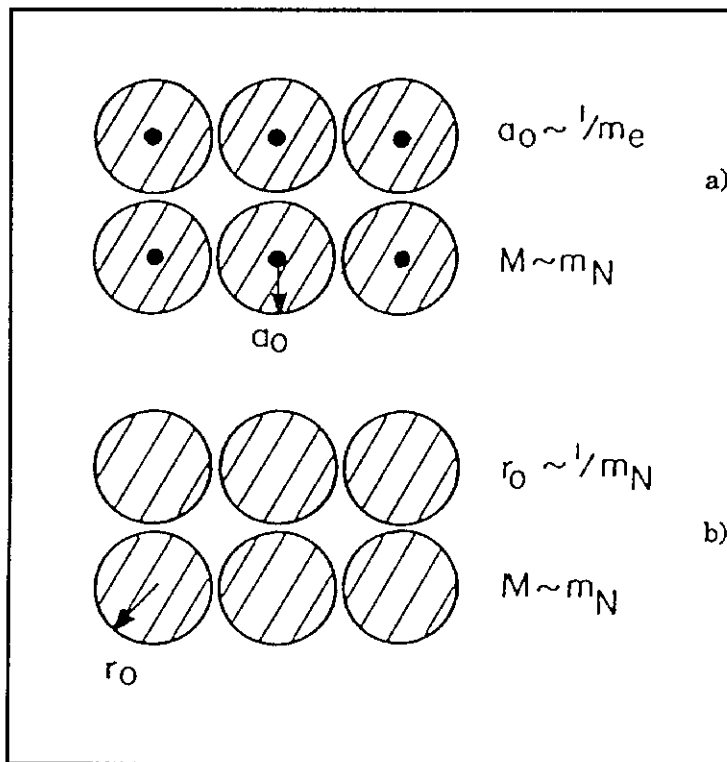


Fig. 8.1: a) Schematic for density of normal matter. b) Schematic for density of nuclear matter.

What about nuclear densities? By using the same arguments, the size is the Yukawa length of the nucleon divided by the strong coupling constant α_s . Because α_s is roughly one, the size is roughly 1fm. Since this volume contains 1 nucleon, there is a nuclear density of 10^{18} kilogram/m³. Figure 8.1b shows the situation in this case where both the zero point energy and the mass of the nucleus are given by the same size scale.

$$\begin{aligned} r_0 &\sim \lambda_N / \alpha_s \sim 1fm \\ \sigma_N &\sim 10^{18} kg / m^3 \\ \sigma_N R^3 &= M_\odot \rightarrow R \sim 12km. \end{aligned} \tag{8.3}$$

An interesting question to ask is: What is the characteristic size of an object of nuclear density which has the mass of one solar mass? The answer is a radius of about 10 kilometers. This, as will be discussed later, is the characteristic size of a neutron star.

Stars are normally thought of as being stable because they burn for a long time. A star burns by fusion processes until it turns into iron, which has the lowest binding energy per nucleon. A crude lifetime estimate of a typical star can be made by taking the solar luminosity given in Appendix A, along with the solar mass. Nuclear physics explains that the binding energy per nucleon from fusion is only about 8 MeV. Assuming all is constant, the lifetime is of order tens of billions of years. Therefore, a star is stable for a long time, but being a finite process, it burns out. The pressure of the fusion reactions can no longer be in equilibrium with gravity. There is nothing to prevent the collapse of the star into a much more compact object.

$$\begin{aligned} B &\sim 8MeV / nucleon \\ \tau_\odot &\sim \frac{B}{m_p} M_\odot c^2 / L_\odot \\ &\sim 40 billion years. \end{aligned} \tag{8.4}$$

To test the stability condition for a burned out star, one needs to see if it is possible to balance gravity against the zero point energy of the electrons, which is the case for a white dwarf, or the

neutrons, which is the case for a neutron star. We proceed in analogy to the discussion in Eq. 8.1, where the balance between the zero point energy and the electromagnetic attraction was derived. First we want to define another characteristic wavelength which is the deBroglie wavelength. It is similar to the Yukawa wavelength except that the mass of the particle is replaced by its momentum divided by c .

Quantum mechanics explains that each phase space cell in position-momentum space is of size \hbar . This can be thought of as the closest possible packing, consistent with the uncertainty principle and the exclusion principle. Given the cell size, N states can be filled in a volume \mathcal{V} up to the Fermi momentum p_F . The Fermi momentum then defines the deBroglie wavelength for this situation.

$$\begin{aligned}
 \lambda_{dB} &\equiv \hbar / p \\
 d\vec{x} d\vec{p} &= \hbar^3 \\
 \mathcal{V} p_F^3 &= N \hbar^3 \\
 (\lambda_{dB})^3 &= \mathcal{V} / N.
 \end{aligned}
 \tag{8.5}$$

The Fermi momentum is related to the Fermi energy in general by the special relativistic formula. In particular, in the non-relativistic case, it is proportional to the square root of the Fermi energy. In the ultra-relativistic case, it is proportional to the first power of the Fermi energy.

$$\begin{aligned}
 \epsilon_F &= p_F^2 / 2m, \quad NR \\
 &= c p_F, \quad UR.
 \end{aligned}
 \tag{8.6}$$

For non-relativistic particles, the lowest mass then dominates the zero point energy, while for ultra-relativistic particles, there is no mass dependence. If the ultra-relativistic situation occurs, Eq. 8.1 shows us that the zero point energy goes as $1/r$. Since the gravitational self energy also goes as $1/r$, we are in an unstable situation. In the non-relativistic case, the zero point energy goes as $1/r^2$. We therefore recover the stable situation, which is analogous to the discussion of the

hydrogen atom. The unstable regime is obviously reached when the Fermi level becomes relativistic. Note that $\beta \sim \alpha$ for the hydrogen atom, so that we remain in the non-relativistic regime. Since α_G grows as M^2 , this will not be the case for gravity.

The Fermi level can be related to the number of states per unit volume. Using Eq. 8.5, the Fermi momentum can be set equal to the mass at the stability boundary when the Fermi momentum is becoming relativistic. We define this to happen at a mass equal to the Chandrasekhar mass. At this mass, the gravitational self energy is equal to the total kinetic energy, which is the number of states times the particle kinetic energy.

$$\begin{aligned}
 p_F &= \hbar(N/V)^{1/3} \sim \frac{\hbar}{R} N^{1/3} \sim mc \\
 &\text{at } M = M_{CH} \\
 GM_{CH}^2 / R &= N(p_F^2 / 2m) \sim N\left(\frac{mc^2}{2}\right).
 \end{aligned} \tag{8.7}$$

Solving for this limiting mass, it is found to be proportional to the Planck Mass.

$$\begin{aligned}
 M_{CH}^2 &\sim NRmc^2 / G \\
 &\sim \frac{Nmc^2}{G} \left[\frac{\hbar N^{1/3}}{mc} \right] \\
 &\sim N^{4/3} M_{PL}^2.
 \end{aligned} \tag{8.8}$$

The limiting number of particles is the total mass of the system divided by the mass of its constituents. This allows us to express the Chandrasekhar limit as a limit on the total number of particles in the system. The limit is the ratio of the Planck mass to the mass of the constituents raised to the 3rd power.

$$\begin{aligned}
N &= M / m \\
M_{CH}^2 &\sim M_{CH}^{4/3} M_{PL}^2 / m^{4/3} \\
M_{CH} &\sim \left(\frac{M_{PL}}{m} \right)^3 m \\
N_{CH} &\leq (M_{PL} / m)^3.
\end{aligned}
\tag{8.9}$$

If the constituents are nucleons, then the Chandrasekhar limit on the mass is about 1.4 solar masses. Masses of pulsars (rotating neutron stars) are shown in Fig. 8.2.

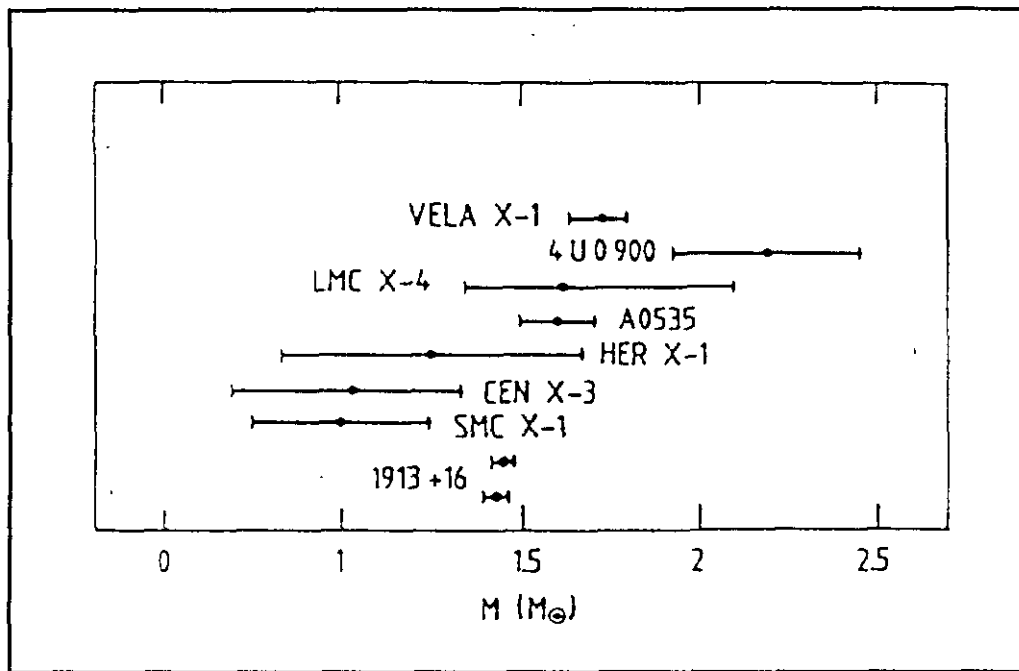


Fig. 8.2: Masses of known pulsars in units of solar masses. Note that no rotating neutron star appears to be much above M_{CH} .

Note that no entry greatly exceeds this mass limit. Since the Planck mass is roughly 10^{19} nucleon masses, the ratio cubed is about 10^{57} . This is roughly the number of nucleons in the sun since the mass of the sun, as seen in Appendix A, is about 10^{30} kilograms. As recalled from the interior Schwartzchild solution discussion, there is a critical density when the radius of the system is equal to the Schwartzchild radius. It is of interest to note that, when the mass of the system is roughly one

stellar mass, the critical density is about 10^{19} kg/m³, which is roughly what we estimated for nuclear densities. One solar mass at nuclear densities, therefore, has a radius equal to its Schwartzchild radius.

$$\begin{aligned}
 M_{CH} &\sim 1.4M_{\odot}, \\
 \sigma_c &\sim 3c^2 / (8\pi G r_s^2) \\
 &\sim 10^{19} \text{ kg / m}^3 \sim \sigma_N.
 \end{aligned}
 \tag{8.10}$$

As an aside, the density at which the system radius is equal to the Schwartzchild radius can be evaluated. That density, the critical density, decreases as the reciprocal of the system mass squared. This reconciles the fact that a very tenuous Universe may be closed (we may be living inside a black hole), whereas an object of near nuclear densities may not close upon itself. Such are the scaling properties of the gravitational self energy.

$$\begin{aligned}
 \frac{2GM}{c^2} &= r_s \\
 \sigma &> (3c^6 / 32\pi G^3 M^2).
 \end{aligned}
 \tag{8.11}$$

The relevant densities can now be evaluated. We start with a star which, when it burns out, will start to collapse under the mutual gravitational attraction of all its elements. If it is a small enough star to be halted by the non-relativistic zero point energy of the electrons, it is called a white dwarf. If it is a higher mass object, it will continue to collapse down to linear dimensions roughly 100,000 times less and finally be made stable by the zero point energy of the nucleons. This behavior obtains because, looking at Eq. 8.1, we see that the linear dimensions of the system go as the inverse of the mass of the constituent which is supplying the stabilizing zero point energy. If the system is yet heavier, (for example, we estimated a few stellar masses), there is no stability condition (as was shown) and the system must collapse into some sort of singularity.

As a side light, you might ask why a neutron star does not decay. When looking in the Particle Data Book, free neutrons are found to decay. In the case of a neutron star you are in a situation with nuclear densities. You know from the existence of various nuclei that neutrons are stable in a nuclear environment characterized by high nuclear densities. This is true because all the low-lying states are filled, due to the high density, which makes the neutron stable. In fact, during the collapse, the reaction $e^- + p \rightarrow n + \nu$ is expected to occur as the immense pressure basically forces the electrons into the protons to make stable neutrons and a pulse of neutrinos.

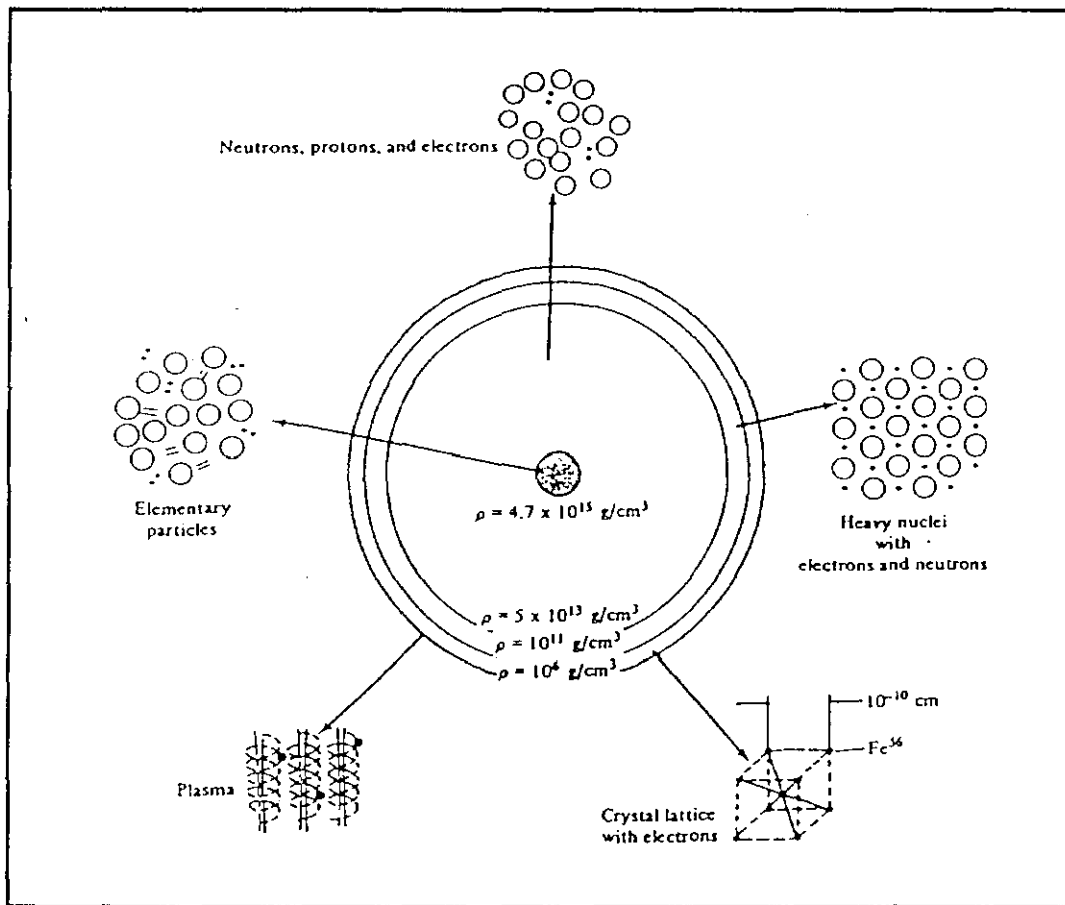


Fig. 8.3: Density and structure for a neutron star.

The structure of the neutron star, which is the most compact, non-collapsed structure imaginable, is shown in Fig. 8.3. The central density, as expected from Eq. 8.3, is characterized by the nuclear density of 10^{15} gm/cm³. At much reduced densities, and much larger sizes, a shell of material can be held in stable equilibrium by the zero point energy of the electrons. The ratio of those densities is, as discussed, related to the mass ratio of the elementary particles providing the zero point stabilizing energy.

For the remainder of this Section not much about black holes will be discussed. There is effectively no observational evidence for the existence of a real singularity and there is some question about the very existence of singularities in one's theory. It is, after all, a classical theory containing no quantum effects. Conversely, quantum effects are expected to become extremely important when we are crashing down to a point singularity with infinite density. Therefore, the fact that the classical theory of gravity predicts point singularities is perhaps irrelevant, and in the absence of any data it is fruitless to speculate.

In the remainder of this Section, we will consider what happens when the burned out nickel-iron core, of order 1 stellar mass, collapses down to a neutron star. We imagine that a substantial fraction of the lost potential energy is available as gravitational radiation; see Section 7. We also imagine that the conversion of electrons + protons to neutrons will give rise to a distinctive neutrino pulse. Let us begin by considering the pressure in a strictly classical Newtonian formulation. The differential equation for the pressure can be found by considering the packing of a shell of matter under gravitational attraction. The attraction leads to a force per unit area, or a pressure element, which is proportional to the thickness of the shell, dr .

$$\begin{aligned} \frac{dP}{dr} &= \frac{G\sigma(r)M(r)}{r^2} \\ \sigma(r) &= \sigma_0, \quad M(r) = M_0(r/R)^3 \\ P(r) &= \left(\left(\frac{r}{R} \right)^2 - 1 \right) \left(\frac{GM_0\sigma_0}{2R} \right). \end{aligned} \tag{8.12}$$

For a constant matter density, the mass scales as the radius to the 3rd power. This allows us to solve the differential equation for pressure as a function of radius. The boundary condition is that the pressure, by definition, vanishes at the surface. The pressure is therefore maximum at the center of the star. This maximum pressure goes like the ratio of the Schwartzchild radius to the system radius and is proportional to the rest energy density. Thus, for a fixed mass it scales like the inverse 4th power of the radius.

$$\begin{aligned}
 (\underline{P})_{MAX} &\sim GM_0\sigma_0/2R \\
 &\sim \left(\frac{r_S}{R}\right)\left(\frac{\sigma_0 c^2}{4}\right) \sim GM^2/R^4.
 \end{aligned}
 \tag{8.13}$$

As a numerical example, if the mass density is a nuclear density and if the radius is equal to the Schwartzchild radius, which is 10 km, there is a pressure of 10^{29} atmospheres. This pressure is 10^{19} times larger than the pressure at the center of the sun, clearly because the problem scales as the 4th power of the radius.

$$\begin{aligned}
 \sigma_0 &= \sigma_N, \quad R = 10km \sim r_S \\
 (\underline{P})_{MAX} &\sim 10^{29} \text{ ATM} \\
 (\underline{P})_{MAX,\odot} &\sim 10^{10} \text{ ATM}.
 \end{aligned}
 \tag{8.14}$$

Recalling the Schwartzchild solution discussion, the tidal stress on a person at the Schwartzchild radius was a mere 10^7 atmospheres. The general relativistic generalization of the differential equation given in Eq. 8.12 is a rather involved non-linear equation due to Tollman, Oppenheimer, and Volkoff. For example, pressure, as seen in Appendix D, has the dimensions of an energy density. Pressure obviously has mass and thus gravitates, therefore resulting in a complicated non-linear equation which must be solved numerically. Since this level of detail is outside the spirit of this note, it will not be discussed further.

If a drastic simplifying assumption is made that there is no pressure gradient, then the mass interior to radius r just goes like r^3 . This assumption allows us to write a partial differential equation relating the mass and the radius. Assuming the system is in free fall, there is a partial differential equation for the acceleration of a mass element. Time can be solved for as a function of the radius using separation of variables.

$$\begin{aligned} \partial r / \partial M &\sim 1 / 4\pi r^2 \sigma \\ \sigma \partial^2 r / \partial t^2 &= \frac{-GM}{r^2} \sigma \\ r(t) &\sim t^{2/3}. \end{aligned} \tag{8.15}$$

As asserted previously, this crude approximation implies a quick power law collapse. The collapse increases rapidly in its later stages, leading to a pulse of neutrinos and gravitational radiation.

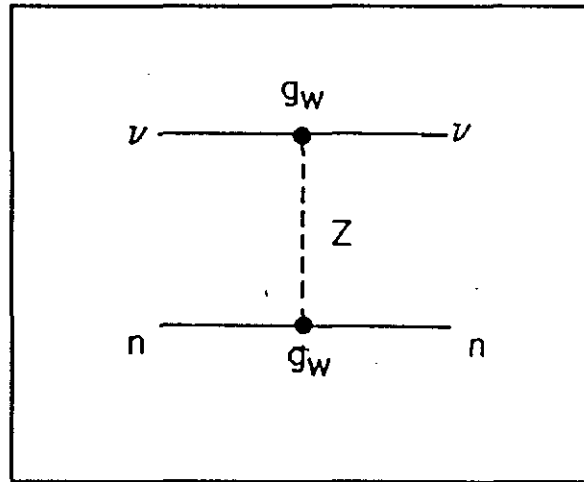


Fig. 8.4: Lowest order neutral current Feynman diagram for neutrino elastic scattering.

Given the power law behavior of the collapse, a rather rapid neutrino pulse is expected. For example, in Supernova '87, there was a neutrino pulse discovered in underground experiments which was coincidental in time with the optical observation of the Supernova. As seen in Fig. 8.4a,

however, there was a considerable spread in the arrival time of the neutrino pulse. How can this be understood? In principle, the neutrinos are rapidly emitted. However, this is an extraordinarily dense substance (nuclear matter); the neutrinos are expected to scatter and diffuse on their way out. This would normally not be expected because low energy neutrinos are very weakly interacting particles. However, the densities involved more than offset the weakness of the interaction.

Figure 8.4 shows the relevant first order diagram for neutral current elastic scattering of neutrinos off neutrons by the exchange of a Z boson. It is clearly observed by coupling constant and dimensional arguments, that the 2 body neutrino scattering cross section is proportional to the weak fine structure constant squared. At high energies Σ_ν is expected to go like $1/s$, however as stated earlier, there is a weak propagator that makes the weak interactions appear weak at low energies. At these energies we expect Σ_ν to be proportional to s .

$$\begin{aligned}
 \Sigma_\nu &\sim \frac{g_W^4}{\pi} \left[s / (s + M_W^2)^2 \right] \\
 &\rightarrow \alpha_W^2 / \pi s \\
 &\rightarrow \alpha_W^2 s / \pi M_W^4.
 \end{aligned}
 \tag{8.16}$$

This expression for the neutrino cross section leads to an easily estimated neutrino mean free path.

$$\begin{aligned}
 L_\nu^{-1} &\sim N_0 \sigma_N \Sigma_\nu \\
 &\sim N_0 \sigma_N \alpha_W^2 (s / M_W^4) \\
 (\Sigma_\nu)_{E_\nu=10\text{MeV}} &\sim 2 \times 10^{-40} \text{ cm}^2 \\
 L_\nu &\sim 10 \text{ cm}.
 \end{aligned}
 \tag{8.17}$$

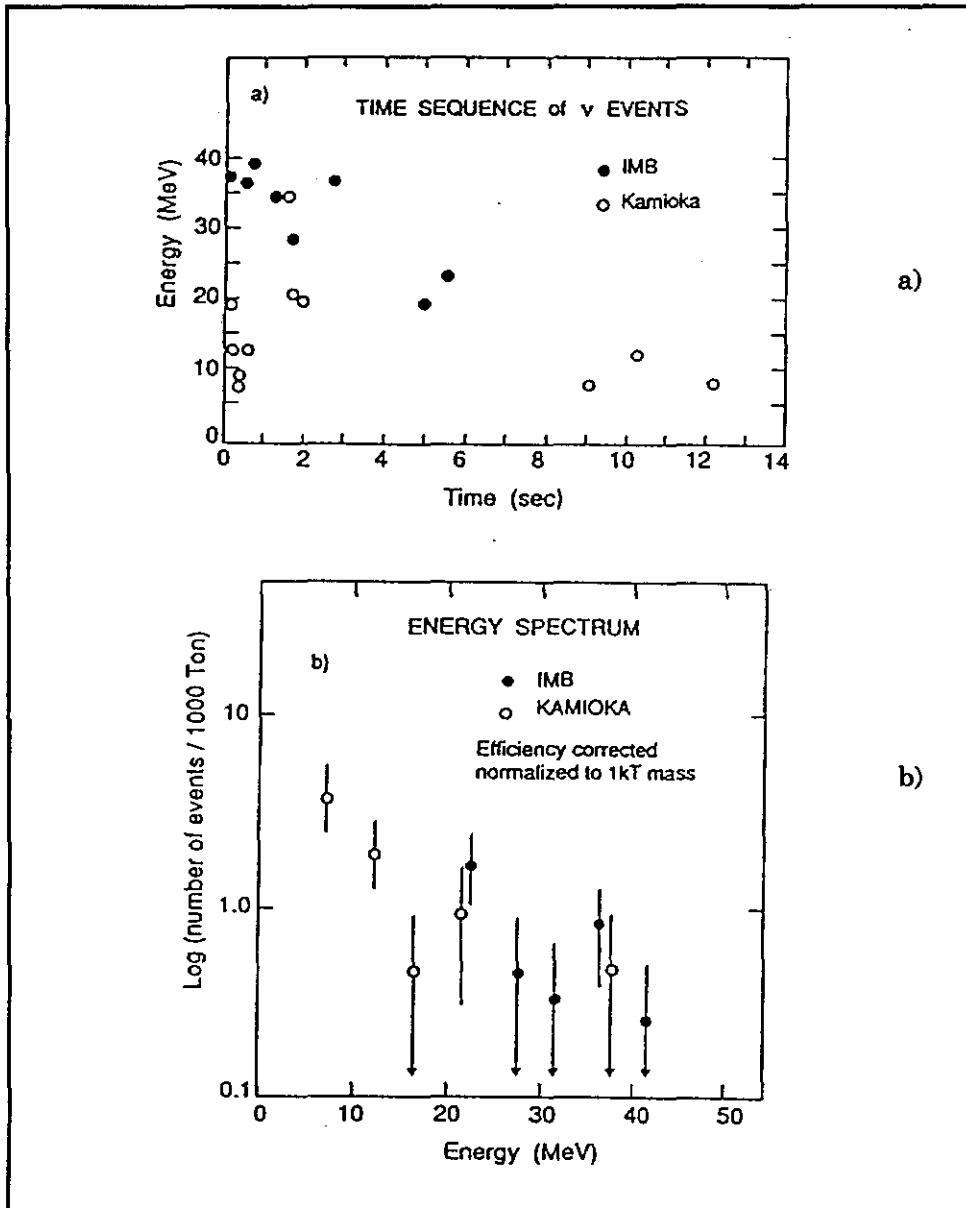


Fig. 8.5: Data from IMB and Kamioka on the Supernova 1987 neutrino burst. a) Arrival time distribution. b) Energy distribution of neutrinos.

To make a numerical estimate, recall that the weak fine structure constant α_w is comparable to the electromagnetic fine structure constant α . This is what is meant by electroweak unification. Given the numerical value of α and the Weinberg angle, α_w is found to be about 1/30. Using Eq. 8.16 for neutrino scattering off nucleons, a 10 MeV, $\epsilon_\nu \sim B$, neutrino (see Fig. 8.4b) has an incredibly small cross section of order 10^{-40} cm². The mean free path at nuclear densities is only about 10 cm. The ratio of the densities is roughly the ratio of the linear dimension of the size of an atom (1Å) to the size of the nucleon (1 fermi), a factor of 10^5 , raised to the 3rd power, or 10^{15} . Since normal densities are 1 gm/cm³, nuclear densities are 10^{15} gm/cm³. Because the source size is of order 10 km and the mean free path is 10 cm, it can be imagined that the neutrinos diffuse out from the core over some substantial period of time. A straight line neutrino time scale is R/c or 10 μ sec for 10 km. For comparison, the scale in Fig. 8.4 is seconds. This spread was observed in Supernova 1987 and gave some important clues as to the dynamics of the collapse. Some supernovae properties are given for reference purposes in Table 8.1.

| Energetics | Light curves and spectra | | |
|--|--------------------------|---------|---------------|
| | | Type I | Type II |
| Maximum Luminosity 10^{44} erg s ⁻¹ | Near Maximum light for | 30 days | 10 days |
| Energy in visual light 10^{48} - 10^{50} erg | Plateau | no | yes, 100 days |
| Total energy output 10^{51} - 10^{52} erg | Duration | 2 years | 1 year |
| Expansion velocity 10^4 km s ⁻¹ | H-lines | no | strong |
| Temperature near maximum light 15000 K | Abundances | Co, Fe? | solar |

Table 8.1: Properties of Supernovae.

What about the situation after the core has collapsed down to a neutron star? In this case there would be a rather dense object, and the question arises - What happens with the core? During collapse the magnetic flux is conserved. Thus, for example, if there is a one Gauss field at a stellar radius, collapse by a factor of 10^5 in linear dimensions (down to 10 km) results in a field of 10^{10} Gauss. This field is far above any imaginable laboratory field that could be produced. For example,

a Fermilab magnet might run at 3 Tesla which is 3×10^4 Gauss, or a million times weaker. A plot of inferred surface magnetic field as a function of pulsar period is given in Fig. 8.6. The scale roughly agrees with our simple estimates.

The angular momentum is another conserved quantity in a collapse, which tells us that ωr^2 is a constant. As an example, there is a pulsar with a 0.33 millisecond period in the Crab Nebula. If we scaled up by $(10^5)^2$, we would get 0.1 years which is certainly comparable to the 30 day rotation period of our sun.

$$\begin{aligned} BR^2 &= \text{CONST} \\ \omega R^2 &= \text{CONST}. \end{aligned} \tag{8.18}$$

What is the implication for energy loss mechanisms? The dipole radiation formula made plausible in the gravitational radiation Section and which was quoted in Appendix D will be used. First we remind ourselves that electric dipole and magnetic dipole radiation are formally exactly the same. The rotational energy is the moment of inertia times ω^2 which is the analog of mv^2 for translational energy. The slowing down rate of the frequency of the system can be found by equating the change in energy per unit time to the radiated power.

$$\begin{aligned} \langle P \rangle_{EM} &\sim \frac{2}{3} c^3 D_B^2 \omega^4 \\ \epsilon &= I \omega^2 \\ d\epsilon / dt &\sim -I \omega d\omega / dt = \langle P \rangle_{EM} \\ I &\sim M_{CH} R^2. \end{aligned} \tag{8.19}$$

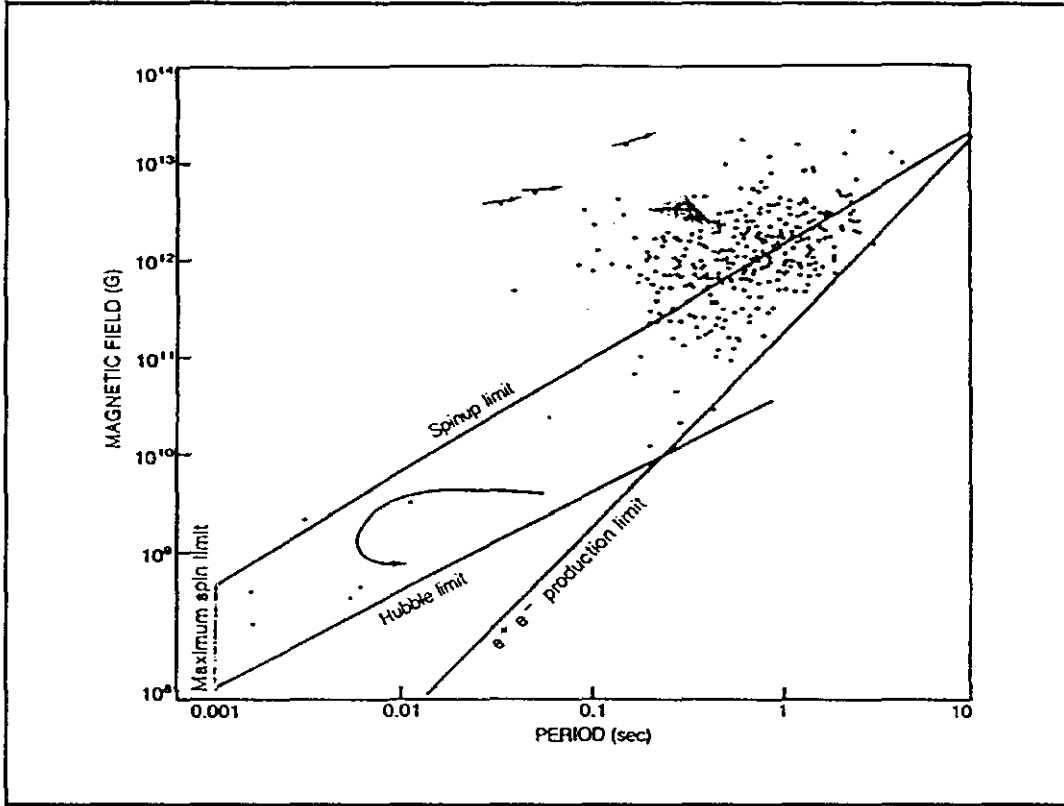


Fig. 8.6: Inferred surface magnetic fields of rotating neutron stars as a function of rotational period.

If a neutron star is taken with parameters roughly equal to those quoted above, the period of slow down due to the emission of magnetic dipole radiation can be found.

$$\begin{aligned}
 \tau_B &\equiv \left(\frac{d\omega}{dt} \right)^{-1} \omega \\
 &= (c^3 M_{CH} R^2) / (D_B^2 \omega^2) \\
 M_{CH} &\sim M_\odot, \quad R \sim 10 \text{ km} \\
 B &\sim 10^{10} \text{ Gauss} \sim D_B / R^3 \\
 \omega &\sim 1 / (3 \times 10^{-4} \text{ sec}) \\
 \tau_B &\sim 1000 \text{ yrs.}
 \end{aligned}
 \tag{8.20}$$

A lifetime of roughly a thousand years can be found for the typical case of a stellar mass of size 10 km with a field 10^{10} Gauss, and with a Crab Nebula pulsar scale frequency of some kilohertz. It is on this scale that the heaviest possible neutron star would radiate away its rotational energy and slow down. As said in the gravitational radiation discussion, if the object has any charge or any magnetic field, it would appear from coupling constant arguments that the slowing down effect would be dominated by electromagnetism and not gravity. It would appear from observation that this time scale is compatible with the slow down of some of the pulsars which have been observed in our galaxy.

Finally, what about the effect of these magnetic fields on particles in the neighborhood of the pulsar? The magnetic field at the surface of the star rotates with a velocity which is proportional to ω . The existence of this velocity implies that there is an electric field via relativistic transformation.

$$\begin{aligned} E &\sim \beta B \sim \omega RB / c \\ \epsilon &\sim eER \sim e\omega BR^2 / c. \end{aligned} \tag{8.21}$$

This electric field would then accelerate particles over a characteristic distance of some kilometers. Therefore, the possibility exists that these point pulsars are sources of enormously high energy cosmic rays. For example, if we take a millisecond pulsar with 10 km radius, β is found to be 0.03. If we take 10^{10} Gauss, then the electric field is 10^{13} Volts per meter, which is quite a Linac. This Linac could be very handy in the Fermilab Upgrade program, because, if it extends over 10 km, it would lead to acceleration energies of 10^{17} eV which is a total lab energy of 100,000 TeV or a center-of-mass energy in nucleon collisions of 10 TeV.

$$\begin{aligned} \beta &\sim 0.03, \quad E \sim 10^{13} \text{ Volt / m} \\ \epsilon &\sim 10^5 \text{ TeV} \\ \sqrt{s} &\sim 10 \text{ TeV}. \end{aligned} \tag{8.22}$$

It is a fascinating speculation that all cosmic rays might be due to these point sources. All the ingredients exist to make immensely high energy accelerating mechanisms. However, this may not be the case and experiments on this topic in Astrophysics are plagued with small sample statistics. It would be interesting to think of this subject as a possible Astrophysics experiment involving Fermilab physicists.

9 HAWKING “EVAPORATION”

The topic in this Section is due to an observation by Hawking. Thus far, any discussion of quantum gravity effects has been studiously avoided. A first attempt would be to try to do quantum field theory for some other interaction on a classical curved space-time (due to gravitation). Few gravitational quantum effects should be expected since the classical curvature radius is large with respect to the Planck length. The Planck length is the characteristic length over which we expect quantum fluctuations in the metric. As mentioned earlier, this should only set in at enormously high energies which are presently inaccessible to direct experiment. Hawking realized, however, that a black hole creates particles as a black body at a temperature which we label as the Hawking temperature. We omit the proof of this assertion.

$$\begin{aligned}(kT)_H &= \hbar a / 2\pi c \\ a &= GM / r_s^2 \\ &= c^4 / 4GM \\ &= c^2 / 2r_s.\end{aligned}\tag{9.1}$$

This thermal radiation leads to a loss of mass or, ultimately to the “evaporation” of black holes. The reason is simply because the surface acceleration at the Schwartzchild radius of a black hole increases as the mass decreases. As the radiation occurs and mass is lost, the surface acceleration rises, and the surface acceleration is proportional to the temperature. At higher temperatures one emits more energy, as is familiar from the Stefan-Boltzmann Law. This is, therefore, a runaway process and the black hole spontaneously evaporates. It was Hawking’s insight that lead to the realization that black holes are not stable under quantum fluctuations.

The particles are created near the horizon, or the Schwartzchild radius, by the strong gravitational fields. It is a vacuum fluctuation during which, for example, one particle falls into the hole and the other escapes. This is similar to the Penrose mechanism for extracting energy from a

rotating black hole. Instead of sending a particle in on some trajectory, however, one allows the vacuum to make the quantum fluctuation resulting in the pair of particles. By calculating, one finds that the characteristic thermal Hawking energy for the sun is roughly 10^{-18} GeV which is completely unobservable as it is much less than the $5,000 K^0$ at the sun's surface.

$$\begin{aligned} T_H &\sim 6.2 \times 10^{-8} K^0 (M_\odot / M) \\ (kT)_H^0 &\sim 1.4 \times 10^{-18} \text{ GeV}. \end{aligned} \tag{9.2}$$

The Stefan-Boltzmann law can be used to derive the lifetime, τ_H , for this evaporation process. In Eq. 9.3, σ is the Stefan-Boltzmann constant. In all previous Sections, σ was the matter density, ρ was the charge density, and Σ was a cross section. The energy per unit area per unit time is U and is proportional to the fourth power of the temperature. If U is set equal to the rest energy of the singularity divided by the evaporation time (or the Hawking time) times the radius squared, then by simple dimensional arguments the evaporation time is found to be proportional to the Schwartzchild radius. If one picks the most extreme environment for which we have evidence, a neutron star with radius equal to the Schwartzchild radius (10 km), the evaporation time is enormously longer than the lifetime of the Universe. Clearly, this quantum evaporation is only important for miniscule black holes with an extremely small Schwartzchild radius, otherwise it is irrelevant to the large scale structure of the Universe.

$$\begin{aligned} U &= \sigma T^4 \\ &\cong (Mc^2) / \tau_H R^2 \\ c\tau_H &\sim \left[\left(\frac{Mc r_S}{\hbar} \right) \left(\frac{r_S}{R} \right)^2 \right] r_S \\ r_S &= 10 \text{ km}, \quad \tau_H \sim 10^{56} \text{ B yr}. \end{aligned} \tag{9.3}$$

The real significance of evaporation, however, may be that it is telling us that quantum mechanics modifies the classical theory in predicting singularities. Since, in this first look one finds that singularities disappear, perhaps they do not exist in the full quantum theory of gravity.

Finally, in a real quantum theory of gravity, the coupling constant diverges and will violate unitarity at sufficiently high energies, of order the Planck mass. The classical theory of gravity, although it has enjoyed enormous success and has been tested (as has been seen) in many different ways to a few percent, must break down at energies of order 10^{19} GeV. Historically there have been a variety of attempts to avoid this problem which are beyond the scope of this simple minded note. At some future point, one can look forward to understanding quantum gravity and thus how the unitarity violation is evaded - this is something "devoutly to be wished for."

The implicit assumption here is that Nature is simple, unified, and ultimately explicable. The goal is to combine gravity and quantum mechanics, and perhaps unify all the forces of Nature.

*"What we call the beginning is often the end and to make
an end is to make a beginning.*

:

*We shall not cease from exploration, and the end of all
our exploring will be to arrive where we started and know
the place for the first time.*

:

A condition of complete simplicity

:

And all shall be well".

T.S. Eliot, Little Gidding

10 ACKNOWLEDGMENTS

~~The patience and care given to this document by Kristen Ford is hereby gratefully and~~
effusively acknowledged. Many comments from the FNAL audience were also incorporated in the
written notes.

11 REFERENCES

- 1) C. Misner, K. Thorne, J. Wheeler, Gravitation, W.H. Freeman, and Co, San Francisco (1973).
- 2) H. Ohanian, Gravitation and Spacetime, W.K. Norton and Co. New York (1976).
- 3) W. Rindler, Essential Relativity, Van Nostrand Reinhold Co., London (1969).
- 4) M.V. Berry, Principles of Cosmology and Gravitation, Roam Hilger, Bristol (1989).
- 5) S. Hawking, G.F.R. Ellis, The Large Scale Structure of Space-Time, Cambridge Press, New York (1973).
- 6) R. Adler, M. Bazin, M. Shiffer, Introduction to General Relativity, McGraw-Hill, New York (1975).
- 7) N. Struamann, General Relativity and Relativistic Astrophysics, Springer-Verlag, Berlin (1984).

APPENDIX A

USEFUL CONSTANTS FOR SOLAR SYSTEM GR TESTS

ASTRONOMICAL CONSTANTS

| | | | |
|--------------------------|--------------------------|---|---------------------|
| Sun: | mass | $M_{\odot} = 1.99 \times 10^{33} \text{ g}$ | |
| | radius | $R_{\odot} = 6.96 \times 10^{10} \text{ cm}$ | |
| | surface gravity | $g_{\odot} = 2.74 \times 10^4 \text{ cm / sec}^2$ | |
| | luminosity | $\mathfrak{L}_{\odot} = 3.9 \times 10^{33} \text{ erg / sec}$ | |
| Earth: | mass | $M_{\oplus} = 5.98 \times 10^{27} \text{ g}$ | |
| | equatorial radius | $R_{\oplus} = 6.38 \times 10^8 \text{ cm}$ | |
| | polar radius | $R'_{\oplus} = R_{\oplus} - 2.15 \times 10^6 \text{ cm}$ | |
| | surface gravity | $g = 9.81 \times 10^2 \text{ cm / sec}^2$ | |
| | moment of inertia: | | |
| | about polar axis | $I^{33} = 0.331 M_{\oplus} R_{\oplus}^2$ | |
| | about equatorial axis | $I^{22} = I^{11} = 0.329 M_{\oplus} R_{\oplus}^2$ | |
| | period of rotation | 1 sidereal day = $8.62 \times 10^4 \text{ sec}$ | |
| | mean distance to sun | 1 A.U. = $1.50 \times 10^{13} \text{ cm}$ | |
| | orbital period | 1 sidereal year = $3.16 \times 10^7 \text{ sec}$ | |
| orbital velocity | 29.8 km / sec | | |
| Moon: | mass | $M_{\text{c}} = 7.35 \times 10^{25} \text{ g}$ | |
| | radius | $R_{\text{c}} = 1.74 \times 10^8 \text{ cm}$ | |
| | mean distance from Earth | $3.84 \times 10^{10} \text{ cm}$ | |
| | orbital period | 1 sidereal month = 27.3 days | |
| Planetary orbits: | | | |
| | Period | Perihelion Distance | Eccentricity |
| Mercury | 0.241 years | $45.9 \times 10^6 \text{ km}$ | 0.206 |
| Venus | 0.615 | 107 | 0.00682 |
| Earth | 1.00 | 147 | 0.0167 |
| Mars | 1.88 | 207 | 0.0933 |
| Jupiter | 11.9 | 741 | 0.0483 |
| Saturn | 29.5 | 1350 | 0.0559 |
| Uranus | 84.0 | 2730 | 0.0471 |
| Neptune | 165 | 4460 | 0.0085 |
| Pluto | 248 | 4420 | 0.249 |

APPENDIX B

SPECIAL RELATIVITY

INTERVAL:

$$g_{\mu\nu}^0 \equiv \begin{bmatrix} -1 & 0 & 0 & 0 \\ 0 & -1 & 0 & 0 \\ 0 & 0 & -1 & 0 \\ 0 & 0 & 0 & 1 \end{bmatrix} \begin{matrix} x \\ y \\ z \\ ct \end{matrix} \quad \text{Flat Space}$$

$$ds^2 = g_{\mu\nu}^0 dx^\mu dx^\nu = dx_\nu dx^\nu = (cdt)^2 - (d\vec{x})^2$$

= invariant length, same in all I. F.

4 VECTORS/TENSORS:

| | | |
|--------------------------------|--|---|
| Position | (\vec{x}, ct) | x^μ |
| Velocity | $\gamma(\vec{v}, c)$ | $U^\mu = dx^\mu / d(s/c)$ |
| Acceleration | $\gamma^2 \begin{pmatrix} \vec{a} + \\ \gamma^2 \vec{\beta}^2 (\vec{\beta} \cdot \vec{a}) \\ , \gamma^2 (\vec{\beta} \cdot \vec{a}) \end{pmatrix}$ | $A^\mu = dU^\mu / d(s/c)$ |
| Momentum | $(\vec{p}, \epsilon/c)$ $m\gamma(\vec{v}, c)$ | $p^\mu = mU^\mu$ |
| Force | (\vec{F}, F^4) $\gamma(\vec{f}, \vec{f} \cdot \vec{\beta})$ | $F^\mu = mA^\mu$ $= dp^\mu / d(s/c)$ |
| $\vec{v} \equiv d\vec{x} / dt$ | | $\beta \equiv v/c$ |
| $\vec{a} \equiv d\vec{v} / dt$ | | $\gamma \equiv 1/\sqrt{1-\beta^2}$ |
| $\vec{f} \equiv d\vec{p} / dt$ | | |

APPENDIX B (con't)

SPECIAL RELATIVITY

4 VECTORS/TENSORS:

| | | |
|-----------------------------|--|---|
| Derivative | $\left(\vec{\nabla}, \frac{\partial}{\partial(ct)} \right)$ $\left(-\vec{\nabla}, \frac{\partial}{\partial(ct)} \right)$ | ∂_μ $(g^0)^{\mu\nu} \partial_\nu = \partial^\mu$ |
| Divergence | $\vec{\nabla} \cdot \vec{A}$ $+ \partial A^4 / \partial(ct)$ | $\partial_\mu A^\mu$ |
| Gradient | $\left(-\vec{\nabla}\phi, \frac{\partial\phi}{\partial(ct)} \right)$ | $\partial^\mu \phi$ |
| Laplacian | $-\nabla^2 \phi + \frac{\partial^2 \phi}{\partial^2(ct)}$ | $\partial_\mu \partial^\mu \phi$ |
| Maxwell's Equations | (\vec{A}, ϕ) | $A^\mu, J^\mu = \rho^* U^\mu$ $(\partial_\nu \partial^\nu) A^\mu = \frac{4\pi}{c} J^\mu$ $\partial_\nu A^\nu = 0$ |
| Mass Tensor | $T^{44} = \sigma c^2$ $T^{4i} = (\sigma \vec{v})^i c$ $\vec{\nabla} \cdot (\sigma \vec{v})$ $= -\partial \sigma / \partial t$ | $T^{\mu\nu} = \sigma^* U^\mu U^\nu$ $\partial_\nu T^{\mu\nu} = 0$ |
| Pressure (Stress Tensor) | $S^{44} = P_0 (\gamma\beta)^2$ $c^2 d[\sigma \mathcal{V}]$ $= -P_0 d\mathcal{V}$ | $S^{\mu\nu} =$ $\frac{P_0}{c^2} [U^\mu U^\nu - c^2 (g^0)^{\mu\nu}]$ $\partial(T^{\mu\nu} + S^{\mu\nu}) = 0$ |

APPENDIX C

COMPARISONS EQUATIONS OF MOTION

| QUANTITY | NEWTONIAN | SR-FREE | SR-EM | LGR |
|----------------|---|--|--|--|
| Source | σ_M | - | $\bar{\rho}_C = \gamma_0 \bar{\rho}_C (1 - \beta_0 \beta_{11})$ $J^\mu = (\bar{J}, c \rho_C)$ $= \rho^* U^\mu$ | $\bar{\sigma}_M = \gamma_0^2 \sigma_M (1 - \beta_0 \beta_{11})^2$ $T^{\mu\nu} = \sigma^* U^\mu U^\nu$ |
| Continuity | $d\varepsilon = -\underline{P}_0 dV$ | - | $\partial_\mu J^\mu = 0$ | $\partial_\mu T^{\mu\nu} = 0$ |
| Field | Φ | - | A^μ | $\phi^{\mu\nu}$ |
| Field Equation | $\nabla^2 \Phi = 4\pi G \sigma_M$ | - | $(\partial_\lambda \partial^\lambda) A^\mu = \frac{4\pi}{c} J^\mu$ | $(\partial_\lambda \partial^\lambda) \phi^{\mu\nu} = -\kappa T^{\mu\nu}$ |
| \mathfrak{L} | $L = \frac{mc^2}{2} \left[\frac{\vec{\beta} \cdot \vec{\beta}}{2\Phi} - \frac{2\Phi}{c^2} \right]$ | $\frac{m}{2} U_\mu U^\mu$ | $\frac{m}{2} U_\mu U^\mu$ $+ \frac{q}{c} U_\mu A^\mu$ | $\frac{m}{2} U_\mu U^\mu$ $+ \frac{m}{2} \kappa \left(\phi_{\mu\nu} - \frac{g_{\mu\nu}^0}{2} \phi \right) U^\mu U^\nu$ |
| \mathfrak{H} | $H = \frac{mc^2}{2} \left[\frac{\vec{\beta} \cdot \vec{\beta}}{2\Phi} + \frac{2\Phi}{c^2} \right]$ | $\frac{m}{2} U_\mu U^\mu$ | $\frac{m}{2} U_\mu U^\mu$ | $\frac{m}{2} \left[g_{\mu\nu}^0 + \kappa \left(\phi_{\mu\nu} - \frac{g_{\mu\nu}^0}{2} \phi \right) \right] U^\mu U^\nu$ |
| Metric | - | $\begin{bmatrix} -1 & 0 & 0 & 0 \\ 0 & -1 & 0 & 0 \\ 0 & 0 & -1 & 0 \\ 0 & 0 & 0 & 1 \end{bmatrix}$ $\equiv g_{SR} = g^0$ | $g_{EM} = g^0$ | $g_{LGR} = g^0 + \kappa \left(\phi_{\mu\nu} - \frac{g_{\mu\nu}^0}{2} \phi \right)$ |

$$\frac{d}{ds} \left[g_{\mu\nu} \left(\frac{dx^\mu}{ds} \right) \left(\frac{dx^\nu}{ds} \right) \right] = 0$$

$$\kappa^2 = 16\pi G / c^4$$

Construct LGR equations to have coupling κ , $\vec{a} = -\vec{\nabla}\Phi$ in NR limit, and satisfy gauge conditions.

APPENDIX D

RADIATION EM vs. LGR

| QUANTITY | EM | LGR |
|-----------------------------------|---|--|
| Wave Equation | $(\partial_\lambda \partial^\lambda) A^\mu = \frac{4\pi}{c} J^\mu$ $\partial_\mu A^\mu = 0$ | $(\partial_\lambda \partial^\lambda) \phi^{\mu\nu} = -\kappa T^{\mu\nu}$ $\partial_\mu \phi^{\mu\nu} = 0$ |
| Integral Wave Equation | $A^\mu(\bar{x}, t) = \frac{1}{c} \int \frac{J^\mu(\bar{x}', t') d\bar{x}'}{ \bar{x} - \bar{x}' }$ $t' = t - \bar{x} - \bar{x}' /c$ $\sim \frac{1}{cr} \int J^\mu\left(\bar{x}', t - \frac{r}{c}\right) d\bar{x}'.$ | $\phi^{\mu\nu}(\bar{x}, t) = \frac{-\kappa}{4\pi} \int \frac{T^{\mu\nu}(\bar{x}', t') d\bar{x}'}{ \bar{x} - \bar{x}' }$ $\sim \frac{-\kappa}{4\pi r} \int T^{\mu\nu}\left(\bar{x}', t - \frac{r}{c}\right) d\bar{x}'.$ |
| Moments of Source Distribution | $\bar{A}(\bar{x}, t) \sim \frac{1}{cr} \left[\left(\bar{D} \right)_{RET} \right]$ | $\phi^{ij}(\bar{x}, t) \sim \frac{-\kappa}{8\pi r} \left[\left(\frac{\ddot{Q}^{ij}}{3} \right)_{RET} \right]$ |
| Time Averaged Radiated Power | $\langle P \rangle = \frac{\omega^4}{3c^3} \bar{D} ^2$ $= \frac{1}{3c^3} \ddot{D} ^2$ | $\langle P \rangle = \frac{G\omega^6}{45c^5} Q^{ij} ^2$ $= \frac{G}{45c^5} \ddot{Q}^{ij} ^2$ |
| Order of Magnitude Estimates | $+q \bullet \uparrow \frac{1}{r} d$ $-q \bullet \downarrow \frac{b}{r}$ $\langle P \rangle \sim \frac{2q^2 d^2}{3c^3} \omega^4$ $\sim \frac{(\delta D)^2}{3c^3} \omega^4$ $D = 2q[b + d \sin \omega t]$ | $M \bullet$ $M \bullet$ $\langle P \rangle \sim \frac{2G}{45c^5} (Mbd)^2 \omega^6$ $\sim \frac{G(\delta Q)^2}{45c^5} \omega^6$ $Q = M[b + d \sin \omega t]^2$ |